Effects of Hyperglycemia in Mouse Models of Atherosclerosis

INVESTIGATING THE EFFECTS OF HYPERGLYCEMIA ON THE VASA VASORUM IN THE DEVELOPMENT OF ATHEROSCLEROSIS AND ESTABLISHMENT OF NOVEL MOUSE MODELS OF DIABETES

By

DANIEL ESTEBAN VENEGAS-PINO, B.SC. (HONOURS),

PHARMACIST (SUMMA CUM LAUDE)

A Thesis Submitted to the School of Graduate Studies in Partial Fulfillment of the Requirements for the Degree Doctor of Philosophy

DOCTOR OF PHILOSOPHY (2015) McMaster University

(Biochemistry and Biomedical Sciences) Hamilton, Ontario

TITLE: Investigating the effects of hyperglycemia on the vasa vasorum in the development of atherosclerosis and establishment of novel mouse models of atherosclerosis

AUTHOR: Daniel Esteban Venegas Pino, B.Sc. in Pharmaceutical Sciences (Honours), Pharmacist (Summa Cum Laude) (University of Chile)

SUPERVISOR: Geoff H. Werstuck, B.Sc., Ph.D.

NUMBER OF PAGES: xviii, 211

ABSTRACT

The prevalence of diabetes is increasing rapidly around the world. People with diabetes are 2–4 times more likely to die from cerebro and cardio-vascular causes than people with no history of diabetes, even after controlling for other risk factors. Atherosclerosis, the underlying cause of most cardiovascular disease (CVD), is accelerated in people with diabetes, but several clinical trials have questioned the efficacy of glucose lowering therapies. A better understanding of the molecular pathways by which diabetes accelerates atherosclerosis will expand the scope of current targets and strategies for more effective therapies. In this thesis we investigate a novel mechanism and establish and characterize new hyperglycemic mouse models for the study of diabetic atherosclerosis.

Firstly, we investigate the effects of hyperglycemia on the vasa vasorum, the microvascular network that surrounds and supplies large vessels, and correlate those effects to the development of atherosclerosis. In normoglycemic $ApoE^{-/-}$ mice, the vasa vasorum expands as atherosclerotic lesions grow. However, in hyperglycemic $ApoE^{-/-}$ mice there is no significant neovascularization of the vasa vasorum despite the enhanced atherosclerotic development. We hypothesize that the ability of hyperglycemia to disrupt vasa vasorum neovascularization may promote the development and progression of atherosclerosis in diabetes.

Secondly, we establish, characterize and manipulate a new model of hyperglycemia-induced atherosclerosis: the $ApoE^{-/-}$:$Ins2^{+/Akita}$ mouse. We describe sex-specific differences of the $ApoE^{-/-}$:$Ins2^{+/Akita}$ mouse model. Male $ApoE^{-/-}$

:$Ins2^{+/Akita}$ mice develop chronic hyperglycemia and accelerated atherosclerosis. Castration slows atherosclerosis in $ApoE^{-/-}$:$Ins2^{+/Akita}$ mice but enhances it in normoglycemic controls. Female $ApoE^{-/-}$:$Ins2^{+/Akita}$ mice are only transiently hyperglycemic but still present with accelerated atherosclerosis. Ovariectomized $ApoE^{-/-}$:$Ins2^{+/Akita}$ mice are chronically hyperglycemic and show indications of advanced atherosclerosis.

Lastly, we investigate the effects of a western-type diet on the hyperglycemic $ApoE^{-/-}$:$Ins2^{+/Akita}$ mice. We demonstrate the pernicious phenotype of the mice leading to a significantly shortened lifespan correlated with massive atherosclerosis that extends to the aortic sinus, ascending and descending aorta, brachiocephalic artery and coronary arteries.

In conclusion we provide insights for a new mechanism by which hyperglycemia may accelerate atherosclerosis and possible role of the vasa vasorum in the progression of atherosclerosis in hyperglycemic mice. We also establish new mouse models that illuminate the action of sex hormones on pancreatic beta-cell function and the vasculature. These models will provide a test bed to further study sex hormone effects, as well as the diabetic pathways that promote atherosclerosis.

AKNOWLEDGEMENTS

I had desired for years being here, doing my PhD. It was a dream that I got when I was at the Instituto Nacional. Its motto—Labor Omnia Vincit—has become a sort of engine in my mind helping me accomplish this dream. There are so many people to thank, but my wife, coincidentally with the meaning of her Spanish name, Pilar has been the greatest support from beginning till the end of this PhD. I would not have done it without you Pilar. Thank you for all your love, company and support! This has been a great journey, but after all we get the sensation that it is just the beginning of a beautiful story, especially, when Leonidas/Giselle is in his/her way. I know we get nervous about it, but I am sure we will do just great!

My life is full of stories and I have had the pleasure to live it since so many scenarios. I was raised in a farm until I was 5–6 years old. So many memories from that time... Then, we moved to the town and I remember with nostalgia the times at school where I made my first friends. It was around that period when my father got in a car accident and we experienced hard times. It is difficult not to be marked for those things, but I realized how important is the 'family' and the real meaning of that word. That's why I cannot let this opportunity go without thanking all of you:

My mother, Esmeralda, thank you for always being there, for being mother and father, for sacrifice everything for your kids even until these days.

My father, Samuel, thank you for never giving up, for show me that life is not easy, but even in the worst unimaginable moments we can arise and triumph.

My sister, Rocio, thank you for sharing all those moments together. I am also happy for you because you finally found your career.

My grandmother, mamita Eliana, it is impossible to quantify all your help and its impact in our lives. I will always admire you and your strength. I have not met another person so special like you. One of my treasures in life is having met you.

My grandfather, tata Carlos, thank you for being there when we needed you the most, for teaching me to fight, and to be brave.

My uncle, Alejandro, thank you for being a father when I needed it, and for bringing me to the Instituto Nacional. All the sacrifice was worth it.

My uncle, Marco, thank you for being my uncle and a close friend. I would like to share this title with you wherever you are.

My mother-in-law, Barbara, since the arrival to Canada you have always being there for us. I am grateful of having you with us. Thank you for all your love.

My father-in-law, José, it is great to have a close relative here that speaks the same language. Thank you for everything Pepe.

My closest friends during this PhD were also an important pillar of strength and a circle of trust. That's why I would like to thank you: Peter Shi, Ying Pei, Yazzed Alshuweishi and Mohammad Khan.

Also I would like to thank my supervisor, Dr. Geoff H. Werstuck, thank you for the great opportunity of working in your laboratory and the excellent guidance during this whole time. Coming from abroad I must say that you have been a key support to the success of this project. I learned a lot from your mentorship, but I selectively take with me the way you manage all your projects and the fluid relationship that you establish with all your peers and students.

Dr. Bernardo Trigatti and Dr. Peter Gross, I would also like to extend my sincere thanks and appreciation to both of you. All the time and commitment from your parts were key elements for the publication of parts of our research project and the accomplishment of this degree.

This research was funded by an operating grant from the Canadian Institutes of Health Sciences (CIHR, Canada) and the Canadian Diabetes Association (CDA, Canada). D.E.V.P. was supported by a scholarship from the Comisión Nacional de Investigación Científica y Tecnológica (CONICYT, Chile).

TABLE OF CONTENTS

LIST OF FIGURES

Chapter 1: General Introduction

Chapter 3: Hyperglycemia is Associated with Impaired Vasa Vasorum Neovascularization and Accelerated Atherosclerosis in Apolipoprotein-E Deficient Mice

Chapter 4: Sex-Specific Differences in an ApoE$^{-/-}$:Ins2$^{+/Akita}$ Mouse Model of Accelerated Atherosclerosis

LIST OF TABLES

Chapter 3: Hyperglycemia is Associated with Impaired Vasa Vasorum Neovascularization and Accelerated Atherosclerosis in Apolipoprotein-E Deficient Mice

LIST OF ABREVIATIONS

ABCA1 ATP-binding cassette transporter member 1

ABCG1 ATP-binding cassette sub-family G member 1

ACCORD Action to control cardiovascular risk in diabetes

ACSL Acyl-CoA synthetase

ADVANCE Action in diabetes and vascular disease: preterax and diamicron MR controlled evaluation

ADP Adenosine diphosphate

AGE Advanced glycation endproduct

ApoA Apolipoprotein-A

ApoB Apolipoprotein-B

ApoC Apolipoprotein-C

ApoE Apolipoprotein-E

ANOVA Analysis of variance

A1C Glycated hemoglobin

CD36 Cluster of differentiation 36

CV Cardiovascular

CVD Cardiovascular disease

Cx Castration, castrated

CXCL16 Chemokine (C-X-C motif) ligand 16

C96Y A tyrosine for cysteine substitution at position 96 of the pre–proinsulin

dKO Double knockout

DAPI 4',6-Diamidino-2-phenylindole

DAB 3,3′-Diaminobenzidine

DCCT Diabetes Control and Complications Trial

DM Diabetes mellitus

DNA Deoxyribonucleic acid

EC Endothelial cell

ECM Extracellular matrix

EDIC Epidemiology of Diabetes Interventions and Complications

ELISA Enzyme-linked immunosorbent assay

eNOS Endothelial nitric oxide synthase

ER Endoplasmic reticulum

FFA Free fatty acids

FSH Follicle stimulating hormone

g Grams

GADD Growth arrest and DNA damage-inducible protein

GAPDH Glyceraldehyde-3-Phosphate Dehydrogenase

GFAT Glutamine:fructose-6-phosphate aminotransferase

GLUT Glucose transporter

GP Glycoprotein

GSH Reduced glutathione

HDL High-density lipoprotein

HF High fat

HFD High fat diet

HIF Hypoxia-inducible factor

HG Hyperglycemia, hyperglycemic

HOMA-IR Homeostatic model assessment for assessing insulin resistance

HOMA-%β Homeostatic model assessment for assessing β-cell function

IAS International Atherosclerosis Society

ICAM Intercellular Adhesion Molecule

IDF International Diabetes Federation

IF Immunofluorescence

IFG Impaired fasting glucose

IgG Immunoglobulin G

IGT Impaired glucose tolerance

IL Interleukin

INF Interferon

IRS Insulin receptor substrate

JoVE Journal of Visualized Experiments

KO Knockout

LDL Low-density lipoprotein

LDLR Low-density lipoprotein receptor

LH Luteinizing hormone

LOX-1 Lectin-like oxidized low-density lipoprotein (LDL) receptor-1

MCP Monocyte chemoattractant protein

M-CSF Macrophage colony-stimulating factor

MI Myocardial infarction

mm Millimeter

mM Millimolar

NBF Neutral buffered formalin

NF-κB Nuclear Factor κB

NG Normoglycemia, normoglycemic

NO Nitric oxide

oxLDL Oxidized low-density lipoprotein

OGTT Oral glucose tolerance test

Ovx Ovariectomy, ovariectomized

PAI Plasminogen activator inhibitor

PARP Poly(ADP-ribose) polymerase

PBS Phosphate buffered saline

PCR Polymerase chain reaction

PITT Peritoneal insulin tolerance test

PKC Protein kinase C

QUICKI Quantitative insulin sensitivity check index

RAGE Receptor for advanced glycation endproduct

RD Regular chow diet

ROS Reactive oxygen species

SEM Standard error of the mean

SMC Smooth muscle cell

Sp1 Specificity protein 1

SR-A Scavenger receptor class A

SR-B1 Scavenger receptor class B1

STZ Streptozotocin

TGF Transforming growth factor

TNF Tumor necrosis factor

T1DM Type 1 diabetes mellitus

T2DM Type 2 diabetes mellitus

UDP-GLcNAc Uridine diphosphate N-acetylglucosamine

UKPDS United Kingdom Prospective Diabetes Study

UPR Unfolded protein response

VADT Veterans Affairs Diabetes Trial

VCAM Vascular cell adhesion molecule

VEGF Vascular endothelial growth factor

VEGF-R2 VEGF receptor 2

VLDL Very low-density lipoprotein

vWF von Willebrand factor

WD Western-type diet

CHAPTER 1: General Introduction

1.1 FOREWORD

Portions of this general introduction are a direct representation of an article and a commentary published in *the Journal of Visualized Experiments* (JoVE) and the *International Atherosclerosis Society* (IAS). The manuscripts were written by Daniel E. Venegas-Pino and Dr. Geoff H. Werstuck in collaboration with others. The complete references are as follows:

Venegas-Pino DE, Banko N, Khan MI, Shi Y, Werstuck GH: Quantitative analysis and characterization of atherosclerotic lesions in the murine aortic sinus. J Vis Exp. 2013, 82:e50933. Copyright © 2013 Journal of Visualized Experiments.

Venegas-Pino DE, Stoute HK, Werstuck GH: Is Accelerated Atherosclerosis a Microvascular Complication of Diabetes? International Atherosclerosis Society. 2014. *www.athero.org/commentaries/comm1171.asp*. Copyright © 2014 International Atherosclerosis Society.

1.2 DIABETES MELLITUS

Definition and diagnosis

The term “Diabetes” actually describes several metabolic diseases characterized by hyperglycemia and glucose intolerance resulting from impaired insulin secretion and/or impaired insulin action [1]. The two most common classes of diabetes mellitus (DM), type 1 diabetes mellitus (T1DM) and type 2 diabetes mellitus (T2DM), account for 5-10% and 85-90% of total cases of diabetes mellitus,

respectively [1, 2]. T1DM involves the autoimmune-driven destruction of pancreatic beta-cells resulting in a severe insulin deficiency. T2DM involves peripheral resistance to circulating insulin, initial hyperinsulinemia, followed by beta-cell death and insulin insufficiency [1]. Normal fasting blood glucose levels (where 'fasting' is no caloric intake for at least 8 hours) should be between 3.9–5.6mM in a healthy individual. DM is diagnosed when fasting blood glucose levels are consistently ≥7.0mM, when A1C levels (glycohemoglobin test) are ≥6.5%, or when blood glucose levels are ≥11.1mM two hours after a 75g oral glucose challenge [1, 2].

Individuals with blood glucose levels above normal, but below the threshold of clinically diagnosed diabetes are considered to have "prediabetes" and are at high risk of developing actual diabetes. Prediabetes includes conditions of impaired fasting glucose (IFG), fasting blood glucose of 5.6–6.9mM, and impaired glucose tolerance (IGT), blood glucose levels of 7.8–11.0mM two hours after a 75g oral glucose challenge, or an A1C of 5.7–6.4% [2, 3].

Prevalence

Increasing urbanization, an ageing population, disproportionate and poor-quality diets, lack of physical activity, and other unhealthy lifestyle and behavioral patterns have led to a drastic increase in the prevalence of T2DM. In the last few decades T2DM has become a serious health burden in all developed and developing countries [4].

The International Diabetes Federation (IDF) analyzed data from 212 countries that corresponded to a sample size equivalent to the 90% of the global population in the age range 20–79 years. They estimated the prevalence of diabetes in 2003 to be 194 million people or 5.1% of the adult global population. The IDF estimated that there will be 333 million people with diabetes by 2025— equivalent to 6.3% of the adult global population [5]. The general picture gets even more dire when individuals with IGT are included. In 2003, 314 million people had IGT (equivalent to 8.2% of the adult global population). This number is predicted to reach 472 million (equivalent to 9%) by 2025 [5].

Complications of diabetes mellitus

DM is a chronic disease that is associated with an array of vascular complications that often lead to premature mortality and morbidity. In most of the developed and developing countries, the main complications of diabetes correspond to retinopathy (responsible for a large number of new cases of blindness every year [6]), nephropathy (leading to renal failure and currently becoming the main cause of dialysis and kidney transplantation [7, 8]), neuropathy (inducing detrimental effects on the peripheral nervous system that eventually may lead to amputations [9–11]), and cerebro and cardio-vascular disease (increasing the risk of stroke and coronary heart disease that account for around 70% of deaths of all diabetic patients [12, 13]).

Although both types of diabetes share 'hyperglycemia' as the main characteristic, T1DM develops suddenly at a younger age (usually <18 years old) [1, 2]. T2DM develops gradually after age 45, however cases of T2DM in adolescence are on the rise [14]. T2DM is often associated with dyslipidemia (high levels of low-density lipoprotein (LDL) and triglycerides, and low levels of high-density lipoprotein (HDL)), obesity and hypertension, as part of the metabolic syndrome [1]. There is currently no cure for T1DM or T2DM. Hyperglycemia can be managed with the adaptation of healthy life habits in combination with medications to help control glucose levels, normalize insulin levels and increase insulin activity [15, 16]. Lowering blood glucose has shown good results with respect to the onset of nephropathy and retinopathy [17, 18], but beneficial effects on cardiovascular disease and stroke have not been strongly supported in randomized controlled trials (UKPDS [17], ACCORD [19], ADVANCE [18] and VADT [20]).

A major complication of DM is the economic impact of the disease around the world. If the IDF predictions of prevalence for 2025 are fulfilled, the world will have to expend between US$200 and US$400 billion to treat this diabetes epidemic. For many countries this will represent a significant proportion (and expansion) of their total healthcare budgets [5].

1.3 VASCULAR PATHOLOGIES OF DIABETES

All of the complications of diabetes are viewed to be vascular in nature and the vascular complications of diabetes are conventionally partitioned into two subtypes; microvascular and macrovascular. Microvascular complications include nephropathy, neuropathy, retinopathy and peripheral circulatory problems [21]. Macrovascular complications involve structural and functional changes in the large arteries that predominately involve the accelerated development of atherosclerosis, potentially leading to increased risk of myocardial infarction and stroke [22]. Traditionally the micro and macro-vascular complications of diabetes have been viewed, studied and treated, as distinct and independent disorders. However, accumulating data from epidemiological and pathophysiological studies suggest that these vascular problems are, in fact, closely interrelated [23, 24].

Macrovascular disease

Diabetes is associated with a cardiovascular (CV) mortality rate that exceeds 70%, and people with diabetes are 2 to 4 times more likely to die from CV causes than people with no history of diabetes, even after controlling for other CV risk factors [25]. The molecular and cellular mechanisms by which diabetes promotes atherosclerosis, the underlying cause of most cardiovascular diseases (CVD) [26], have not been clearly defined. Mounting evidence, showing that the normalization of glucose levels improves CV outcomes, supports a causative role for elevated blood glucose levels in the pathogenesis of atherosclerosis [27].

However, the apparent lack of a blood glucose threshold for CV risk, and confounding data from clinical trials (UKPDS, ACCORD, ADVANCE, VADT, and some ongoing trials) that examine the effects of glucose lowering on CV risk, indicate that the relationship between blood glucose levels and CV risk is even more complex than previously believed [17–20]. Our ability to effectively prevent and/or treat diabetic CVD is currently impeded by our lack of understanding of the mechanisms that underlie disease development and progression.

Microvascular disease

Microvascular disease involves the disruption of the structure and function of the capillary networks that supply nutrients and oxygen to various tissues and organs.

In contrast to diabetic macrovascular disease, it is very well established that the incidence of microvascular disorders is tightly linked to blood glucose levels. In fact, the glycemic parameters that define/diagnose diabetes mellitus (fasting blood glucose ≥7mM) were chosen because they effectively differentiate individuals at high risk for developing retinopathy from those at low risk [1], and not because these glucose levels have any connection to CV risk.

It has been proposed that conditions of hyperglycemia disrupt normal microvascular structure and function by mechanisms involving oxidative stress, inflammation, pericyte loss and/or increased extracellular matrix deposition, which leads to increased vascular permeability and vessel leakage [28]. Depending upon

the tissue/organ being considered, and perhaps the duration of the condition, the effects of hyperglycemia on the microvasculature can lead to excessive neovascularization, as in proliferative diabetic retinopathy [29] and nephropathy [30], or attenuated neovascularization, contributing to pre–proliferative retinopathy [21], impaired coronary collateral vessel development [31], impaired wound healing [32], and transplant rejection in diabetic recipients [33]. The concurrent existence of pro- and anti-neovascularization responses in diabetes has been called the "angiogenesis paradox" [34]. The angiogenesis paradox is most strikingly illustrated by the fact that experimental treatments for proliferative diabetic retinopathy and nephropathy have involved targeting vascular endothelial growth factor (VEGF) for inhibition [35], whereas application of exogenous VEGF facilitates wound healing in diabetic patients [36].

1.4 POTENTIAL LINK BETWEEN MICROVASCULAR AND MACROVASCULAR DISEASE: VASA VASORUM

The walls of large arteries consist of three distinct layers. The innermost layer is called the intima. The intima contains a monolayer of endothelial cells that is in direct contact with the circulating blood. The sub-endothelial part of the intima consists of extracellular connective tissue built mainly of proteoglycans and collagen. The second layer of the artery wall is the media, characterized by a thicker and organized arrangement of vascular smooth muscles cells. The medial layer provides strength and flexibility to the artery wall. The third layer, the adventitia,

provides structure and support and is composed of connective tissue with interspersed fibroblasts, vascular smooth muscle cells and the vasa vasorum [37].

The vasa vasorum consists of a network of small arterioles, capillaries and venules that supply the cells that constitute the adventitia and tunica media of large blood vessels, including the aorta and coronary arteries (See Figure 1.1 [38]). Vasa vasorum literally means "vessels of the vessels," and therefore, by definition, it is the place where the microvasculature and the macrovasculature meet. A role for the vasa vasorum in the progression of atherosclerosis is not a new idea—but it has historically been a contentious one [39]. A general correlation between vasa vasorum neovascularization and atherosclerotic lesion size has been observed in (non-diabetic) humans [40] and in dyslipidemic ApoE/Ldlr dKO mice [41]. The cause-effect relationship between lesion neovascularization and atherogenesis in these systems is not clear—does lesion growth promote vasa vasorum angiogenesis, or does vasa vasorum expansion drive lesion growth?

Relatively early in atherogenesis, the increased oxygen demands associated with inflammation together with thickening of the artery wall create localized regions of hypoxia that are detectable, even in mice [42]. Several studies have shown that systemic application of pro-angiogenic stimuli is associated with enhanced atherosclerosis [43], and anti-angiogenic therapies attenuate atherosclerosis [44]. However, it is important to note that the majority of these studies failed to detect any changes in plaque neovascularization during the course

of the experiments, suggesting that these treatments/interventions may be affecting atherogenesis in ways that are independent of vasa vasorum angiogenesis.

Since the fundamental purpose of the vasa vasorum is to facilitate the supply, maintenance, and repair of the healthy arterial wall, disruption of this microvascular network can be detrimental. Occlusion of the vasa vasorum has been associated with localized ischemia in the arterial media that may lead to the proliferation of smooth muscle cells, localized intimal/medial thickening, and increased synthesis of collagen fibers [45]. Other studies have suggested that the vasa vasorum plays an important role in reverse cholesterol transport/removal of lipids from the artery wall [46].

Thus, the pro- and/or anti-atherogenic potential of alterations to the vasa vasorum has yet to be determined. Furthermore, it is important to note that the studies carried out thus far have been performed in non-diabetic animal models and, despite the established effects of hyperglycemia on microvascular beds in the retina, kidney and peripheral tissues, virtually nothing is known about the effect of diabetes/hyperglycemia on the vasa vasorum, or the potential role of these microvascular effects on diabetes-associated accelerated atherosclerosis.

Figure 1.1. Vasa vasorum. Three-dimensional images captured by computed tomography of the vasa vasorum running longitudinally (+135º) along the adventitial surface of a coronary artery (arrows indicating first-order vasa vasorum), and running around and surrounding (+90º) the coronary artery (triangles indicating second-order vasa vasorum).

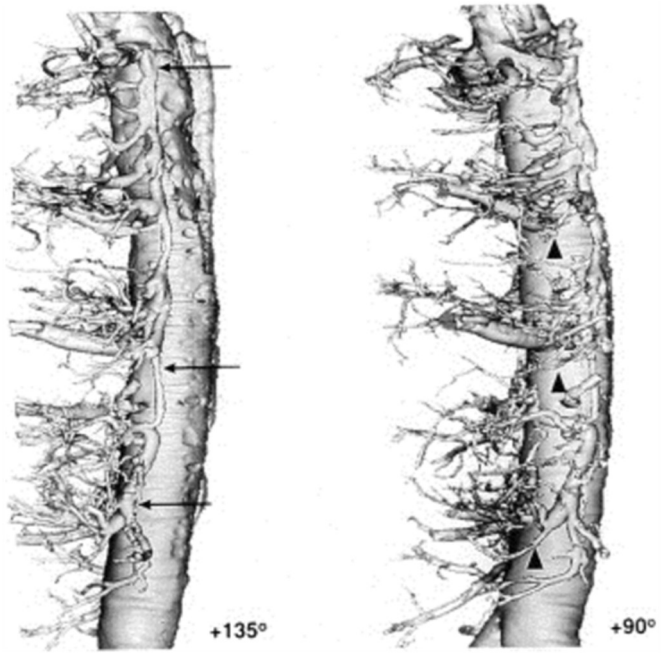

Reprinted with permission from:

Kwon HM, Sangiorgi G, Ritman EL, Lerman A, McKenna C, Virmani R, Edwards WD, Holmes DR, Schwartz RS: Adventitial vasa vasorum in balloon-injured coronary arteries: visualization and quantitation by a microscopic three-dimensional computed tomography technique. J Am Coll Cardiol. 1998, 32:2072–2079. Copyright © 1998 by the American College of Cardiology. License Number 3741560811404

1.5 ATHEROSCLEROSIS

Pathology of atherosclerosis

Atherosclerosis is characterized by progressive lipid accumulation and chronic inflammation of the arterial wall leading to the formation of atherosclerotic lesions (Figure 1.2). Generally the lesions tend to appear at specific arterial locations, branches and bifurcations, where changes in the hemodynamic forces, including decreased shear stress and increased turbulent blood flow would favor the lesion development [47].

The earliest events that lead to atherosclerotic lesion formation occur in the endothelial cells that are in direct contact with the lumen content. Several risk factors (hyperlipidemia, hypertension, DM, insulin resistance, obesity, smoking, lack of exercise, high fat diet and infectious agents [47, 48]) induce the endothelial permeability through specific mediators including proinflammatory cytokines (TNF-α, IL-1β), bacterial (lipopolysaccharide) and endogenous toxins (oxLDL), vasoconstrictors (angiotensin II, endothelin-1 and Thromboxane A2), and extracellular matrix proteins (fibronectin, fibrinogen) [49–51]. Increased endothelial permeability leads to the retention of LDLs that interact with the underlying extracellular matrix (ECM). This interaction retains the LDL which becomes trapped in the vessel wall where it can undergo progressive oxidation by reactive oxygen species (ROS) and/or glycation under hyperglycemic conditions. Trapped and modified LDL induces a profound change of the phenotype of endothelial cells through the activation of the proinflammatory transcription

nuclear factor κB (NF-κB), up-regulation of the expression of adhesion molecules (P-selectin, E-selectin, ICAM-1, VCAM-1), chemokines (IL-8, monocyte chemotactic protein-1 (MCP-1)), and cytokines (IL-1β, TNFα, macrophage colony-stimulating factor (M-CSF)). Modified LDL also inhibits the production of nitric oxide (NO), a vasodilator with anti-atherogenic properties [52, 53], leading to endothelial dysfunction. Upon the activation of the endothelium, leukocytes (monocytes, T-cells and neutrophils) commence to interact with selectins on the endothelial surface and also bind to ICAM-1 and VCAM-1 to undergo directed migration into the artery wall mediated by MCP-1. Once these recruited leukocytes are in the intima, M-CSF stimulates the proliferation and differentiation of macrophages that express high levels of scavenger receptors (CD36, SR-A, LOX-1 and CXCL16) [54]. The macrophages over-expressing scavenger receptors are able to engulf modified LDL, accumulating cholesteryl ester and becoming foam cells, which accumulate to form fatty streaks in the artery wall. The accumulation of cholesterol may be driven, in part, by a dysregulation of the ATP binding cassette transporters (ABCA1 and ABCG1) that regulate and control cholesterol efflux and reverse cholesterol transport in macrophages [55–59]. As lesion development progresses, activated macrophages, foam cells and T cells further stimulate the inflammatory process and induce the migration and proliferation of SMCs from the media. The proliferation of SMC results in the formation of the fibrous cap, composed of elastic proteins, including collagen and elastin, which are secreted by SMCs. The fibrous cap stabilizes the lesion and also protects the lesion from the

circulating blood thereby avoiding the contact with the intimal mixture of monocytes, macrophages, T-cells, SMCs, foam cells, modified lipids and the necrotic core characteristic of advanced lesion. Necrosis and apoptosis of macrophages, foam cells and SMCs in the lesion are the main contributors to the formation of this necrotic core composed mainly of apoptotic cell bodies, debris, modified lipids and cholesterol crystals. Macrophages are responsible for the clearance of apoptotic cells (efferocytosis), but the excessive cholesterol uptake induces endoplasmic reticulum (ER) stress in these cells [60–62], leading to their death and the release of their total lipid content. This process creates a cycle in which the local inflammatory response is sustained and the size of this necrotic area continues to increase. The fact that over 60% of heart attacks are associated with plaques that occlude less than 50% of the lumen [63] suggests that plaque rupture and eventual thrombus formation are the main factors responsible for the artery occlusion and infarction. Plaque rupture probably occurs as an imbalance between the forces that control and maintain the fibrous cap. For example, collagen provides most of the biomechanical resistance to the disruption of the fibrous cap. Therefore, factors that decrease the collagen synthesis or increase the degradation of elastic proteins will favor this process. Also, the growing necrotic core and the neovascularization *in situ* are thought to contribute to the weakening process because new microvessels can induce internal hemorrhage increasing the chances of contact between the lesion content and the blood (Figure 1.3 [47]).

Figure 1.2. Atherosclerosis development. Atherosclerotic lesions at the aortic sinus and coronary arteries of an ApoE-deficient mouse fed a high-fat diet. Picture taken by Daniel E. Venegas-Pino.

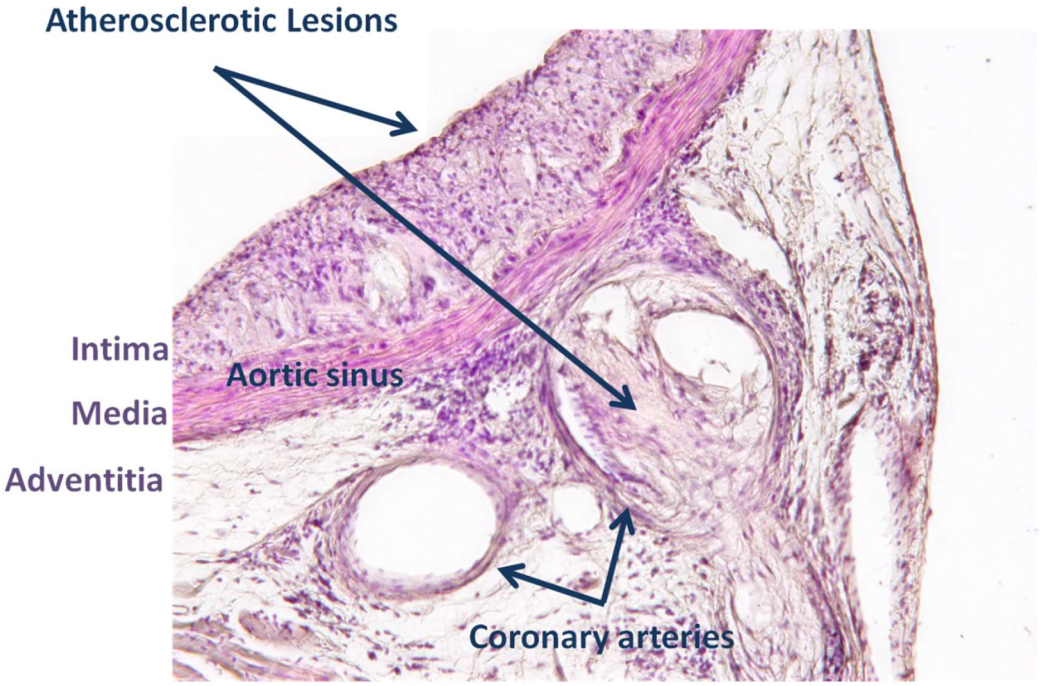
Atherosclerotic Lesions
Intima
Media
Adventitia
Aortic sinus
Coronary arteries

Figure 1.3. Schematic representation of atherosclerosis progression. (A) Initiating events: atherosclerosis is initiated at sites of endothelial injury. These areas have increased endothelial permeability and sub-endothelial LDL accumulation. Trapped LDL can be modified by progressive oxidation. The activated endothelium expresses adhesion molecules (ICAM, VCAM, P-selectin and E-selectin) and leukocytes bind these adhesion molecules and undergo directed migration (MCP-1 mediated) into the artery wall. (B) Fatty-streak formation: intimal monocytes are induced to differentiate into macrophages by M-CSF. Macrophages proliferate and over-express scavenger receptors that allow them to engulf modified LDLs. The accumulation of cholesteryl ester in macrophages results in the formation of foam cells which form the characteristic fatty streak in the artery wall. (C) Advanced plaque: lesion development progresses with SMC migration and proliferation leading to the formation of the fibrous cap composed of SMCs and elastic proteins such as collagen and elastin which protect and stabilize the growing lesion. Foam cells undergo apoptosis forming an acellular necrotic core, which is believed to destabilize the lesion. (D) The plaque rupture: an imbalance between the factors that contribute to a stable fibrous cap may lead to its weakening or thinning. The internal hemorrhage of the plaques can also affect the lesion stability and induce the eventual thrombus formation.

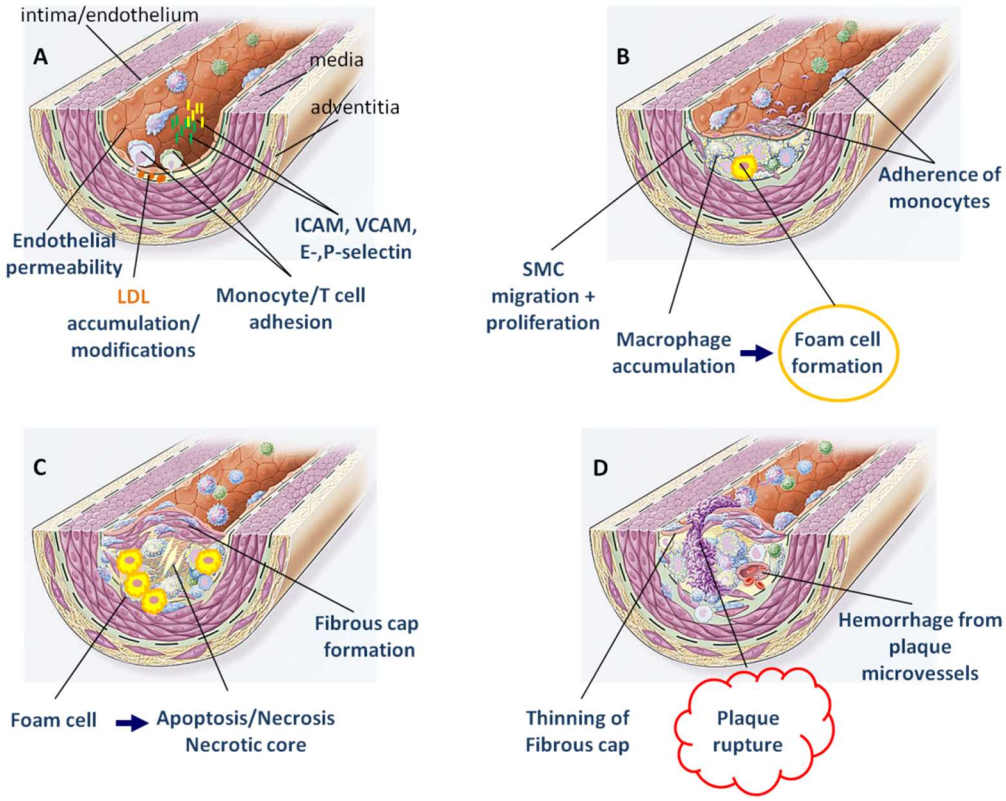

Reproduced with permission from:

Ross R: Atherosclerosis—an inflammatory disease. N Engl J Med. 1999, 340:115–126. Copyright © 1999 Massachusetts Medical Society.

Atherosclerosis and diabetes

Even though morphological characteristics of atherosclerotic plaques are similar between people with diabetes and without the disease, it is generally believed that the process is accelerated in diabetes with more calcification, larger necrotic cores, an increased presence of leukocyte infiltration, and a higher incidence of hemorrhage in atherosclerotic plaques from diabetic patients. In addition, diabetes accelerates lesion growth and impairs lesion regression [64–66].

The mechanism by which diabetes exerts its effects on the development of atherosclerosis is likely linked to hyperglycemia and insulin resistance. Endothelial cells represent a good candidate for the initial damage induced by chronically high glucose levels because these cells retain the expression of insulin-independent glucose transporters (GLUT) allowing intracellular glucose concentrations similar to those observed in blood [67, 68]. ROS levels would increase inside the cells by direct glucose auto-oxidation [69] and mitochondrial superoxide production [70]. It has been demonstrated that hyperglycemia-induced ROS reduce glyceraldehyde 3-phosphate dehydrogenase (GAPDH) activity by modifying this enzyme with polymers of ADP-ribose [71]. Poly(ADP-ribose) polymerase (PARP) resides in the nucleus and is activated by damage of DNA, producing in response these polymers of ADP-ribose. Increased ROS in the mitochondria induce DNA strand breaks, thereby activating PARP in the nucleus. GAPDH is constantly relocating from the cytosol to the nucleus which allows the encounter with polymers of ADP-ribose and the structural modification [72, 73]. Du et al. (2000) showed a 66% reduction

in the activity of GAPDH as a result of hyperglycemia, and the subsequent activation of four detrimental pathways: polyol pathway, AGEs, PKCs, and the hexosamine pathway [74].

The polyol pathway is based on the enzyme aldose reductase and the depletion of NADPH. When glucose concentrations become abnormally high in the cell (endothelial cells), glucose flux into this pathway increases 10X [75, 76]. Glucose then is reduced by aldose reductase to sorbitol consuming NADPH in the process and inducing its depletion [77]. Thereby, the lack of NADPH available to regenerate reduced glutathione (GSH) lays the cells in a vulnerable stage against oxidative stress. Causative studies have shown that overexpression of human aldose reductase (aldose reductase in mouse is not comparatively expressed to humans [78]) in diabetic mice resulted in accelerated atherosclerosis and reduced expression of genes that maintain GSH [79].

AGEs are modifications of proteins that become nonenzymatically glycated after prolonged contact with sugars. The AGE formation process starts with the nonenzymatic reaction of the carbonyl group of glucose with proteins producing the Amadori products. These highly reactive intermediate carbonyl groups accumulate, and also react with amino, sulfhydryl, and guanidine functional groups in proteins. Stable AGE precursors include methylglyoxal (which is the major precursor and it is derived from the glycolytic intermediate glyceraldehyde-3 phosphate), 3-deoxyglucosone and glyoxal [80]. AGEs may injure endothelial cells by modification of intracellular proteins and their functionality, by interacting and

modifying extracellular matrix components and matrix receptors, and by modifying circulating proteins that then interact and activate AGE receptors (RAGEs)—which are also found on macrophages, endothelial and smooth muscle cells. The AGE–RAGE interaction triggers the production of intracellular reactive oxidative species that initiate an inflammatory response activating the proinflammatory transcription factor NF-κB [80]. Removal of AGE effects or AGEs, by RAGE deficiency [81] or a soluble form of RAGE [82], has then shown positive effects on mouse models of atherosclerosis.

As a result of the impaired GAPDH activity (by intracellular hyperglycemia), there is accumulation of glyceraldehyde-3-phosphate that can be transformed to diacylglycerol—a key activator of PKCs [83, 84]. Activation of PKC has a wide scope of detrimental effects. PKC inhibits endothelial nitric oxide synthase (eNOS) expression, decreasing the production of the vasodilator nitric oxide (NO). PKC increases the vasoconstrictors endothelin-1 and thromboxane-A2 expression. PKC also up-regulates plasminogen activator inhibitor type-1 (PAI-1) and NF-κB exacerbating the hypercoagulable and proinflammatory state [85–87].

Decreased activity of GAPDH is also accompanied by a concomitant 2.5-fold increase in the hexosamine pathway activity [74]. The glycolytic intermediate fructose-6-phosphate enters the pathway and is transformed by the rate-limiting enzyme glutamine:fructose-6-phosphate amidotransferase (GFAT) to glucosamine-6-phosphate that then after further modifications is converted to uridine diphosphate N-acetylglucosamine (UDP-GlcNAc) [88]. UDP-GlcNAc acts as

precursor for all amino sugars used for the post–translational changes and synthesis of glycoproteins, glycolipids, and proteoglycans. The post–translational protein O-GlcNAcylation modification has been reported to play a role in the vascular complications of diabetes [88, 89]. For example, O-GlcNAcylation of eNOS decreases its activity leading to a deficiency of NO [90, 91], and the same post–translational modification of the transcription factor Sp1 (Specificity protein 1) activates the TGF-β1 and PAI-1 expression [74].

Hyperglycemia has also been reported to induce changes in myeloid cells favouring the atherogenic progression. In mouse models, isolated peritoneal macrophages from hyperglycemic mice presented higher expression of chemokines and cytokines [92, 93]. Atherosclerotic lesion macrophages, in lesion regression studies, from hyperglycemic mice also had a higher inflammatory component than macrophages from normoglycemic mice [94, 95]. Observations that are supported by cytokine expression in monocytes from diabetic patients [96–99] where the proinflammatory transcription factor NF-κB seems to be one of the pathways activated and playing a role in this greater proinflammatory phenotype of monocytes, at least in T1DM patients [99–101]. Also acyl-CoA synthetase-1 (ACSL-1) has been identified to play a role in the proinflammatory phenotype of monocytes in hyperglycemic mice. Targeting ACSL-1 expression in myeloid cells prevented the hyperglycemia-induced inflammatory effect on monocytes and macrophages and protected from atherosclerosis development [93]. Diabetes has been also associated with a higher expression of macrophage receptors that allow

the engulfment of modified lipids (SR-A [102], CD36 [103] and LOX-1 [104]) and reduced ABCG1 expression (in human [105] and mouse [106]). Furthermore, exacerbated myelopoiesis has been described in diabetic mice [95] specifically of a monocyte variation that has been identified in atherosclerosis [107].

SMCs also seem to suffer the effects of hyperglycemia. Vascular calcification is increased in patients with diabetes mellitus [66], and connecting to calcification SMCs have been identified to differentiate into chondrocyte-like cells, which contribute to calcification [108]. However, still more research is needed to establish a direct connection between hyperglycemia and SMC differentiation. Also, recently it was described in human coronary artery that SMCs play a major role (than previously thought) in cholesterol accumulation and foam cell formation. 50% of total foam cells were found to be SMC derived due to a decrease in ABCA1 expression in intimal SMCs in late-stage disease [109]. This obviously opens the possibility for a greater effect of hyperglycemia on SMCs.

On the other hand, insulin resistance has also shown to have direct effects, independent from hyperglycemia, on the development of atherosclerosis. First, the increase of circulating free fatty acids (FFA) from adipocytes [110] has shown to produce, in aortic endothelial cells, similar mitochondrial overproduction of ROS and inducing the same damaging pathways described above for hyperglycemia [111]. Second, insulin resistance has been shown to affect endothelial cells [112] and myeloid cells [113, 114] in mouse models. Direct effects on atherosclerosis were observed when a heterozygous null mutation in the *insulin receptor substrate-*

2 (*IRS-2*) gene [115] or heterozygous null mutations in the *insulin receptor* and the *insulin receptor substrate-1* (*IRS-1*) genes [116] were introduced in the ApoE$^{-/-}$ mouse, accelerating the progression of the disease.

1.6 MOUSE MODELS

Mice have become the preferred model for the study of atherosclerosis for most basic science laboratories. Mouse models provide several distinct advantages including; i) mice can be genetically manipulated, ii) atherosclerosis develops relatively quickly in genetically-modified mice (within 2–3 months) and lesions appear to be very similar to those seen in human patients, iii) mice are inexpensive compared to other animal models, iv) experiments can be carried out using relatively large treatment groups. However, when compared to human beings, still there are important limitations that we should be aware of as these may restrict the translation of findings into humans. Generally the lipid profiles of mice are different to those observed in humans. Wild type mice have high levels of circulating athero-protective HDL and low levels of pro-atherogenic very low-density lipoprotein (VLDL) and LDL particles [117]. This is likely a major reason why wild type mice are resistant to the development of atherosclerosis. Also for this reason, the majority of the existing mouse models for the study of atherosclerosis involve the disruption of this non-atherogenic lipid profile through atherogenic diets and/or genetic interventions. There are other important limitations with mouse models including the differences in vessel diameters and hemodynamic forces (heart rate, blood flow

and pressure) [118], relative to humans. These factors have a major impact in the locations of the atherosclerotic lesions guiding our focus mainly on the aortic sinus of the mice where human atherosclerosis does not present a major threat.

Apolipoprotein E-deficient ($ApoE^{-/-}$) mice have been widely used in the study and characterization of atherosclerosis. ApoE is a component of the VLDL and LDL particles and functions as an important ligand for LDL receptors and LDL receptor-related proteins. $ApoE^{-/-}$ mice develop marked hyperlipidemia (high levels of circulating VLDL and LDL particles) and early and spontaneous atherosclerosis, even when fed a standard low fat diet. ApoE is also synthesized by monocytes and it plays a role in reverse cholesterol transport from peripheral tissue, affecting then the cholesterol removal from the atherosclerotic lesions [119]. The atherosclerotic lesions developed by $ApoE^{-/-}$ mice present with similar characteristics to those observed in humans, growing from fatty streaks to advanced, necrotized, multilayered lesions [120–124]. $ApoE^{-/-}$ mice have been used by our laboratory in several studies to investigate the link between diabetes and the progression of atherosclerosis [125–127]. Another mouse model has also helped to expand the study of atherosclerosis, the low density lipoprotein receptor knockout ($Ldlr^{-/-}$) mouse. Under a low fat diet or normal chow diet, $Ldlr^{-/-}$ mice show a modest alteration in plasma cholesterol levels and the atherosclerosis development is quite limited. However, when fed a western-type diet, $Ldlr^{-/-}$ mice show a clear increase of plasma cholesterol levels, a lipoprotein profile more similar to humans than $ApoE^{-/-}$ mice, and advanced atherosclerosis [128, 129].

Currently, there is no perfect mouse model for the study of the diabetic atherosclerosis. However, we count on some mouse models that have been widely used during the last decades. Among those mouse models for T2DM atherosclerosis, we have the ob/ob mice [130, 131] that develop obesity and diabetes. As a result of leptin deficiency there is no hypothalamic suppression of the appetite. Similarly, the db/db mice present no leptin action in the hypothalamus due to a mutation in the leptin receptor [132, 133]. Both models have been crossed to ApoE$^{-/-}$ [134, 135] and Ldlr$^{-/-}$ [136] backgrounds originating diabetic mouse models with accelerated atherosclerosis. Within the mouse models for T1DM atherosclerosis, we have the transgenic mouse model that expresses viral glycoprotein (GP) causing an immune reaction that specifically destroy beta-cells expressing this glycoprotein [137, 138]. This mouse then has been crossed to an Ldlr$^{-/-}$ background producing the Ldlr$^{-/-}$:GP mouse that develops diabetes-induced accelerated atherosclerosis when fed a western-type diet [139]. Hyperglycemia can also be induced chemically in mice through the administration of the aminoglycoside antibiotic streptozotocin (STZ). This has been used for several decades not only in mice but in a range of animals [140, 141]. STZ can be administered intraperitoneally in one large dose or in multiple low doses to induce hyperglycemia. STZ is a DNA alkylating agent that is selectively toxic to pancreatic beta-cells because its uptake is mediated by glucose transporter 2 (GLUT-2) [140]. GLUT-2 is highly expressed in pancreatic beta cells, but also in tubular cells and hepatocytes which explains the damage to kidneys and liver sometimes described

[142–146]. There is some evidence that multiple low dose injections induce limited beta cell death that activates an autoimmune response against the remaining beta cells [147–149]. However both high dose and multiple low dose STZ injection generally induce severe hyperglycemia and insulinopenia. The obvious limitations of the STZ model have led to the need for alternative and practical strategies to induce hyperglycemia in mice. One alternative to chemically-induced hyperglycemia is the $Ins2^{+/Akita}$ mouse or simply Akita mouse, established by Yoshioka et al. (1997) [150]. This mouse carries a point mutation (C96Y) in one of the alleles of the gene for insulin 2. This mutation impedes the formation of a disulfide bond between the A and B chains of insulin, inducing a sensitive conformational change in this protein [151]. The mal-formed insulin is non-functional and the mouse cannot adequately control blood glucose levels. Early reports characterizing the $Ins2^{+/Akita}$ mouse suggested that the accumulation of mutant insulin induced pancreatic beta cell apoptosis by a mechanism involving endoplasmic reticulum (ER) stress [151–153]. These studies suggested that the lack of beta cells caused the hyperglycemia. Subsequent studies have demonstrated that the mutant proinsulin forms aggregates that sequester the wild type proinsulin. This results in the ER retention and ultimate degradation of mutant and native insulin leading to hyperglycemia [154, 155]. Importantly, these later studies suggest the beta cells, although dysfunctional, maintain viability [154, 155].

CHAPTER 2: General Hypothesis and Objectives

2.1 HYPOTHESIS

Diabetes-associated hyperglycemia will alter the structure of the vasa vasorum in hyperglycemic mice. This microvascular disruption will contribute to the accelerated growth of atherosclerotic lesions in the aorta.

2.2 OBJECTIVES

I. To investigate the effect of hyperglycemia on different microvascular beds, such as retina and the vasa vasorum, and to investigate the possible correlation between hyperglycemia-induced microvascular changes and atherosclerosis.

II. To develop and extensively characterize an $ApoE^{-/-}$:$Ins2^{+/Akita}$ mouse model of hyperglycemia-induced accelerated atherosclerosis.

CHAPTER 3: Hyperglycemia is Associated with Impaired Vasa Vasorum Neovascularization and Accelerated Atherosclerosis in Apolipoprotein-E Deficient Mice

KJ Veerman[a]*, DE Venegas-Pino[b,c]*, Y Shi[a], MI Khan[a], HC Gerstein[c,d,e], GH Werstuck[a,b,c]

[a] Thrombosis and Atherosclerosis Research Institute, [b] Department of Biochemistry and Biomedical Sciences, [c] Department of Medicine, [d] Department of Clinical Epidemiology and Biostatistics, [e] Population Health Research Institute, McMaster University, Hamilton, Ontario, Canada

* These authors contributed equally to this study

3.1. FOREWORD

Here we investigate the effects of hyperglycemia on the vasa vasorum and correlates them with the development of atherosclerosis. Normoglycemic ApoE$^{-/-}$ mice have vasa vasorum expansion as atherosclerotic lesions grow. However, hyperglycemic ApoE$^{-/-}$ mice have no significant neovascularization of the vasa vasorum despite the enhanced atherosclerotic development.

This work was published in the journal *Arteriosclerosis*. The experiments in this study were conducted by KJ Veerman and DE Venegas-Pino with assistance from co-authors. The manuscript was written by KJ Veerman, DE Venegas-Pino and Dr. Geoff Werstuck. The content of Chapter 3 is a representation of this publication. The complete reference is as follows:

KJ Veerman*, DE Venegas-Pino*, Y Shi, MI Khan, HC Gerstein, GH Werstuck: Hyperglycemia is Associated with Impaired Vasa Vasorum Neovascularization and Accelerated Atherosclerosis in Apolipoprotein-E Deficient Mice. Atherosclerosis. 2013, 227:250–258.

3.2. ABSTRACT

Objective: A direct correlation between blood glucose levels and the microvascular complications of diabetes is well established. However, the effects of hyperglycemia on the vasa vasorum, a microvascular network which surrounds and supplies the walls of large arteries, is not known. The objective of this study is to investigate the effects of hyperglycemia on the vasa vasorum and to examine correlations between these effects and the development of atherosclerosis in a mouse model.

Methods: The micro- and macrovascular effects of hyperglycemia were examined in streptozotocin-injected apolipoprotein-E deficient ($ApoE^{-/-}$) mice. Retina and aortic sinus were isolated from hyperglycemic mice and normoglycemic controls at 5–20 weeks of age. Retinal and vasa vasorum microvessel densities were quantified and correlated to atherosclerotic lesion development. The expression levels of pro-angiogenic factors including vascular endothelial growth factor (VEGF) and VEGF receptor 2 were examined.

Results: In normoglycemic $ApoE^{-/-}$ mice atherogenesis is associated with vasa vasorum expansion, which likely corresponds to the increasing blood supply

demands of the thickening artery wall. In hyperglycemic ApoE$^{-/-}$ mice there is no significant neovascularization of the vasa vasorum, despite the fact that lesions are significantly larger. This defect may result from a localized deficiency in VEGF.

Conclusions: These findings are the first evidence that hyperglycemia alters the structure of the vasa vasorum. Such microvascular changes directly correlate, and may contribute to, the development and progression of atherosclerosis in hyperglycemic ApoE-deficient mice.

3.3. INTRODUCTION

The vascular complications of diabetes have been conventionally partitioned into two subtypes; microvascular and macrovascular. Microvascular complications manifest clinically as microangiopathies of the retina, kidney, nerve and peripheral vasculature, significantly contribute to diabetic morbidity [1, 2]. Macrovascular complications involve structural and functional changes in the large arteries that predominately involve the accelerated development of atherosclerosis, leading to increased risk of myocardial infarction and stroke [3]. As a consequence, diabetes is associated with a cardiovascular disease (CVD) mortality rate that exceeds 70%, and a 2- to 4-fold increased risk of dying from heart attack or stroke [4]. Traditionally the micro- and macrovascular complications of diabetes have been viewed and treated as distinct and independent disorders. However, accumulating data from epidemiological and pathophysiological studies suggest that these vascular problems are, in fact, closely interrelated. For example,

retinopathy, microalbuminuria, and large-fiber nerve dysfunction have each been independently associated with increased CVD risk in diabetes [2, 5, 6]. Thus, the pathogenesis of diabetes-associated microvascular dysfunction may be mechanistically linked to the pathogenesis of diabetic macrovascular diseases, including atherosclerosis.

Despite the potential relationship between micro- and macrovascular disease, there is a fundamental difference in how these disorders respond to glucose lowering. It is well established that reducing fasting blood glucose levels below 7.0mM significantly decreases the risk of microvascular disease [7]. In contrast, accumulating evidence suggests that normalization of glucose levels improves CVD outcome, a similar blood glucose threshold does not exist for cardiovascular (CV) risk [8]. Data from clinical trials examining the effects of intensive glucose lowering indicate that the relationship between blood glucose levels and CV risk is complex [9, 10].

The vasa vasorum is a distinct microvascular network which surrounds and supplies the cells within the walls of large muscular arteries [11]. A general correlation has been observed between vasa vasorum expansion/neovascularization and atherosclerotic lesion development, and it has been suggested that such neovascularization may play a role in the pathophysiology of atherosclerosis [12]. Experiments performed in $ApoE^{-/-}$ mice have shown that vasa vasorum neovascularization is associated with atherosclerotic plaque growth, and that inhibition of neovascularization reduces plaque size [13]. However, all of these

observations have been reported in non-diabetic/normoglycemic models [12–14]. In fact, very little is known about the potential effects of diabetes and hyperglycemia on the vasa vasorum and the potential role of the vasa vasorum in diabetic atherosclerosis has not been explored. Because the vasa vasorum plays a significant role in vessel wall maintenance, regulating local oxygen delivery and facilitating solute transport in and out of the vascular tissue, its dysfunction may significantly alter the structure, function and/or health of large blood vessels which it supplies.

Based on the established effects of hyperglycemia on several independent microvascular networks, and the established relationship between the vasa vasorum, arterial wall health and atherosclerosis, we hypothesize that diabetes-associated hyperglycemia disrupts the vasa vasorum and that this effect may play a role in the accelerated development of atherosclerosis. To test this hypothesis, we have used an ApoE$^{-/-}$ mouse model. ApoE$^{-/-}$ mice are dyslipidemic, relative to wild type mice, and they spontaneously develop atherosclerotic lesions by approximately 10 weeks of age [15]. Streptozotocin-induced hyperglycemia accelerates the development of atherosclerosis in ApoE$^{-/-}$ mice and significantly larger lesions are observed by 15 weeks of age [16]. We have previously shown that significantly larger atherosclerotic lesions can be detected prior to hyperglycemia-associated increases in plasma lipid levels [16, 17]. These results suggest that, in this model, elevated plasma glucose levels are sufficient to accelerate atherogenesis.

In this study, we use a hyperglycemic ApoE$^{-/-}$ mouse model to investigate the possible effects of hyperglycemia on the vasa vasorum, the underlying alterations in angiogenic mechanisms, and the association of these microvascular defects with the accelerated development of atherosclerosis.

3.4. METHODS

Mouse models

Five week old female ApoE$^{-/-}$ (B6.129P2-ApoE^{tm1Unc}) mice were placed on standard chow diet (TD92078; Harlan Teklad, Madison, WI) and randomized to one of two treatment groups. Hyperglycemia was induced in one group (n = 46) by administering two sets of five low-dose streptozotocin (STZ) injections (30–40mg/kg) as previously described [15]. To control for potential non-specific effects of STZ, a subgroup of STZ mice (n = 10) received a slow-release insulin pellet implant (LinBit, Toronto, ON) at eight weeks of age to normalize glucose levels. The second treatment group (n = 36) was given two sets of five intraperitoneal injections of citrate buffer over the same three week period. Mice were sacrificed at 10, 15, and 20 weeks of age (n = 10–12 per group). An additional group was sacrificed prior to injection, at 5 weeks of age (n = 5). Plasma and tissue samples were collected from each mouse for further examination. All animal procedures were approved by the McMaster University Animal Research Ethics Board.

Histology and immunohistochemistry

Two hours prior to sacrifice, mice were injected with 60mg/kg pimonidazole hydrochloride (Hypoxyprobe^{TM}-1; Hypoxprobe Inc., Burlington, MA). Mice were then anaesthetized with isoflurane, flushed with 1x PBS, and perfusion-fixed with 10% neutral buffered formalin. Upon excision of the heart and ascending aorta, the apex of the heart was sectioned transversely, and the remaining cardiac tissue embedded in paraffin. Using the valve leaflets as a point of orientation, serial sections (4μm) of the aortic root were collected and stained with hematoxylin and eosin for lesion and necrotic core measurement (Supplementary Figure 1, Appendix 1), or with specific antibodies, as indicated, for immunohistochemical and immunofluorescence analysis [16, 18, 19].

Immunohistochemical labeling was performed using standard immunoperoxidase techniques, with biotinylated secondary antibodies, Vectastain ABC Kits (Vector Labs, Burlington, ON), and both DAB (Dako, Burlington, ON) and Nova Red (Vector Labs) chromogenic substrates. Fluorescence staining was performed using secondary antibodies tagged with Alexa 488 and Alexa 594 (Invitrogen, Burlington, ON), followed by DAPI nuclear counterstain.

Primary antibodies that were used include: polyclonal rabbit anti-human von Willebrand Factor (Dako), monoclonal mouse anti-mouse HIF-1 alpha (Novus Biologicals, Oakville, ON), polyclonal rabbit anti-mouse VEGF-A (Santa Cruz Biotechnology, Inc., Santa Cruz CA), monoclonal rabbit anti-mouse VEGF Receptor 2 (Cell Signaling Technology, Pickering, ON), Hypoxyprobe^{TM} mouse

monoclonal antibody (Hypoxyprobe^{TM}), and polyclonal goat anti-mouse CD105 (Endoglin) (R&D Systems). Non-specific staining was controlled by incubating similar aortic sections with pre-immune IgG.

Light microscopy images were captured with an Olympus DP71 digital camera (Olympus America Inc. Center Valley, PA) mounted on a Leitz Laborlux S bright field microscope (Leica Microsystems, Germany). Fluorescence images were taken with an Olympus DP71 digital camera mounted on an Olympus BX41 microscope (Olympus America Inc.).

Quantification of vasa vasorum density

Microvessels were visualized by fluorescent microscopy using an antibody against von Willebrand factor (vWF) to specifically stain the endothelial cells. For statistical analysis of vWF staining, positively labeled vasa vasorum microvessels residing within the intima, media, and adventitia of the aortic root were tallied. Vasa vasorum density was defined as the total number of microvessels within the defined regions per aortic cross-section.

India Ink injection and retinal analysis

Additional control and hyperglycemic ApoE$^{-/-}$ mice of 5, 6, 7, 8, 9, 10 and 15 weeks of age (n = 4 per group) were anaesthetized with isoflurane, flushed with 1x PBS, and perfused with 1–2mL of India Ink. Mouse eyes were excised and retinal flat mounts prepared. Capillary density was estimated using a method

outlined by Browning et al [20]. Briefly, a quantification template comprised of 64 sampling boxes aligned along 8 axes was centered upon the optic disk (Supplemental Figure 2, Appendix 1). The number of vessel intersections with the edges of each sampling box was tallied for central, mid, and peripheral regions of the vasculature. Regional and total capillary densities are presented as the total number of vessel intersections per number of boxes analyzed.

Data analysis and statistics

Data were analyzed by one- or two-way ANOVA and the Bonferroni multiple comparison test for all groups. Data are expressed as arithmetic means ± SEM. For all experiments a p value of 0.05 was considered statistically significant.

3.5. EXPERIMENTAL RESULTS

Hyperglycemia is associated with accelerated development of atherosclerosis at the aortic sinus

Five week old female ApoE$^{-/-}$ mice were given multiple low dose intraperitoneal injections of STZ to induce hyperglycemia. Glucose levels were significantly elevated by 10 weeks of age with a mean blood glucose concentration of 32.3mM compared to 8.5mM in citrate injected controls (p<0.01). Blood glucose levels remained chronically elevated at every subsequent time point examined throughout the course of the study (Table 3.1).

By 15 weeks of age, STZ-induced hyperglycemic ApoE$^{-/-}$ mice developed atherosclerotic lesions at the aortic sinus that were 2X larger in cross-sectional area than normoglycemic controls (Figure 3.1A–C). In addition, hyperglycemic ApoE$^{-/-}$ mice had significantly increased lesion volume in the ascending aorta (Figure 3.1D). Lesions at the sinus reached a maximum area by approximately 20 weeks of age, at which point differences in plaque cross-sectional area at the aortic sinus were no longer significant. Hyperglycemic mice continued to exhibit significantly increased lesion volume as a result of increased plaque growth in the ascending aorta. Plaque composition was analyzed in 15 week old mice by measuring the necrotic cross-sectional area within each atherosclerotic lesion. Lesions from hyperglycemic mice had significantly larger necrotic cores than those isolated from normoglycemic control animals (Figure 3.1E).

To control for any possible effects of STZ-injection that are independent of hyperglycemia, a subgroup of STZ-injected ApoE$^{-/-}$ mice were implanted with slow-release insulin pellets to normalize blood glucose levels. Blood glucose levels in STZ-injected ApoE$^{-/-}$ mice supplemented with insulin were not significantly different than those of normoglycemic ApoE$^{-/-}$ mice (Table 3.1). Lesion cross-sectional area was analyzed in 15 week old mice, as described above. Lesion areas in insulin-supplemented mice were similar in size to age matched, citrate-injected normoglycemic mice (Figure 3.1B).

Table 3.1. Metabolic Parameters. Metabolic parameters of normoglycemic (NG), STZ-induced hyperglycemic (STZ-HG), and STZ-injected, insulin supplemented (STZ+insulin) ApoE$^{-/-}$ and C57Bl/6J mice. Ages and *N* values are indicated. Vasa vasorum density defined as the total number of microvessels per aortic cross section. n = 5–12 mice per group; mean ± SEM.

* $p<0.05$, ** $p<0.01$, *** $p<0.001$ relative to age-matched ApoE$^{-/-}$ NG control; † $p<0.001$ relative to age-matched ApoE$^{-/-}$ STZ-HG.

	5 weeks	*10 weeks*		*15 weeks*			*20 weeks*	
	NG	**NG**	**STZ-HG**	**NG**	**STZ-HG**	**STZ+insulin**	**NG**	**STZ-HG**
Plasma								
glucose (mM)	5.9±0.3	8.5±0.9	32.3±1.4 ***	7.9±0.3	23.0±1.4 ***	9.4±0.8 †	7.7±0.4	26.8±3.1 ***
triglycerides (mM)	0.57±0.06	1.5±0.2	1.5±0.4	0.49±0.04	0.64±0.09	1.7±0.4	0.63±0.08	1.00±0.31
cholesterol (mM)	4.6±0.1	7.6±0.7	9.2±0.6	6.74±0.70	7.0±1.0	9.6±2.1	5.4±1.1	6.3±1.5 *
Tissues								
body weight (g)	14.6±0.4	19.1±0.3	14.5±0.8 ***	20.2±0.4	17.9±0.5 ***	16.7±0.2	19.8±0.8	17.7±0.5 *
lesion area (10^{-2} mm^2)	0	1.1±0.4	0.55±0.21	3.8±0.7	11.4±1.5 **	2.6±0.5 †	16.0±2.0	16.9±2.5
vasa vasorum density	1.8±0.4	6.5±0.5	4.8±0.4 *	8.6±0.7	5.9 ± 0.6 **	7.5±0.9	14.9±1.1	8.3±0.8 **
n	*5*	*12*	*12*	*12*	*12*	*10*	*12*	*12*

Table 3.1

Figure 3.1. Hyperglycemia is associated with accelerated development of atherosclerosis at the aortic sinus in ApoE$^{-/-}$ mice. A) Representative images of haematoxylin and eosin stained aortic cross-sections from 15 week old normoglycemic (NG), STZ-induced hyperglycemic (STZ-HG), and STZ-treated insulin-supplemented (STZ-insulin) ApoE$^{-/-}$ mice. Atherosclerotic lesions (black arrows), lesion thickness (black bars) and aortic lumen (L) are indicated (scale = 100μm). B) Quantification of plaque cross-sectional area at the aortic sinus in 15 week old ApoE$^{-/-}$ mice (NG, STZ-HG and STZ-insulin). Plaque area (C), total plaque volume (D), and necrotic content (E) in 5, 10, 15, and 20 week old normoglycemic and STZ-induced hyperglycemic ApoE$^{-/-}$ mice, as indicated. n = 8–12 mice per group; mean ± SEM. * $p<0.05$, ** $p<0.01$.

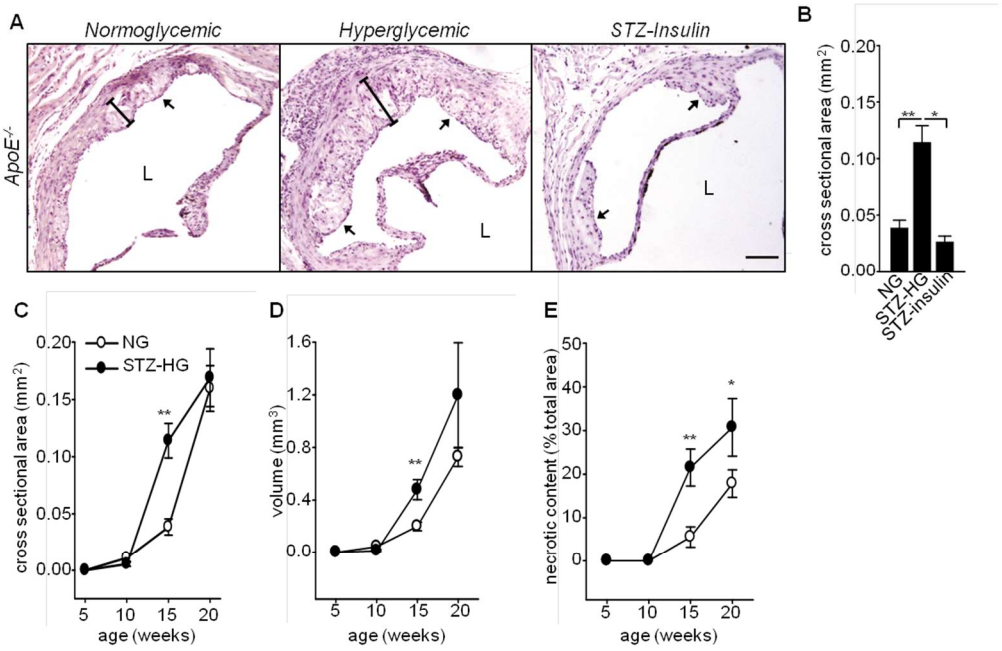
A
Normoglycemic
Hyperglycemic
STZ-Insulin
ApoE-/-
L
L
L
B
cross sectional area (mm2)
0.20
0.15
0.10
0.05
0.00
**
*
NG
STZ-HG
STZ-insulin
C
NG
STZ-HG
cross sectional area (mm2)
0.20
0.15
0.10
0.05
0.00
**
5
10
15
20
age (weeks)
D
volume (mm3)
1.6
1.2
0.8
0.4
0.0
**
5
10
15
20
age (weeks)
E
necrotic content (% total area)
50
40
30
20
10
0
**
*
5
10
15
20
age (weeks)

Figure 3.1

Hyperglycemia is associated with microvascular changes in the retina

We next examined the potential effect of chronic hyperglycemia on the retinal microvasculature in this mouse model. STZ injected hyperglycemic ApoE$^{-/-}$ mice and normoglycemic controls were perfused with India Ink. Retinas were mounted on glass slides and retinal microvessel density was quantified under a light microscope (Figure 3.2). There was a significant reduction in microvessel density in the retinas of 6–8 week old hyperglycemic ApoE$^{-/-}$ mice relative to age-matched normoglycemic controls. After 15 weeks of age a significant expansion of the microvasculature was observed in the retinas of hyperglycemic ApoE$^{-/-}$ mice.

Figure 3.2. Hyperglycemia is associated with microvascular changes in the retina. Representative images of retinal flat mounts from 6 week old normoglycemic (NG) (A) and hyperglycemic (STZ-HG) (B) ApoE$^{-/-}$ mice perfused with India Ink taken at low (left, scale = 500μm) and high (right, scale = 100μm) magnification. *C*) Quantification of retinal microvessel density in NG and STZ-HG ApoE$^{-/-}$ mice, from 5 to 15 weeks of age. n = 4 mice per group; mean ± SEM. * $p<0.05$.

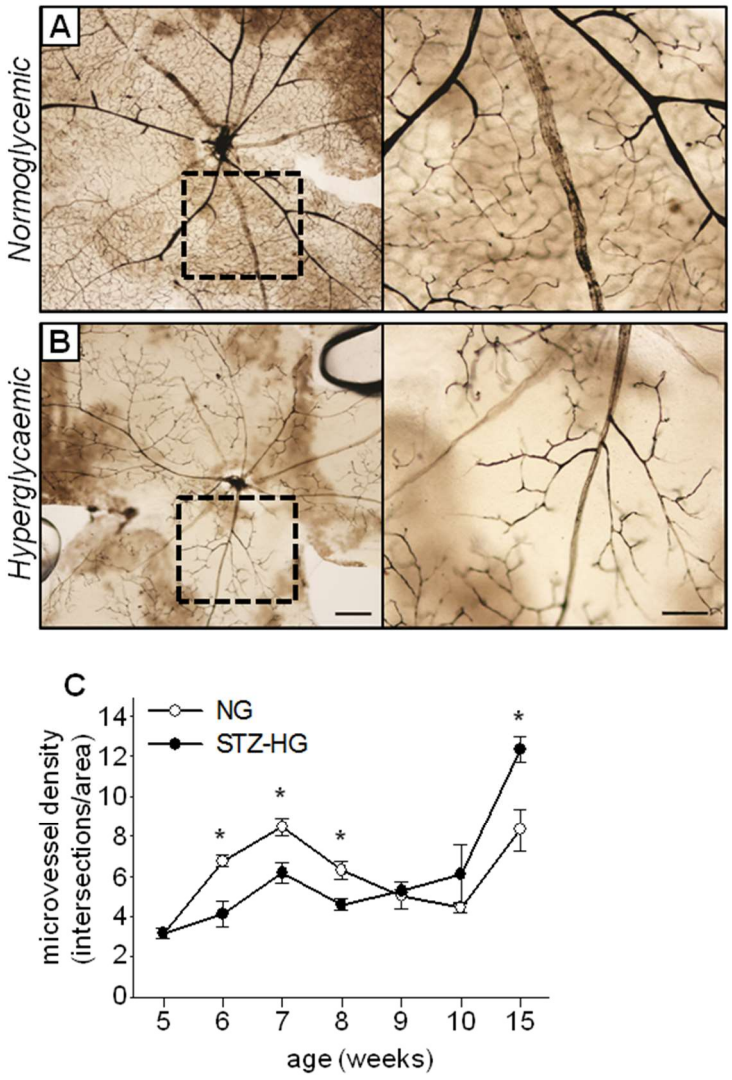
A
Normoglycemic
B
Hyperglycaemic
C
NG
STZ-HG
microvessel density
(intersections/area)
0
2
4
6
8
10
12
14
5
6
7
8
9
10
15
age (weeks)
*
*
*
*

Figure 3.2

Chronic hyperglycemia is associated with vasa vasorum deficiency at the aortic sinus of ApoE$^{-/-}$ mice

To examine the effects of hyperglycemia on the vasa vasorum, cross-sections of aorta from normoglycemic and hyperglycemic ApoE$^{-/-}$ mice were immunostained with an antibody against vWF (Figure 3.3A), a specific endothelial cell (EC) marker. Vasa vasorum density, defined as the total number of microvessels residing within the intima, media, and adventitia per aortic cross-section, was quantified for each experimental group. In normoglycemic ApoE$^{-/-}$ mice, there was a progressive and significant increase in vasa vasorum density at the aortic sinus from 5 to 20 weeks of age (Figure 3.3B). In contrast, hyperglycemic ApoE$^{-/-}$ mice showed a non-significant increase in vasa vasorum density at the aortic sinus over time, and had significantly fewer microvessels relative to normoglycemic controls at each time point examined. STZ-injected ApoE$^{-/-}$ mice that were supplemented with insulin had a vasa vasorum density similar to normoglycemic controls (Figure 3.3D; Table 3.1). Significant changes in vasa vasorum density were not observed in the ascending aorta until 20 weeks of age (Figure 3.3C).

Figure 3.3. Hyperglycemia is associated with reduced vasa vasorum density at the aortic sinus. A) Low (left) and high (right) magnification images of cross-sections of the aortic sinus from 15 week old normoglycemic (NG) and hyperglycemic (STZ-HG) ApoE$^{-/-}$ mice, immunostained with an antibody against vWF. Vasa vasorum microvessels within the arterial wall are indicated (arrows). An image of a representative section stained with a non-immune IgG antibody is provided. (scale = 100μm). Quantification of vasa vasorum density in 5, 10, 15, and 20 week old NG and STZ-HG ApoE$^{-/-}$ mice. Vasa vasorum density defined as the total number of vasa vasorum microvessels residing within the intima, media and adventitia, per aortic cross-section of aortic sinus (B) or ascending aorta (C). n = 8–10 mice per group; mean ± SEM. * $p<0.05$; ** $p<0.01$. D) Quantification of vasa vasorum density at the aortic sinus in 15 week old NG, STZ-HG, and STZ-insulin ApoE$^{-/-}$ mice and, as indicated. n = 6–8 mice per group; mean ± SEM. * $p<0.05$. L = Lumen.

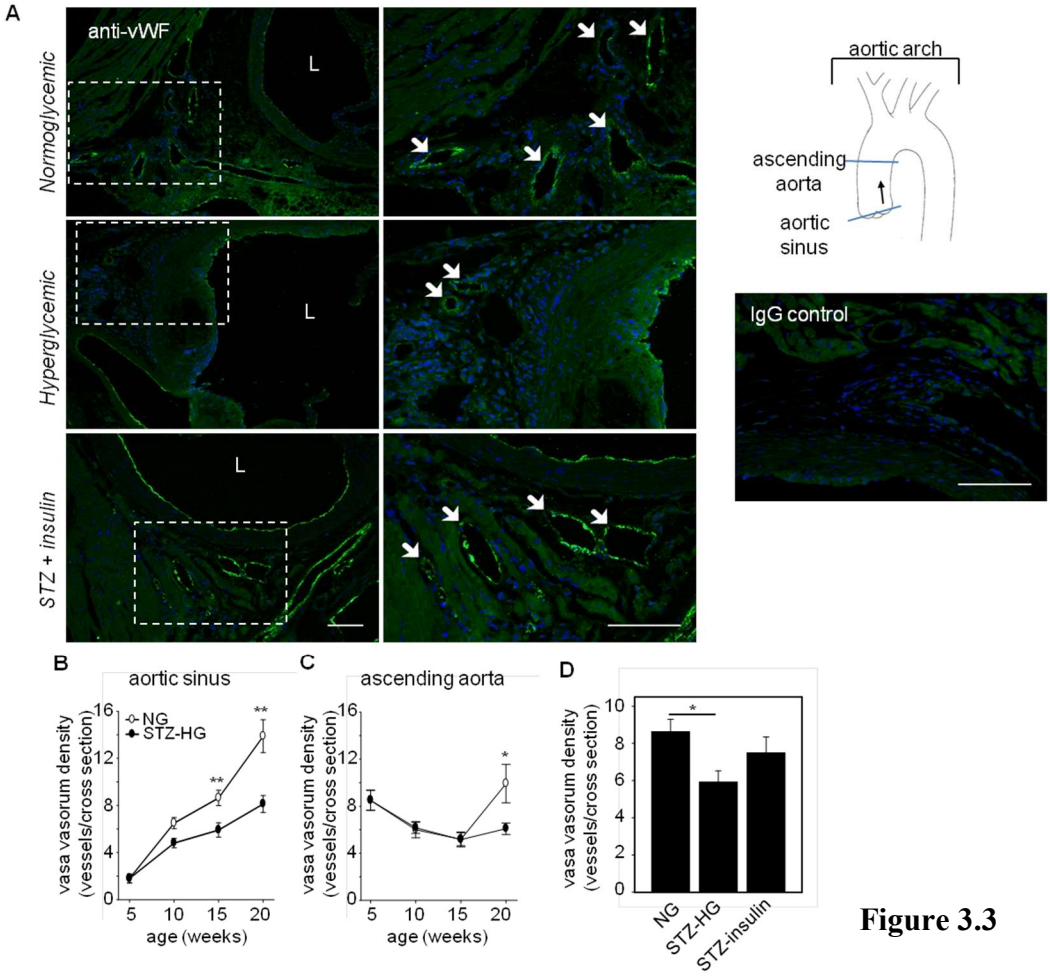
A
anti-vWF
Normoglycemic
Hyperglycemic
STZ + insulin
L
aortic arch
ascending aorta
aortic sinus
IgG control
B
aortic sinus
C
ascending aorta
D
vasa vasorum density (vessels/cross section)
NG
STZ-HG
age (weeks)
STZ-insulin

Figure 3.3

Accelerated atherogenesis is associated with hypoxia and elevated levels of HIF-1α

To investigate the possible role of hypoxia in vasa vasorum neovascularization, 15 week old normoglycemic and hyperglycemic ApoE$^{-/-}$ mice were injected with pimonidazole hydrochloride to detect regions of relative oxygen depletion. As shown in Figure 3.4A, hyperglycemic ApoE$^{-/-}$ mice had more hypoxic cells within the adventitia than normoglycemic controls. Regions staining most intensely for hypoxia were localized directly in atherosclerotic lesions where the vascular wall is the thickest.

HIF-1α protein levels were assessed by immunofluorescence. Serial aortic cross-sections were stained with an antibody against HIF-1α. Relative to normoglycemic controls, hyperglycemic ApoE$^{-/-}$ mice had increased staining for HIF-1α (Figures 3.4B), which is consistent with HIF-1α stabilization under conditions of hypoxia.

Figure 3.4. Hyperglycemia is associated with elevated levels of hypoxia and HIF-1α at the aortic sinus. A) Aortic cross-sections from 15 week old normoglycemic and hyperglycemic ApoE$^{-/-}$ mice stained with an antibody against pimonidazole hydrochloride, an indicator of hypoxia. Arrows indicate positively stained hypoxic cells. B) Cross sections of the aortic root from normoglycemic, hyperglycemic, and STZ-injected insulin supplemented (STZ-insulin) ApoE$^{-/-}$ mice immunostained with an antibody against HIF-1α. Representative images were taken at low (left) and high (right) magnification (scale = 100μm). n = 6–8 mice per group.

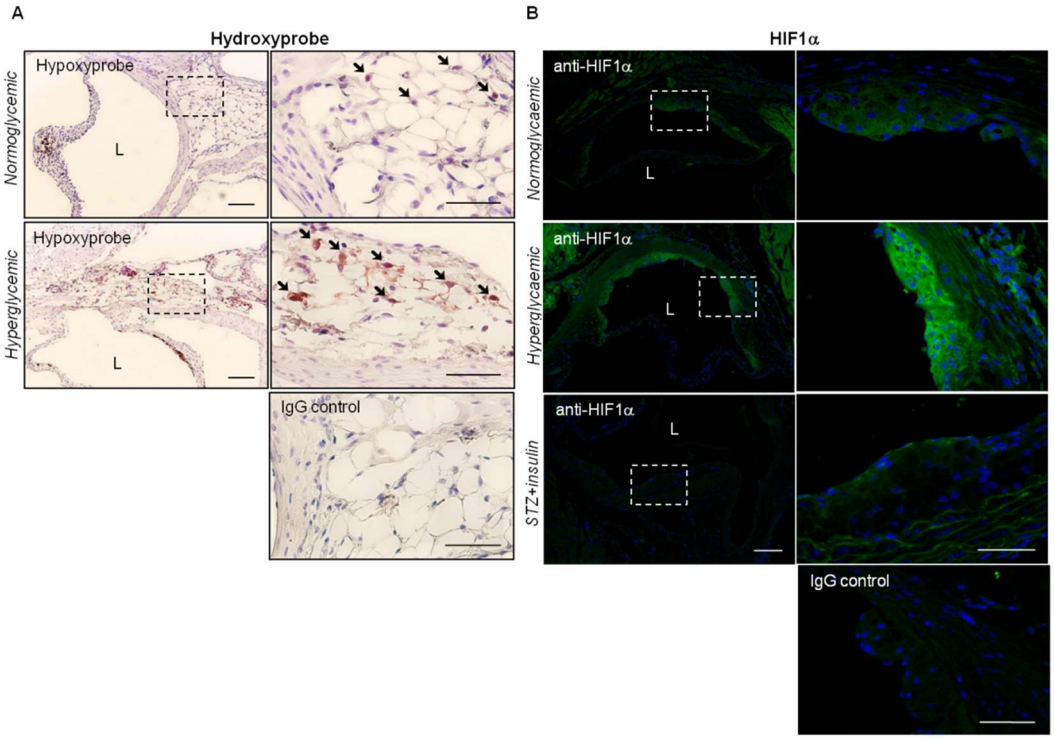
A
Hydroxyprobe
Normoglycemic
Hyperglycemic
Hypoxyprobe
Hypoxyprobe
L
L
IgG control
B
HIF1α
Normoglycaemic
Hyperglycaemic
STZ+insulin
anti-HIF1α
anti-HIF1α
anti-HIF1α
L
L
L
IgG control

Figure 3.4

Hyperglycemic mice show indications of endothelial cell activation at the aortic sinus

To further examine hypoxia-induced endothelial cell activation in our mice, aortic cross-sections from normoglycemic and hyperglycemic ApoE$^{-/-}$ mice were stained with an antibody against endoglin (Figure 3.5A). The total number of endoglin-positive vessels residing within the intima, media, and adventitia was quantified. By 15 weeks of age, hyperglycemic ApoE$^{-/-}$ mice had significantly more endoglin-positive microvessels than normoglycemic controls (Figure 3.5B).

Figure 3.5. Hyperglycemia is associated with endothelial activation. A) Aortic cross-sections from 15 week old normoglycemic (NG) and hyperglycemic (HG) $ApoE^{-/-}$ mice stained with an antibody against endoglin. Endoglin-positive microvessels are indicated by arrows. B) Quantification of endoglin-positive microvessels at the aortic root in 5, 10, 15, and 20 week old NG and STZ-HG $ApoE^{-/-}$ mice. n = 6–9 mice per group; mean ± SEM. * $p<0.05$.

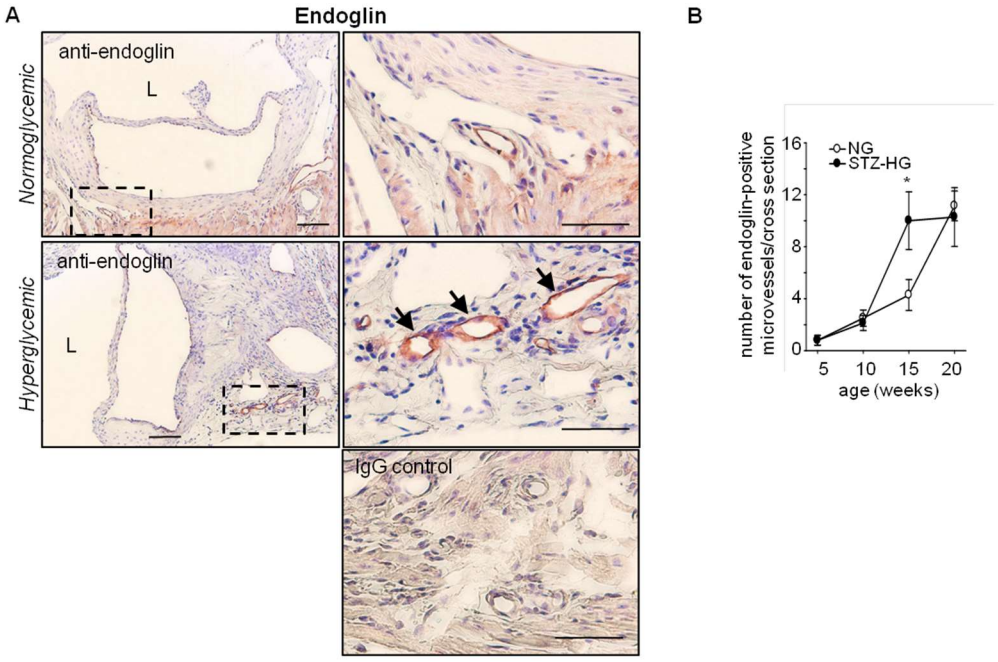
A
Endoglin
anti-endoglin
L
Normoglycemic
anti-endoglin
L
Hyperglycemic
IgG control
B
number of endoglin-positive microvessels/cross section
NG
STZ-HG
*
16
12
8
4
0
5
10
15
20
age (weeks)

Figure 3.5

Hyperglycemic mice have a relative deficiency of VEGF-A and VEGF receptor 2

The protein levels of HIF-1α inducible factors, including VEGF-A and VEGF-R2 were analyzed by immunofluorescence staining of cross sections of aortic sinus from 15 week old normoglycemic and hyperglycemic $ApoE^{-/-}$ mice. Hyperglycemic mice showed decreased staining for VEGF-A (Figure 3.6A, C) within the lesions and surrounding adventitia. VEGF-R2 expression, which is regulated by VEGF-A in an autocrine manner was significantly reduced within the lesions of hyperglycemic mice compared to controls (Figure 3.6B).

Figure 3.6. VEGF-A and VEGF-R2 expressions are reduced in atherosclerotic lesions of hyperglycemic mice. Aortic cross-sections from 15 week old normoglycemic (NG), hyperglycemic (STZ-HG) and insulin-supplemented (STZ-insulin) ApoE$^{-/-}$ mice were immunostained with antibodies against A) VEGF-A or B) VEGF-R2, as indicated. Low (left) and high (right) magnified images are shown (scale = 20μm). C) Quantification of VEGF-A density within the lesion of NG, STZ-HG, and STZ-insulin ApoE$^{-/-}$ mice. n = 6–8 mice per group; mean ± SEM. * $p<0.05$, ** $p<0.01$.

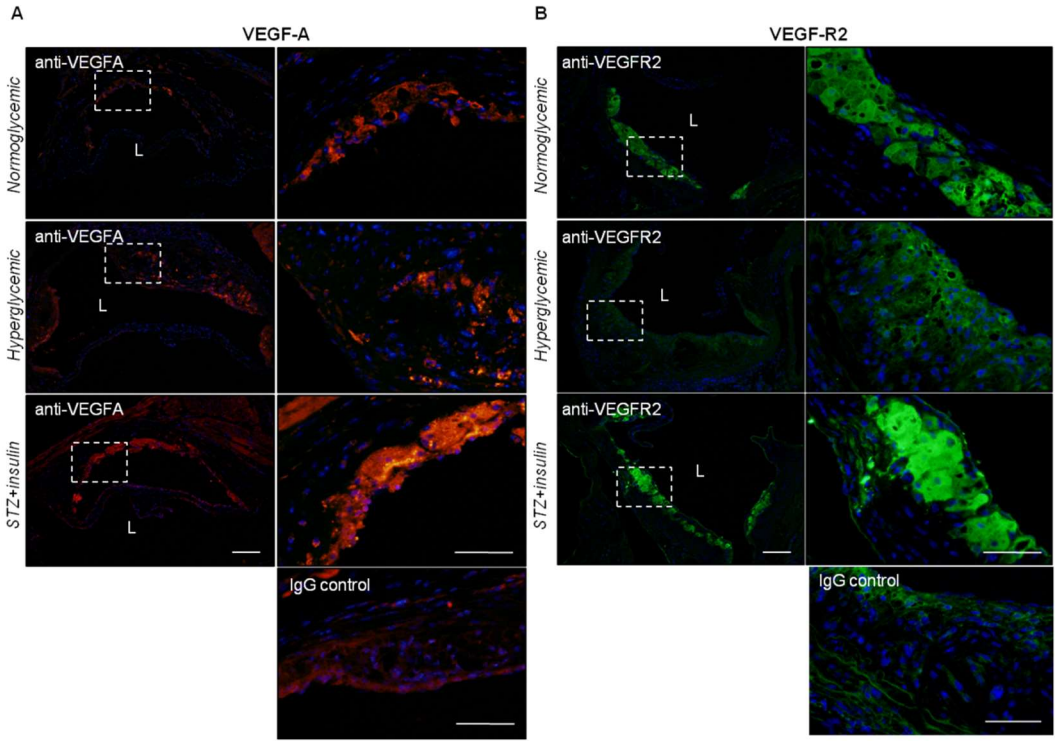
A
VEGF-A
anti-VEGFA
Normoglycemic
Hyperglycemic
STZ+insulin
L
IgG control
B
VEGF-R2
anti-VEGFR2
Normoglycemic
Hyperglycemic
STZ+insulin
L
IgG control

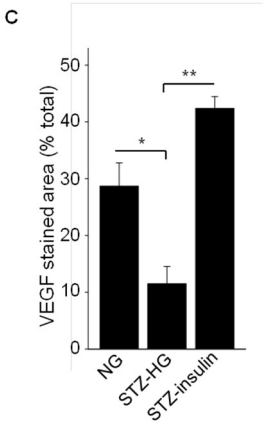
C
VEGF stained area (% total)
50
40
30
20
10
0
*
**
NG
STZ-HG
STZ-insulin

Figure 3.6

3.6. DISCUSSION

Chronic hyperglycemia is associated with both microvascular and macrovascular pathologies. Hyperglycemic ApoE$^{-/-}$ mice have larger and more advanced atherosclerotic lesions at the aortic root relative to normoglycemic ApoE$^{-/-}$ mice. By 15 weeks of age, lesions were >2-fold larger in cross sectional area, volume and necrotic content, relative to age matched controls. The initial acceleration in atherogenesis correlated directly to blood glucose concentrations but not to plasma lipid levels because significant elevations in plasma cholesterol were not observed until 20 weeks of age. This finding was consistent with previous observations in this model [16, 17]. Normalization of blood glucose by supplementation with insulin attenuated lesion development. Hyperglycemic ApoE$^{-/-}$ mice also showed indications of early-onset microvessel deficiencies in the retina. This was followed by significant capillary neovascularization at later time points. Despite the established effects of hyperglycemia on specific microvascular networks, little is known about the potential effects of hyperglycemia on the vasa vasorum. Using this model, we investigated the effects of chronic hyperglycemia on the microvessels of the vasa vasorum.

The effects of hyperglycemia on the microvasculature can lead to excessive neovascularization, as in proliferative diabetic retinopathy [21] and nephropathy [22], or attenuated neovascularization, contributing to impaired coronary collateral vessel development [23], impaired wound healing [24] and transplant rejection in diabetic recipients [25]. The concurrent existence of pro- and anti-

neovascularization responses in diabetes is known as the “angiogenesis paradox”. The effect of hyperglycemia on the vasculature may be dependent upon the tissue/organ being considered as well as the duration of the hyperglycemia. For example, an early complication of diabetes is pre-proliferative diabetic retinopathy, involving pericyte and endothelial cell death leading to retinal ischemia [26]. Excessive retinal neovascularization, or proliferative diabetic retinopathy, is a common complication in more advanced diabetes [6, 21]. Consistent with this pattern, in our model, we observed a deficiency in retinal microvessels in 6–8 week old mice followed by a significant increase in retinal vascularization in 15 week old mice.

In normoglycemic ApoE$^{-/-}$ mice, spontaneous atherosclerotic lesion growth at the aortic sinus was associated with vasa vasorum expansion. High fat diet fed ApoE$^{-/-}$ mice also exhibit accelerated atherosclerosis and increased vasa vasorum neovascularization (see Supplemental Table 1 and Supplemental Figure 3, Appendix 1). These observations are consistent with previously reported results from other studies carried out in non-diabetic mouse models [12–14]. Together, these data support the theory that neovascularization may play a causative role in atherosclerosis by providing new conduits for lipid and inflammatory cell entry, facilitating lesion growth and perhaps predisposing atherosclerotic lesions to intraplaque hemorrhage [12–14].

In contrast, there was no evidence of vasa vasorum expansion in hyperglycemic ApoE$^{-/-}$ mice, despite the development of significantly larger more

advanced atherosclerotic lesions. As a result there was a relative deficiency in vasa vasorum microvessels in the aortic sinus of hyperglycemic mice, compared to age-matched normoglycemic controls, at every time point examined (Figure 3.3B and Supplemental Figure 4, Appendix 1). Normalization of blood glucose levels with insulin restored vasa vasorum density, attenuated atherogenesis, and restored HIF-1α, VEGF-A and VEGF-R2 levels to those seen in control mice. These findings suggest that; i) in addition to affecting the microvascular structure in the retina, conditions of hyperglycemia impair normal vasa vasorum expansion, and ii) neovascularization of the vasa vasorum is not required to support or promote the accelerated development of atherosclerotic lesions in this model.

The function of the vasa vasorum is to facilitate the supply, maintenance, and repair of the healthy arterial wall [11]. Limiting blood flow to the artery wall would presumably lead to tissue hypoxia in the arterial media and adventitia, particularly in regions proximal to arterial damage, where inflammation would increase local oxygen demand [27]. Ischemic injury is known to promote intimal/medial thickening due to vascular smooth muscle cell proliferation and collagen deposition, which may exacerbate lesion growth [28, 29]. In support of this mechanism, we found indications of adventitial hypoxia in our hyperglycemic mice that directly correlate to accelerated atherosclerosis. A deficiency in microvessel density may also impair lipid removal by reverse cholesterol transport, promoting an accumulation of lipids and inflammatory cells, accelerated plaque growth, necrosis, and further hypoxic stimulus [30]. Impaired neo-vasa vasorum

formation has previously been associated with neointimal thickening and reactive oxygen species production in saphenous vein grafts in a diabetic pig model [29].

Conditions of hypoxia are known to trigger angiogenesis by stabilizing HIF-1α and increasing the expression of pro-angiogenic signaling proteins. We observed a significant increase in HIF-1α staining in the lesions of hyperglycemic mice. Endoglin is an auxiliary receptor for the TGF-β family of cytokines, which plays a key role in angiogenesis by regulating EC growth [30], vascular smooth muscle cell development [31], and the production and turnover of extracellular matrix [32]. Since endoglin expression can be induced by hypoxia, upregulation of endoglin in our hyperglycemic ApoE$^{-/-}$ mice suggests that the hypoxia-regulated angiogenic response is at least partially intact. However, we observed a deficiency in the expression of VEGF-A and VEGF-R2 at the aortic sinus. These results are consistent with the findings of Thangarajah et al. (2009) who reported that hypoxia-induced VEGF expression was impaired in a db/db mouse hind limb wound healing model [33]. The authors attributed the impaired VEGF upregulation to hyperglycemia-associated methylglyoxal-induced modification of the transcriptional coactivator, p300, which is essential for HIF-1α-regulated gene expression [34]. This mechanism could explain the decreased expression of the hypoxia-regulated VEGF and VEGF-R2 proteins in the aortas of STZ-induced hyperglycemic ApoE$^{-/-}$ mice. A mechanism involving a hyperglycemia-induced defect in hypoxia-regulated angiogenesis is consistent with the lack of effect on the vasa vasorum in the ascending aorta of ApoE$^{-/-}$ mice, which is relatively resistant

to the development of atherosclerosis. It was only at 20 weeks of age, as the lesion grows up from the aortic sinus, that the deficiency in vasa vasorum neovascularization was significant. Together, these findings suggest that conditions of hyperglycemia disrupt vasa vasorum angiogenesis rather than the maintenance of existing microvessels. Additional studies will be required to verify the molecular mechanisms that underlie these effects. In addition, it will be useful to examine the longer term effects of hyperglycemia on the vasa vasorum to determine if the observed initial deficiencies in the vasa vasorum are followed by proliferative vascularization, analogous to the pathogenesis of diabetic retinopathy.

In summary, using a model of STZ-induced hyperglycemia, we have demonstrated that chronically elevated blood glucose levels are associated with impaired neovascularization of the vasa vasorum. Accelerated development of the atherosclerotic lesion proceeds in hyperglycemic mice despite the vasa vasorum deficiency at the aortic root. In fact, the significant increase in atherosclerotic necrosis and lesion growth may be a direct result of impaired neovascularization. This would imply a protective role for vasa vasorum neovascularization in maintenance of arterial wall health. To our knowledge, this is the first evidence to suggest a potential role for impaired vasa vasorum neovascularization in diabetic atherosclerosis.

3.7. REFERENCES FOR CHAPTER 3

[1] The Diabetes Control and Complications Trial Research Group: The effect of intensive treatment of diabetes on the development and progression of long-term complications in insulin-dependent diabetes mellitus. N Engl J Med. 1993, 329:977–986

[2] UK Prospective Diabetes Study (UKPDS) Group: Intensive blood-glucose control with sulphonylureas or insulin compared with conventional treatment and risk of complications in patients with type 2 diabetes (UKPDS 33). Lancet. 1998, 352:837–853

[3] Beckman JA, Creager MA, Libby P: Diabetes and atherosclerosis: epidemiology, pathophysiology, and management. JAMA. 2002, 287:2570–2581

[4] Haffner SM, Lehto S, Ronnemaa T, Pyorala K, Laakso M: Mortality from coronary heart disease in subjects with type 2 diabetes and in nondiabetic subjects with and without prior myocardial infarction. N Engl J Med. 1998, 339:229–234

[5] Valmadrid CT, Klein R, Moss SE, Klein BE: The risk of cardiovascular disease mortality associated with microalbuminuria and gross proteinuria in persons with older-onset diabetes mellitus. Arch Intern Med. 2000, 160:1093–1100

[6] Juutilainen A, Lehto S, Rönnemaa T, Pyörälä K, Laakso M: Retinopathy predicts cardiovascular mortality in type 2 diabetic men and women. Diabetes Care. 2007, 30:292–299

[7] Klein R, Klein BE, Moss SE: Relationship of glycemic control to diabetic microvascular complications in diabetes mellitus. Ann Intern Med. 1996, 124:90–96

[8] Norhammar A, Tenerz A, Nilsson G, Hamsten A, Efendíc S, Rydén L, Malmberg K: Glucose metabolism in patients with acute myocardial infarction and no previous diagnosis of diabetes mellitus: a prospective study. Lancet. 2002, 359:2140–2144

[9] The ADVANCE Collaborative Group: Intensive Blood Glucose Control and Vascular Outcomes in Patients with Type 2 Diabetes. N Engl J Med. 2008, 358:2560–2572

[10] ACCORD Study Group, Gerstein HC, Miller ME, Genuth S, Ismail-Beigi F, Buse JB, Goff DC Jr, Probstfield JL, Cushman WC, Ginsberg HN, Bigger JT, Grimm RH Jr, Byington RP, Rosenberg YD, Friedewald WT: Long-term effects of intensive glucose lowering on cardiovascular outcomes. N Engl J Med. 2011, 364:818–828

[11] Ritman EL, Lerman A: The dynamic vasa vasorum. Cardiovasc Res. 2007, 75:649–658

[12] Langheinrich AC, Michniewicz A, Sedding DG, Walker G, Beighley PE, Rau WS, Bohle RM, Ritman EL: Correlation of vasa vasorum neovascularization and plaque progression in aortas of apolipoprotein E(-/-)/low-density lipoprotein(-/-) double knockout mice. Arterioscler Thromb Vasc Biol. 2006, 26:347–352

[13] Moulton KS, Vakili K, Zurakowski D, Soliman M, Butterfield C, Sylvin E, Lo KM, Gillies S, Javaherian K, Folkman J: Inhibition of plaque neovascularization reduces macrophage accumulation and progression of advanced atherosclerosis. Proc Natl Acad Sci USA. 2003, 100:4736–4741

[14] Moulton KS, Heller E, Konerding MA, Flynn E, Palinski W, Folkman J: Angiogenesis inhibitors endostatin or TNP-470 reduce intimal neovascularization and plaque growth in apolipoprotein E-deficient mice. Circulation. 1999, 99:1726–1732

[15] Reddick RL, Zhang SH, Maeda N: Atherosclerosis in mice lacking apo E. Evaluation of lesional development and progression. Arterioscler Thromb Vasc Biol. 1994, 14:141–147

[16] Werstuck GH, Khan MI, Femia G, Kim AJ, Tedesco V, Trigatti B, Shi Y: Glucosamine-induced endoplasmic reticulum dysfunction is associated with accelerated atherosclerosis in a hyperglycemic mouse model. Diabetes. 2006, 55:93–101

[17] Khan MI, Pichna BA, Shi Y, Bowes AJ, Werstuck GH: Evidence supporting a role for endoplasmic reticulum stress in the development of atherosclerosis in a hyperglycaemic mouse model. Antioxid Redox Signal. 2009, 11:2289–2298

[18] Paigen B, Morrow A, Holmes PA, Mitchell D, Williams RA: Quantitative assessment of atherosclerotic lesions in mice. Atherosclerosis. 1987, 68:231–240

[19] Shai SY, Sukhanov S, Higashi Y, Vaughn C, Kelly J, Delafontaine P: Smooth muscle cell-specific insulin-like growth factor-1 overexpression in Apoe$^{-/-}$ mice does not alter atherosclerotic plaque burden but increases features of plaque stability. Arterioscler Thromb Vasc Biol. 2010, 30:1916–1924

[20] Browning J, Wylie CK, Gole G: Quantification of oxygen-induced retinopathy in the mouse. Invest Ophthalmol Vis Sci. 1997, 38:1168–1174

[21] Aiello LP, Bursell SE, Clermont A, Duh E, Ishii H, Takagi C, Mori F, Ciulla TA, Ways K, Jirousek M, Smith LE, King GL: Vascular endothelial growth factor-induced retinal permeability is mediated by protein kinase C in vivo and suppressed by an orally effective beta-isoform-selective inhibitor. Diabetes. 1997, 46:1473–1480

[22] Cooper ME, Vranes D, Youssef S, Stacker SA, Cox AJ, Rizkalla B, Casley DJ, Bach LA, Kelly DJ, Gilbert RE: Increased renal expression of vascular endothelial growth factor (VEGF) and its receptor VEGFR-2 in experimental diabetes. Diabetes. 1999, 48:2229–2239

[23] Abaci A, Oguzhan A, Kahraman S, Eryol NK, Unal S, Arinç H, Ergin A: Effect of diabetes mellitus on formation of coronary collateral vessels. Circulation. 1999, 99:2239–2242

[24] Galiano RD, Tepper OM, Pelo CR, Bhatt KA, Callaghan M, Bastidas N, Bunting S, Steinmetz HG, Gurtner GC: Topical vascular endothelial growth factor accelerates diabetic wound healing through increased angiogenesis and by mobilizing and recruiting bone marrow-derived cells. Am J Pathol. 2004, 164:1935–1947

[25] Vasir B, Reitz P, Xu G, Sharma A, Bonner-Weir S, Weir GC: Effects of diabetes and hypoxia on gene markers of angiogenesis (HGF, cMET, uPA and uPAR, TGF-alpha, TGF-beta, bFGF and Vimentin) in cultured and transplanted rat islets. Diabetologia. 2000, 43:763–772

[26] Joussen AM, Poulaki V, Le ML Koizumi K, Esser C, Janicki H, Schraermeyer U, Kociok N, Fauser S, Kirchhof B, Kern TS, Adamis AP: A central role for inflammation in the pathogenesis of diabetic retinopathy. FASEB J. 2004, 18:1450–1452

[27] Parathath S, Mick SL, Feig JE, Joaquin V, Grauer L, Habiel DM, Gassmann M, Gardner LB, Fisher EA: Hypoxia is present in murine atherosclerotic plaques and has multiple adverse effects on macrophage lipid metabolism. Circ Res. 2011, 109:1141–1152

[28] Nakata Y, Shionoya S: Vascular lesions due to obstruction of the vasa vasorum. Nature. 1966, 212:1258–1259

[29] Bloor J, Shukla N, Smith FC, Angelini GD, Jeremy JY: Folic acid administration reduces neointimal thickening, augments neo-vasa vasorum formation and reduces oxidative stress in saphenous vein grafts from pigs used as a model of diabetes. Diabetologia. 2010, 53:980–988

[30] Sviridov D, Nestel P: Dynamics of reverse cholesterol transport: protection against atherosclerosis. Atherosclerosis. 2002, 161:245–254

[31] Mazure NM, Chen EY, Laderoute KR, Giaccia AJ: Induction of vascular endothelial growth factor by hypoxia is modulated by a phosphatidylinositol 3-kinase/Akt signaling pathway in Ha-ras-transformed cells through a hypoxia inducible factor-1 transcriptional element. Blood. 1997, 90:3322–3331

[32] Carvalho RL, Jonker L, Goumans MJ, Larsson J, Bouwman P, Karlsson S, Dijke PT, Arthur HM, Mummery CL: Defective paracrine signalling by TGFbeta in yolk sac vasculature of endoglin mutant mice: a paradigm for hereditary haemorrhagic telangiectasia. Development. 2004, 131:6237–6247

[33] Blobe GC, Schiemann WP, Lodish HF: Role of transforming growth factor beta in human disease. N Engl J Med. 2000, 342:1350–1358

[34] Thangarajah H, Yao D, Chang EI, Shi Y, Jazayeri L, Vial IN, Galiano RD, Du XL, Grogan R, Galvez MG, Januszyk M, Brownlee M, Gurtner GC: The molecular basis for impaired hypoxia-induced VEGF expression in diabetic tissues. Proc Natl Acad Sci USA. 2009, 106:13505–13510

CHAPTER 4: Sex-Specific Differences in an ApoE$^{-/-}$:Ins2$^{+/Akita}$ Mouse Model of Accelerated Atherosclerosis

DE Venegas-Pino, PW Wang, HK Stoute, NA Singh-Pickersgill, BY Hong, MI Khan, Y Shi, GH Werstuck

From the Departments of Biochemistry and Biomedical Sciences (D.E.V.P., G.H.W.), Medicine (H.K.S., G.H.W.), and the Thrombosis and Atherosclerosis Research Institute (D.E.V.P., H.K.S., P.W.W., N.A.S.P., B.Y.H., M.I.K., Y.S., G.H.W.), McMaster University, Hamilton, Ontario, Canada

4.1 FOREWORD

Here we establish, characterize and manipulate a new model of hyperglycemia-induced atherosclerosis: the ApoE$^{-/-}$:Ins2$^{+/Akita}$ mouse. We describe sex-specific differences of the ApoE$^{-/-}$:Ins2$^{+/Akita}$ mouse model. Male ApoE$^{-/-}$:Ins2$^{+/Akita}$ mice develop chronic hyperglycemia and accelerated atherosclerosis. Castration slows atherosclerosis in ApoE$^{-/-}$:Ins2$^{+/Akita}$ mice but enhances it in normoglycemic controls. Female ApoE$^{-/-}$:Ins2$^{+/Akita}$ mice are only transiently hyperglycemic but still present with accelerated atherosclerosis. Ovariectomized ApoE$^{-/-}$:Ins2$^{+/Akita}$ mice are chronically hyperglycemic and show indications of advanced atherosclerosis.

This work was published in the journal *The American Journal of Pathology,* and the content of this chapter 4 is a representation of that manuscript. The experiments in this study were conducted by Daniel E. Venegas-Pino with

assistance from the co-authors. The manuscript was written by Daniel E. Venegas-Pino in collaboration with Dr. Geoff Werstuck. The complete reference is as follows:

Venegas-Pino DE, Wang P, Stoute HK, Singh-Pickersgill NA, Hong BY, Khan MI, Shi Y, Werstuck GH: Sex-Specific Differences in an ApoE$^{-/-}$:Ins2$^{+/Akita}$ Mouse Model of Accelerated Atherosclerosis. Am J Pathol. 2015, 186:67–77.

4.2 ABSTRACT

Diabetic patients have a 2- to 4-fold increased risk of cardiovascular disease (CVD). Despite a vast amount of research, the underlying mechanisms that predispose individuals with diabetes to the development of CVD are unclear. To further our understanding of how diabetes promotes atherosclerosis we have established, characterized and manipulated a new model of hyperglycemia-induced atherosclerosis: the ApoE$^{-/-}$:Ins2$^{+/Akita}$ mouse. All mice were fed a standard chow diet. Male ApoE$^{-/-}$:Ins2$^{+/Akita}$ mice developed chronic hyperglycemia which significantly accelerated atherosclerosis. Female ApoE$^{-/-}$:Ins2$^{+/Akita}$ mice presented hyperglycemia that normalized by 15 weeks of age. Despite the transient hyperglycemia, advanced atherosclerosis was observed at 15 weeks of age compared to ApoE$^{-/-}$ females. To better understand these differences, subsets of mice were castrated or ovariectomized at 5 weeks of age. Castrated ApoE$^{-/-}$:Ins2$^{+/Akita}$ mice showed a reduction in blood glucose levels which correlated with

the amelioration of atherosclerosis. Interestingly, castrated normoglycemic ApoE$^{-/-}$ mice developed larger atherosclerotic lesions than sham-operated controls. Ovariectomized ApoE$^{-/-}$:Ins2$^{+/Akita}$ mice presented chronic hyperglycemia and atherosclerosis appeared to be advanced. We have characterized the distinctive sex-specific phenotypes exhibited by the ApoE$^{-/-}$:Ins2$^{+/Akita}$ mouse model and present evidence for the action of sex hormones on pancreatic beta-cell function and the vasculature that affect the regulation of blood glucose levels and the development of atherosclerosis. This model will provide a test bed to further delineate these effects.

4.3 INTRODUCTION

A strong correlation exists between diabetes mellitus (DM) and the prevalence and severity of large vessel disease. Angiographic and autopsy studies have reported that, compared to nondiabetic patients, people with diabetes have a greater degree of both high grade and subclinical atherosclerosis, the underlying cause of most coronary artery disease [1, 2]. DM is associated with a cardiovascular disease mortality rate that exceeds 70%, and diabetic patients have a 2- to 4-fold increased risk of dying from myocardial infarction or stroke [3].

Our understanding of the molecular mechanisms that link diabetes to the accelerated development and progression of atherosclerosis is complicated by the interdependence of circulating glucose and insulin concentrations, as well as the close association of DM with other cardiovascular risk factors, including

dyslipidemia, obesity and hypertension [4]. To facilitate the investigation and identification of the relevant molecular mechanisms and pathways, several different mouse models of diabetes-induced atherosclerosis have been developed. The majority of these models involve the induction of hyperglycemia, in the presence or absence of insulin resistance, in dyslipidemic, atherosclerosis-prone apolipoprotein E deficient ($ApoE^{-/-}$) or low density lipoprotein receptor deficient ($Ldlr^{-/-}$) mice [5].

The most common, and direct, strategy to induce hyperglycemia in rodents and other experimental animals, has been through a single, or multiple, intraperitoneal injections of streptozotocin (STZ). STZ is a DNA alkylating agent that is selectively toxic to pancreatic beta cells, resulting in severe insulinopenia [6]. Many studies have shown that STZ-induced hyperglycemia can promote atherosclerosis in $ApoE^{-/-}$ mice [7–10]. However, there are several disadvantages associated with the use of STZ including; i) possible toxicity to other tissues and organs [11, 12], ii) the severity of the hyperglycemia [7, 8], and iii) the potential for subsequent beta cell regeneration [13].

The $Ins2^{+/Akita}$ mouse represents a genetic alternative to chemically induced hyperglycemia. This mouse carries a point mutation (C96Y) in one allele of the *insulin 2* gene, which disrupts a disulfide bond between the insulin A and B chains. The resulting proinsulin polypeptide cannot be properly processed and therefore accumulates, causing endoplasmic reticulum (ER) stress and beta cell dysfunction [14]. It has been postulated that ER stress-induced beta cell death is the major cause

of insulinopenia in $Ins2^{+/Akita}$ mice. Subsequent studies have suggested that the formation of mutant proinsulin-derived aggregates sequester the wild type proinsulin, leading to ER retention and degradation of mutant and wild type proinsulin, as the underlying cause of the decrease in circulating insulin and development of hyperglycemia [15–19].

We have independently created an $ApoE^{-/-}$:$Ins2^{+/Akita}$ mouse strain in a C57BL/J6 genetic background and have carried out an extensive characterization of this strain. In this report we show that glucose regulation and atherosclerotic progression varies significantly between male and female $ApoE^{-/-}$:$Ins2^{+/Akita}$ mice. We use castration and ovariectomy to expose the roles played by sex hormones in the development of hyperglycemia and atherosclerosis.

4.4 MATERIALS AND METHODS

Mice

Male $ApoE^{+/+}$:$Ins2^{+/Akita}$ mice (Jackson Laboratory) were crossed with female $ApoE^{-/-}$:$Ins2^{+/+}$ mice. The resulting male $ApoE^{+/-}$:$Ins2^{+/Akita}$ offspring were crossed with female $ApoE^{-/-}$:$Ins2^{+/+}$ mice. The male $ApoE^{-/-}$:$Ins2^{+/Akita}$ offspring produced from this cross and female $ApoE^{-/-}$:$Ins2^{+/+}$ were set up as breeding pairs to produce the $ApoE^{-/-}$:$Ins2^{+/Akita}$ and control $ApoE^{-/-}$:$Ins2^{+/+}$ littermates that were used in the following experiments. Genotypes were confirmed by PCR using primers specific for *Ins2* and *ApoE* genes (Supplemental Figure 1, Appendix 2). Primers used were Ins2: forward, 5'-TGCTGATGCCCTGGCCTGCT-3', and

reverse, 5'-TGGTCCCACATATGCACATG-3'; and ApoE: forward, 5'-GCCGCCCCGACTGCATCT-3', WT reverse, 5'-TGTGACTTGGGAGCTCTGCAGC-3', and KO reverse, 5'-GCCTAGCCGAGGGAGAGCCG-3'. The restriction enzyme Fnu4HI was used to identify the presence of the $Ins2^{Akita}$ mutation. All the mice used in this study were fed a standard chow diet (2018 Teklad Global 18 % Protein Rodent Diet; Harlan Teklad) *ad libitum* with free access to water. Atherosclerosis was assessed at 5, 15 and 25 weeks of age in male $ApoE^{-/-}$ (n = 25), male $ApoE^{-/-}$:$Ins2^{+/Akita}$ (n = 25), female $ApoE^{-/-}$ (n = 21) and female $ApoE^{-/-}$:$Ins2^{+/Akita}$ (n = 25) mice. For castration and ovariectomy experiments, mice were stratified by glucose levels and body weight, and then randomly allocated into each group. All the animal procedures were approved by the McMaster University Animal Research Ethics Board.

Castration

Five-week-old mice were anaesthetized with isoflurane and administered a dose of buprenorphine (100µl of a 0.015mg/mL solution) for pain control. A 5mm incision was made through the skin along the midline of the scrotal sac. After crossing the skin, another 5mm incision was made on the left side on the scrotal sac membrane. The left testis was then dissected. The incision made on the scrotal sac membrane and the skin was then sutured. The process was repeated to remove the right testis (n = 12 $ApoE^{-/-}$ and 12 $ApoE^{-/-}$:$Ins2^{+/Akita}$ mice). Identical incisions were made on the sham-operated mice, but testicles were not removed (n = 9 $ApoE^{-/-}$ and

8 $ApoE^{-/-}$:$Ins2^{+/Akita}$ mice). After surgery, mice recovered on a heating bed, to stabilize corporal temperature, and were returned to sterile cages where they were monitored daily.

Ovariectomy

Five-week-old mice were anaesthetized with isoflurane and administered a dose of buprenorphine for pain control. Hair was removed from the incision site and skin was cleaned with 70% ethanol. A 10mm lateral incision was made through the skin of the left side of the back. After crossing the skin, another 10mm incision was made to cross the muscle layer. The ovary and oviduct were located and the ovary was removed. Then the muscle and skin incisions were sutured. The process was repeated to remove the right ovary (n = 8 $ApoE^{-/-}$ and 9 $ApoE^{-/-}$:$Ins2^{+/Akita}$ mice). Identical incisions were made on the sham-operated groups, but ovaries were not removed (n = 7 $ApoE^{-/-}$ and 9 $ApoE^{-/-}$:$Ins2^{+/Akita}$ mice). After surgery, mice recovered on a heating bed, to stabilize corporal temperature, and were returned to sterile cages where they were monitored daily.

Harvesting and storing

Mice were anesthetized with isoflurane and blood was extracted. Mice were sacrificed by cervical dislocation and the vasculature was rinsed with 5mL of 0.9% saline. Liver and fat pad were removed and the vasculature was perfusion fixed

with 10% neutral buffered formalin (NBF). The heart, pancreas and aorta were extracted. All the organs were stored in 10% NBF at room temperature.

Analysis of atherosclerosis

Paraffin-embedded hearts were sectioned with a microtome and 4.5μm serial sections from the aortic sinus were collected on glass slides until atherosclerotic lesions were no longer observed. Sections were stained with hematoxylin and eosin (Sigma) and lesion areas and volumes were determined, as previously described [20]. The necrotic core of the atherosclerotic lesions was estimated by Masson's trichrome staining (Sigma) [21]. Calcified lesion areas were detected and quantified by von Kossa staining [22]. Smooth muscle cell (SMC) and macrophage/foam cells were quantified in the atherosclerotic lesions by immunofluorescent staining for α-actin (Santa Cruz Biotechnology) and Mac-3 (BD Pharmingen), respectively. All images were captured with an Olympus DP71 digital camera (Olympus) mounted on a Leitz Laborlux S bright field microscope (Leica Microsystems), and assessed using Image J software.

***En face* aortas**

The fixed aortas were cleaned of surrounding muscle and adventitial fat. They were longitudinally opened and stained for lipid content with Sudan IV (Sigma). Images of the whole aorta were captured using a L320 digital camera

(Nikon) and the percentage of the atherosclerotic area was assessed using Image J software.

Analysis of pancreata

Paraffin-embedded pancreata were sectioned (6µm thick) and consecutive sections were collected on glass slides. The antibody against GADD153 (Santa Cruz Biotechnology) was utilized to detect the percentage of cells under ER stress [23]. Images were taken with an Olympus DP72 digital camera (Olympus) mounted on an Olympus BX41 microscope (Olympus).

Analysis of plasma

Nonfasting and fasting (6 hours) blood glucose levels were measured using a glucometer (LifeScan). Plasma lipid levels were determined in nonfasting and fasting conditions using the colorimetric diagnostic kit for total cholesterol and triglyceride (Thermal DMA). Fasting plasma lipoproteins were separated by fast protein liquid chromatography, and total cholesterol was measured in each fraction. ELISA kits were used to measure insulin (Crystal Chem), estradiol (Calbiotech), progesterone and testosterone (ALPCO) under fasting conditions.

Surrogate indexes of beta cell function, insulin resistance and sensitivity were calculated from fasting blood glucose and plasma insulin concentrations as follows: HOMA-%β = $[(20 * I_0) / (G_0 - 3.5)]$ where G_0 is fasting glucose (mmol/l) and I_0 is fasting insulin (µIU/ml); HOMA-IR = $[(G_0 * I_0) / 22.5]$ where G_0 is fasting

glucose (mmol/l) and I_0 is fasting insulin (μIU/ml); and QUICKI = [1 / (log(I_0) + log(G_0))] where I_0 is fasting insulin (μIU/ml) and G_0 is fasting glucose (mg/dl) [24, 25].

Oral glucose tolerance test (OGTT) and peritoneal insulin tolerance test (PITT)

Independent groups of mice were prepared for OGTT and PITT in male $ApoE^{-/-}$ (n = 11) and $ApoE^{-/-}$:$Ins2^{+/Akita}$ (n = 15) or female $ApoE^{-/-}$ (n = 12) and $ApoE^{-/-}$:$Ins2^{+/Akita}$ (n = 12) mice. 20-week-old mice were fasted for 4 hours and then blood samples were collected from the tail vein. After the first collection (time 0), glucose (Sigma) (2g/kg body weight of a 200mg/mL solution) was administrated by oral gavage and blood samples were collected at time points of 15, 30, 60 and 120 minutes. Glucose levels were determined using a colorimetric glucose assay reagent (Sigma).

For PITT, 20-week-old mice were fasted for 4 hours and then blood glucose levels were measured with a glucometer (time 0). After the first measurement, bovine insulin (Sigma) was then injected intraperitoneally (0.75U/kg body weight of a 200mU/mL solution) and blood glucose was measured at time points of 15, 30, 60 and 120 minutes.

Data analysis

Data were analyzed by Student t-test to compare two groups. To compare multiple groups, one or two-way ANOVA was used, followed by the Bonferroni multiple comparison test between all groups. Data are expressed as arithmetic means ± SEM. For all experiments a *p value* of 0.05 was considered statistically significant. * $p<0.05$; ** $p<0.01$; *** $p<0.001$.

4.5 RESULTS

Sex effects on hyperglycemia in ApoE$^{-/-}$:Ins2$^{+/Akita}$ mice

Male and female ApoE$^{-/-}$:Ins2$^{+/Akita}$ mice developed hyperglycemia spontaneously by 5 weeks of age relative to age matched ApoE$^{-/-}$ controls. Nonfasting blood glucose levels for 5-week-old male mice were 20.4±1.1mM vs. 8.7±0.4mM ($p<0.001$), respectively. For female mice blood glucose levels were 18.0±1.1mM vs. 8.8±0.2mM ($p<0.001$). Hyperglycemia was sustained for the entire lifespan of the male mice. The blood glucose levels of female ApoE$^{-/-}$:Ins2$^{+/Akita}$ mice normalized by 15 weeks of age (Figure 4.1A). Normalization of blood glucose in female ApoE$^{-/-}$:Ins2$^{+/Akita}$ mice was at least partially dependent on ApoE-deficiency as blood glucose levels in heterozygous ApoE$^{+/-}$:Ins2$^{+/Akita}$ females remained significantly elevated at 15 weeks of age (Supplemental Figure 2, Appendix 2).

OGTT and PITT were performed at 20 weeks of age. Male ApoE$^{-/-}$:Ins2$^{+/Akita}$ mice were clearly glucose intolerant (Figure 4.1B) and also exhibited an

impaired response to exogenous insulin (Figure 4.1C). Female ApoE$^{-/-}$:Ins2$^{+/Akita}$ mice showed marginally impaired glucose tolerance and normal insulin sensitivity (Figure 4.1B–C). In addition to chronic hyperglycemia, male ApoE$^{-/-}$:Ins2$^{+/Akita}$ mice also developed enhanced hypercholesterolemia (Figure 4.1D), but showed no defined changes in triglycerides (Figure 4.1E) by 25 weeks of age. There were no differences in plasma lipid levels in female ApoE$^{-/-}$:Ins2$^{+/Akita}$ mice relative to ApoE$^{-/-}$ controls (Figure 4.1D–E).

At the end of the study, the average body weight of the hyperglycemic male mice was 5 g less than male ApoE$^{-/-}$ controls (Figure 4.1F). The hyperglycemic male mice had virtually no epididymal fat pad (Figure 4.1G). There was no significant difference in liver weight between the male hyperglycemic mice compared to controls (data not shown). Transiently hyperglycemic ApoE$^{-/-}$:Ins2$^{+/Akita}$ and normoglycemic ApoE$^{-/-}$ female mice presented similar metabolic parameters throughout the study (Figure 4.1F–G).

Figure 4.1. Analysis of metabolic parameters in male and female ApoE$^{-/-}$:Ins2$^{+/Akita}$ mice and age matched controls. (A) Nonfasting blood glucose levels (n = 8–12/group). (B) OGTT (n = 4–5/group). (C) PITT (n = 7–10/group). (D) Nonfasting plasma cholesterol and (E) triglycerides (n = 5–11/group). (F) Body weight (n = 8–12/group). (G) Fat pad (n = 6–12/group).

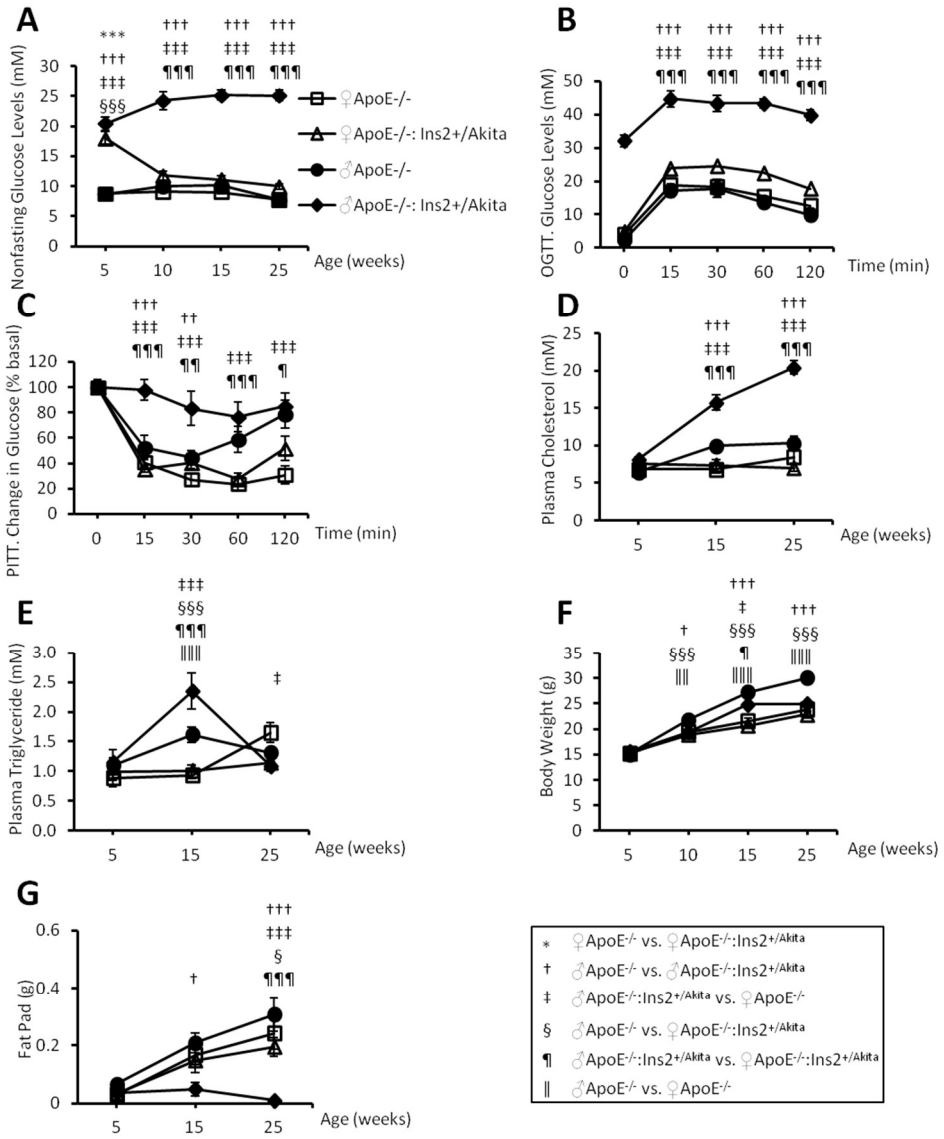
A
Nonfasting Glucose Levels (mM)
Age (weeks)
♀ApoE-/-
♀ApoE-/-: Ins2+/Akita
♂ApoE-/-
♂ApoE-/-: Ins2+/Akita
B
OGTT. Glucose Levels (mM)
Time (min)
C
PITT. Change in Glucose (% basal)
Time (min)
D
Plasma Cholesterol (mM)
Age (weeks)
E
Plasma Triglyceride (mM)
Age (weeks)
F
Body Weight (g)
Age (weeks)
G
Fat Pad (g)
Age (weeks)
* ♀ApoE-/- vs. ♀ApoE-/-:Ins2+/Akita
† ♂ApoE-/- vs. ♂ApoE-/-:Ins2+/Akita
‡ ♂ApoE-/-:Ins2+/Akita vs. ♀ApoE-/-
§ ♂ApoE-/- vs. ♀ApoE-/-:Ins2+/Akita
¶ ♂ApoE-/-:Ins2+/Akita vs. ♀ApoE-/-:Ins2+/Akita
‖ ♂ApoE-/- vs. ♀ApoE-/-

Figure 4.1

Accelerated atherosclerosis in ApoE$^{-/-}$:Ins2$^{+/Akita}$ mice

Atherosclerosis was analyzed in 5-, 15- and 25-week-old male and female ApoE$^{-/-}$ and ApoE$^{-/-}$:Ins2$^{+/Akita}$ mice. No atherosclerotic lesions were detected in any of the 5-week-old mice (data not shown). Atherosclerotic lesions in the aortic sinus of 15-week-old male ApoE$^{-/-}$:Ins2$^{+/Akita}$ mice were relatively small and not significantly different compared to controls (Supplemental Figure 3A, Appendix 2). However, the examination of the whole aortas revealed an increase of lipid accumulation, predominantly in the aortic arch of the hyperglycemic male mice (Supplemental Figure 3B, Appendix 2). At 25 weeks of age, hyperglycemic male ApoE$^{-/-}$:Ins2$^{+/Akita}$ mice presented with advanced atherosclerosis when compared to age and sex matched normoglycemic ApoE$^{-/-}$ controls. Atherosclerotic lesion volume from male ApoE$^{-/-}$:Ins2$^{+/Akita}$ mice was at least 4X larger (p<0.001) in the aortic sinus (Figure 4.2A). Similarly, *en face* aortas from male ApoE$^{-/-}$:Ins2$^{+/Akita}$ mice showed 3X (p<0.05) more atherosclerotic lesion area (Figure 4.2B).

Transiently hyperglycemic female ApoE$^{-/-}$:Ins2$^{+/Akita}$ mice developed accelerated atherosclerosis in the aortic sinus compared to female ApoE$^{-/-}$ controls, at 15 weeks of age (p<0.01) (Figure 4.2C). A similar trend was observed when the whole aortas were examined for lipid accumulation (Figure 4.2D). Lesion volume in the aortic sinus (Supplemental Figure 3C, Appendix 2) and lipid accumulation in the descending aorta (Supplemental Figure 3D, Appendix 2) increased in female ApoE$^{-/-}$ and ApoE$^{-/-}$:Ins2$^{+/Akita}$ mice by 25 weeks of age, however there were no longer statistically significant differences in area or volume.

Figure 4.2. Chronically hyperglycemic male ApoE$^{-/-}$:Ins2$^{+/Akita}$ and transiently hyperglycemic female ApoE$^{-/-}$:Ins2$^{+/Akita}$ mice develop accelerated atherosclerosis. (A) Atherosclerotic lesion area and volume were quantified in the aortic sinus (n = 12/group) and (B) lipid accumulation was determined in *en face* aortas with Sudan-IV staining (n = 5/group) in 25-week-old male mice. (C) Atherosclerotic lesion area and volume were quantified in the aortic sinus (n = 9–10/group) and (D) lipid accumulation was determined in *en face* aortas with Sudan-IV staining (n = 9–10/group) in 15-week-old female mice.

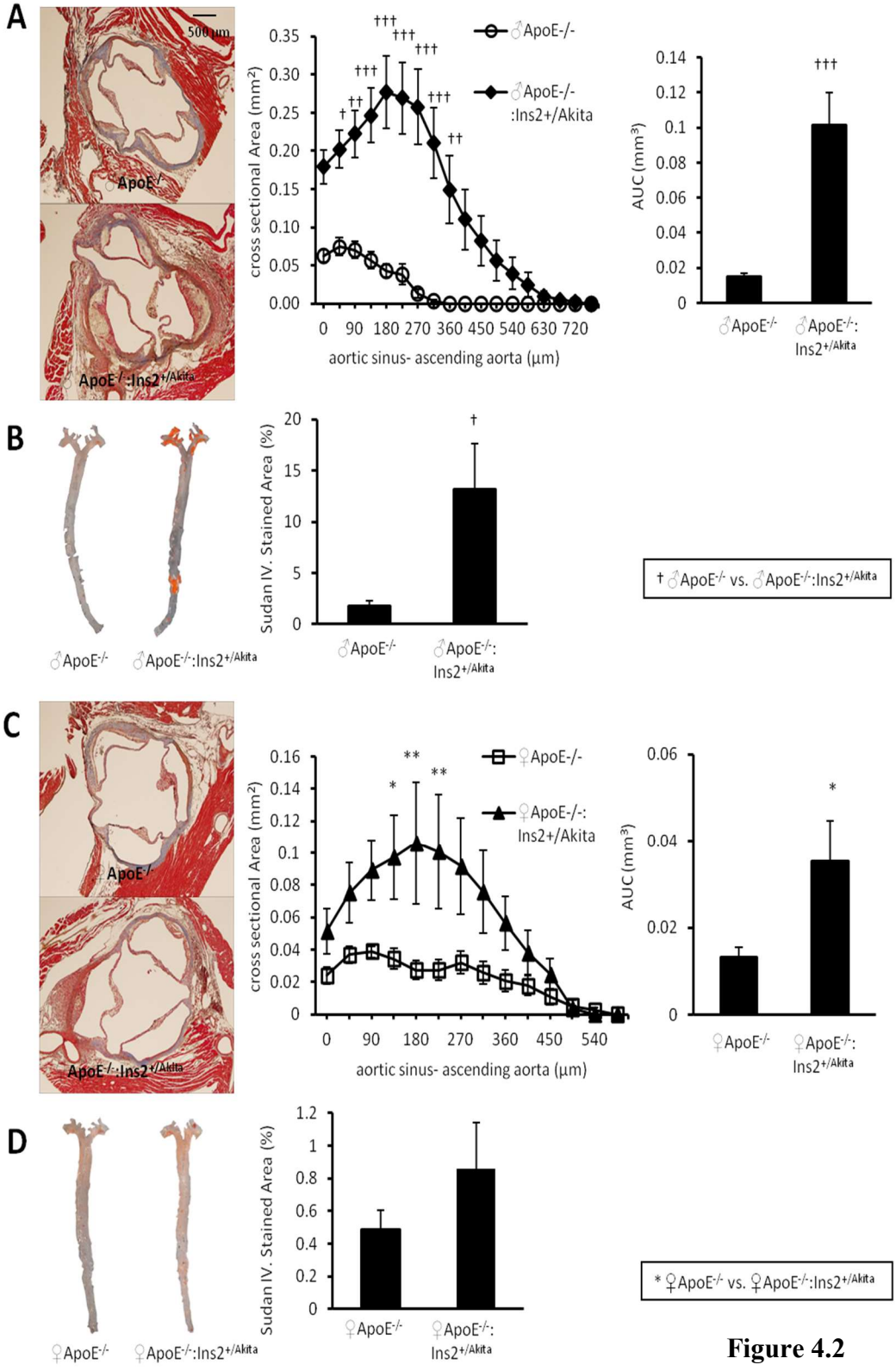
A
500 µm
♂ApoE-/-
♂ApoE-/-:Ins2+/Akita
cross sectional Area (mm²)
aortic sinus- ascending aorta (µm)
AUC (mm³)
B
Sudan IV. Stained Area (%)
† ♂ApoE-/- vs. ♂ApoE-/-:Ins2+/Akita
C
♀ApoE-/-
♀ApoE-/-:Ins2+/Akita
D
* ♀ApoE-/- vs. ♀ApoE-/-:Ins2+/Akita

Figure 4.2

Ovariectomized ApoE$^{-/-}$:Ins2$^{+/Akita}$ mice develop chronic hyperglycemia

To further examine the effects of sex, ApoE$^{-/-}$:Ins2$^{+/Akita}$ and ApoE$^{-/-}$ mice were ovariectomized (Ovx) at 5 weeks of age. Sham-operated female ApoE$^{-/-}$:Ins2$^{+/Akita}$ and ApoE$^{-/-}$ mice were used as controls. In contrast to the transient hyperglycemia observed in female ApoE$^{-/-}$:Ins2$^{+/Akita}$-Sham mice, ovariectomized ApoE$^{-/-}$:Ins2$^{+/Akita}$ mice remained hyperglycemic for the duration of the study (Figure 4.3A). Examination of the pancreatic islets of 25-week-old mice showed that ovariectomization resulted in a significant increase of GADD153-stained nuclei (40% stained nuclei/islet) (Figure 4.3B). Consistent with this finding, beta cell function, evaluated by HOMA-%β (Supplemental Figure 4A, Appendix 2), and the glucose-induced insulin secretion (Supplemental Figure 5, Appendix 2) were impaired in the ovariectomized group. HOMA-IR and QUICKI indexes were also significantly altered in the ovariectomized ApoE$^{-/-}$:Ins2$^{+/Akita}$ mice relative to sham-operated controls (Figure 4.3C and Supplemental Figure 4B, Appendix 2). Ovariectomization had no significant effect on fasting blood glucose levels, GADD153 expression, insulin sensitivity or beta cell function in the ApoE$^{-/-}$ control mice (Figure 4.3A–C and Supplemental Figure 4A–B, Appendix 2).

Examination of other metabolic parameters showed no significant differences in body weight, fat pad, liver weight, or plasma lipid levels between 25-week-old ApoE$^{-/-}$:Ins2$^{+/Akita}$-Ovx and ApoE$^{-/-}$:Ins2$^{+/Akita}$-Sham mice (Figure 4.3D–G and Supplemental Figure 6A, Appendix 2). 25-week-old ApoE$^{-/-}$-Ovx mice showed a significant increase of body weight respect to all the other groups (Figure

4.3D). This increase of body weight was accompanied by an increase in epididymal fat pad (Figure 4.3E) but no changes in liver weight (Supplemental Figure 6A, Appendix 2). ApoE$^{-/-}$-Ovx mice also had increased fasting plasma cholesterol levels (Figure 4.3F) that correlated with an elevation of the VLDL-cholesterol and LDL-cholesterol peaks (Supplemental Figure 7A, Appendix 2). As expected, ovariectomized mice had significantly reduced plasma estrogen (estradiol) and progesterone levels compared to sham-operated controls (Supplemental Figure 8A–B, Appendix 2).

Figure 4.3. Female ApoE$^{-/-}$:Ins2$^{+/Akita}$ mice develop chronic hyperglycemia after ovariectomy. (A) Fasting blood glucose levels in ovariectomized (Ovx) and sham-operated (Sham) mice (n = 7–9/group). (B) GADD153 expression in pancreatic islets at 25 weeks of age (n = 3/group). (C) HOMA-IR (n = 4–6/group). (D) Body weight progression, (E) fat pad weight, (F) fasting plasma cholesterol and (G) triglycerides at 25 weeks of age (n = 7–9/group).

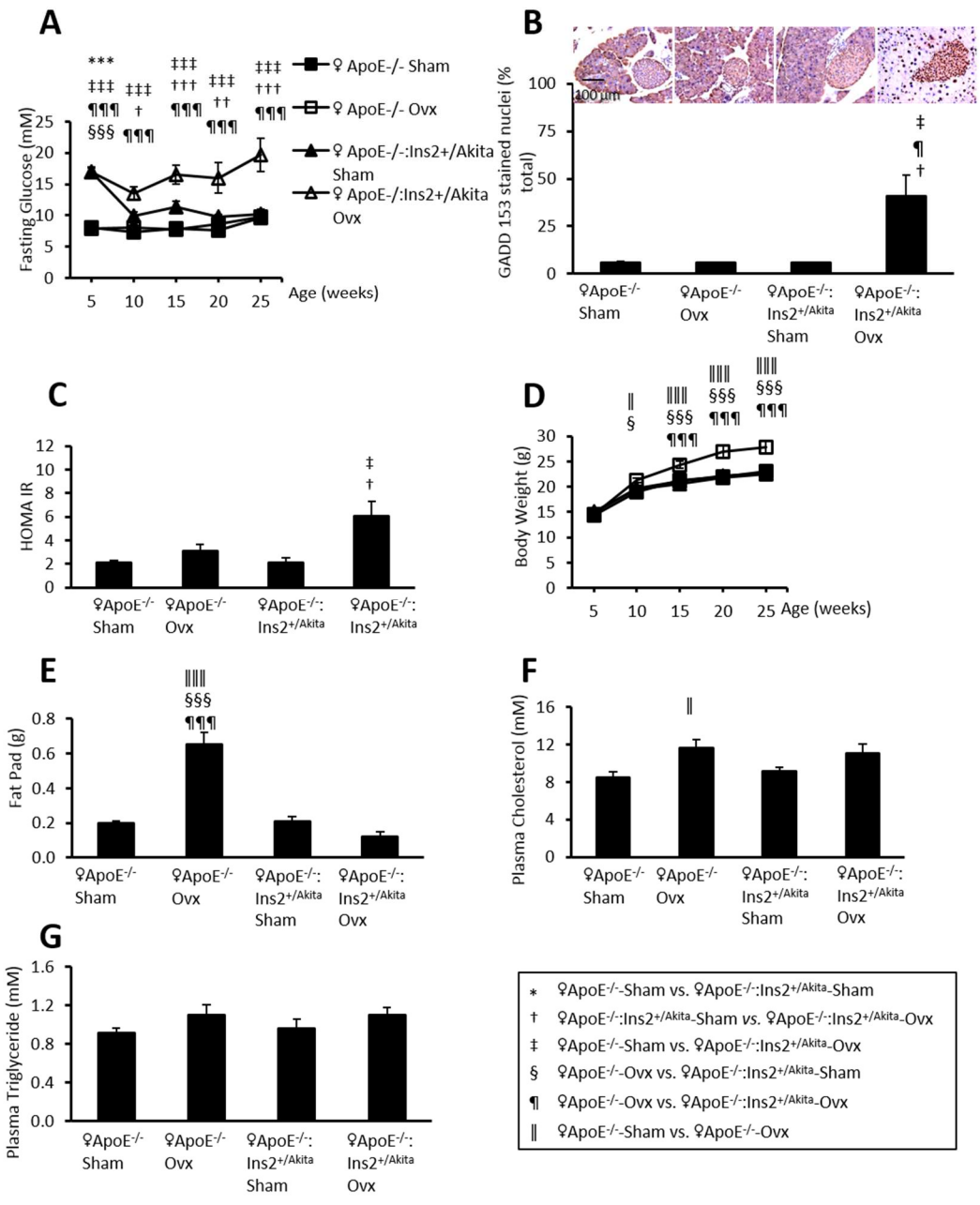
A
Fasting Glucose (mM)
Age (weeks)
♀ ApoE-/- Sham
♀ ApoE-/- Ovx
♀ ApoE-/-:Ins2+/Akita Sham
♀ ApoE-/:Ins2+/Akita Ovx
B
GADD 153 stained nuclei (% total)
100 µm
♀ApoE-/- Sham
♀ApoE-/- Ovx
♀ApoE-/-: Ins2+/Akita Sham
♀ApoE-/-: Ins2+/Akita Ovx
C
HOMA IR
D
Body Weight (g)
Age (weeks)
E
Fat Pad (g)
F
Plasma Cholesterol (mM)
G
Plasma Triglyceride (mM)
* ♀ApoE-/--Sham vs. ♀ApoE-/-:Ins2+/Akita-Sham
† ♀ApoE-/-:Ins2+/Akita-Sham vs. ♀ApoE-/-:Ins2+/Akita-Ovx
‡ ♀ApoE-/--Sham vs. ♀ApoE-/-:Ins2+/Akita-Ovx
§ ♀ApoE-/--Ovx vs. ♀ApoE-/-:Ins2+/Akita-Sham
¶ ♀ApoE-/--Ovx vs. ♀ApoE-/-:Ins2+/Akita-Ovx
‖ ♀ApoE-/--Sham vs. ♀ApoE-/--Ovx

Figure 4.3

Ovariectomized ApoE$^{-/-}$:Ins2$^{+/Akita}$ mice developed advanced atherosclerosis

No differences in atherosclerosis were observed at the aortic sinus among 25-week-old ovariectomized and sham-operated mice (Figure 4.4A, Supplemental Figure 9A and Supplemental Figure 10A, Appendix 2). However, the atherosclerotic lesions found in 25-week-old ApoE$^{-/-}$:Ins2$^{+/Akita}$-Ovx mice showed a trend toward larger necrotic cores (Figure 4.4B) and increased artery calcification (Figure 4.4C). Similarly, examination of *en face* aortas showed that 25-week-old ApoE$^{-/-}$:Ins2$^{+/Akita}$-Ovx mice presented with increased atherosclerotic area in the descending aorta (Figure 4.4D).

Figure 4.4. Ovariectomized ApoE$^{-/-}$:Ins2$^{+/Akita}$ mice have more advanced atherosclerotic lesions than sham-operated controls. (A) Atherosclerotic lesion area and volume (n = 7–9/group), (B) necrotic core (n = 7–9/group), (C) calcification in the aortic sinus (n = 7–9/group) and (D) lipid accumulation in *en face* aortas (n = 7–9/group) were quantified in 25-week-old female mice.

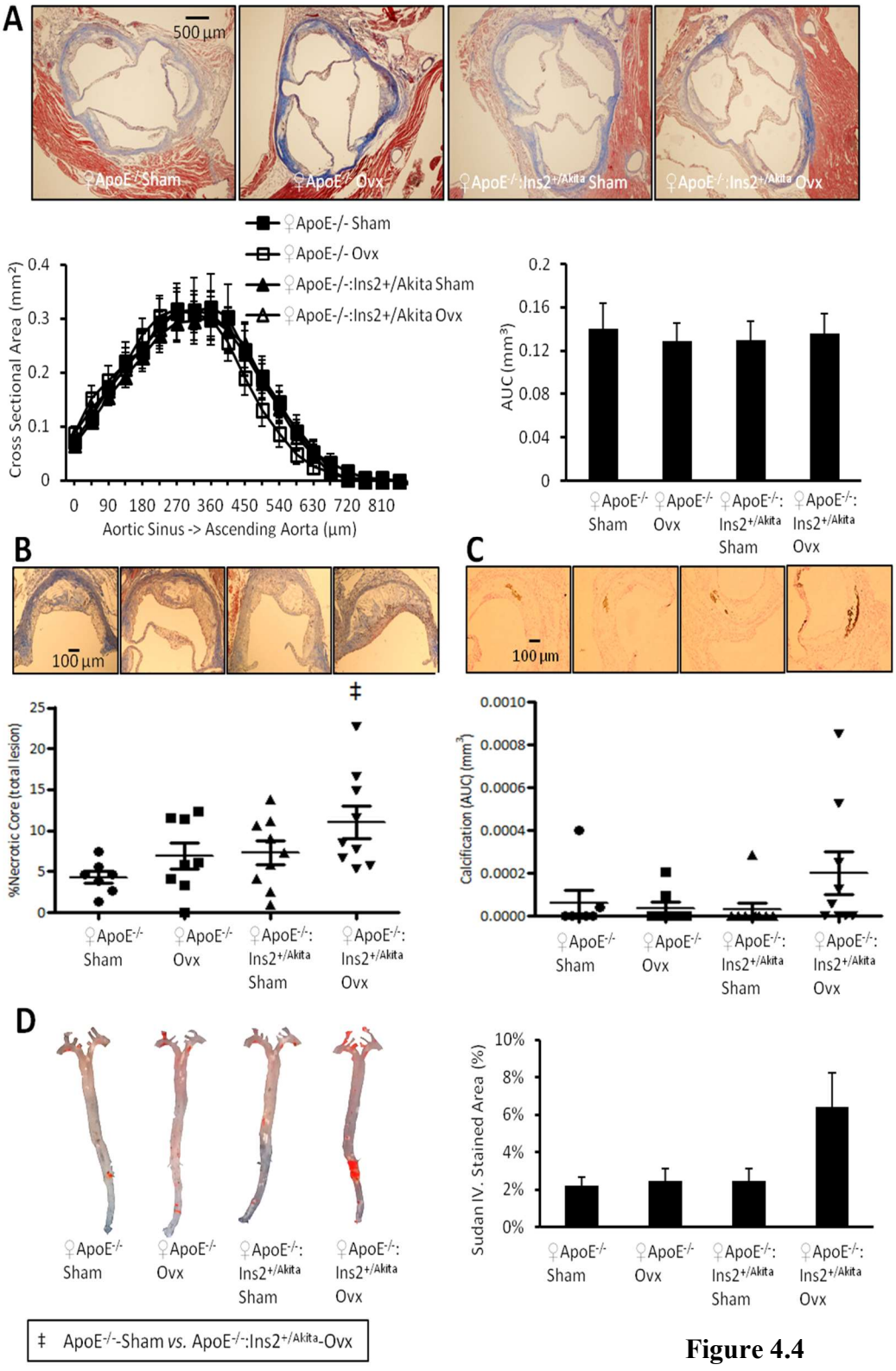
A
500 µm
♀ApoE-/- Sham
♀ApoE-/- Ovx
♀ApoE-/-:Ins2+/Akita Sham
♀ApoE-/-:Ins2+/Akita Ovx
♀ApoE-/- Sham
♀ApoE-/- Ovx
♀ApoE-/-:Ins2+/Akita Sham
♀ApoE-/-:Ins2+/Akita Ovx
Cross Sectional Area (mm²)
0 0.1 0.2 0.3 0.4
0 90 180 270 360 450 540 630 720 810
Aortic Sinus -> Ascending Aorta (µm)
AUC (mm³)
0 0.04 0.08 0.12 0.16 0.2
♀ApoE-/- Sham
♀ApoE-/- Ovx
♀ApoE-/-: Ins2+/Akita Sham
♀ApoE-/-: Ins2+/Akita Ovx
B
100 µm
%Necrotic Core (total lesion)
0 5 10 15 20 25
‡
♀ApoE-/- Sham
♀ApoE-/- Ovx
♀ApoE-/-: Ins2+/Akita Sham
♀ApoE-/-: Ins2+/Akita Ovx
C
100 µm
Calcification (AUC) (mm²)
0.0000 0.0002 0.0004 0.0006 0.0008 0.0010
♀ApoE-/- Sham
♀ApoE-/- Ovx
♀ApoE-/-: Ins2+/Akita Sham
♀ApoE-/-: Ins2+/Akita Ovx
D
♀ApoE-/- Sham
♀ApoE-/- Ovx
♀ApoE-/-: Ins2+/Akita Sham
♀ApoE-/-: Ins2+/Akita Ovx
Sudan IV. Stained Area (%)
0% 2% 4% 6% 8% 10%
♀ApoE-/- Sham
♀ApoE-/- Ovx
♀ApoE-/-: Ins2+/Akita Sham
♀ApoE-/-: Ins2+/Akita Ovx
‡ ApoE-/--Sham vs. ApoE-/-:Ins2+/Akita-Ovx

Figure 4.4

Castration reduces blood glucose levels in ApoE$^{-/-}$:Ins2$^{+/Akita}$ mice

Male ApoE$^{-/-}$:Ins2$^{+/Akita}$ and ApoE$^{-/-}$ mice were castrated (Cx) at 5 weeks of age. After the surgery, ApoE$^{-/-}$:Ins2$^{+/Akita}$-Cx mice presented with a moderate but significant decrease in fasting glucose levels when compared to male ApoE$^{-/-}$:Ins2$^{+/Akita}$-Sham mice. At 25 weeks of age this reduction in blood glucose was no longer observed (Figure 4.5A). In 25-week-old male ApoE$^{-/-}$:Ins2$^{+/Akita}$ mice, castration did not alter the percentage of GADD153-positive nuclei in pancreatic islets (Figure 4.5B). Beta cell function, evaluated by HOMA-%β index, was significantly impaired in both the sham-operated and castrated ApoE$^{-/-}$:Ins2$^{+/Akita}$ mice (Supplemental Figure 4C, Appendix 2). However, castration did result in an improved HOMA-IR and QUICKI indexes (Figure 4.5C and Supplemental Figure 4D, Appendix 2). In ApoE$^{-/-}$ mice, castration had no effect on fasting blood glucose levels, the percentage of GADD153-positive nuclei, insulin resistance or sensitivity, and beta cell function (Figure 4.5A–C and Supplemental Figure 4C–D, Appendix 2).

Castration did not affect body weight of 25-week-old ApoE$^{-/-}$:Ins2$^{+/Akita}$-Cx mice (Figure 4.5D), but they did recover the capability to store fat in the abdominal cavity (Figure 4.5E). In addition, these mice presented a decrease of liver weight (Supplemental Figure 6B, Appendix 2) which was accompanied by lower plasma cholesterol levels (Figure 4.5F). Consistent with these findings, there was a reduction of the VLDL-cholesterol and LDL-cholesterol peaks in the lipid profile (Supplemental Figure 7B, Appendix 2). 25-week-old ApoE$^{-/-}$-Cx mice had reduced

body weight, epididymal fat pad and liver weight (Figure 4.5D–E and Supplemental Figure 6B, Appendix 2). No changes in plasma lipids were detected (Figure 4.5F–G and Supplemental Figure 7B, Appendix 2). Castration effectively reduced plasma testosterone levels. However, testosterone levels were already significantly reduced in the hyperglycemic ApoE$^{-/-}$:Ins2$^{+/Akita}$-Sham relative to normoglycemic ApoE$^{-/-}$-Sham mice (Supplemental Figure 8C, Appendix 2).

Figure 4.5. Blood glucose levels are reduced in male $ApoE^{-/-}$:$Ins2^{+/Akita}$ mice after castration. (A) Fasting blood glucose levels in castrated (Cx) and sham-operated (Sham) mice. (n = 8–12/group). (B) GADD153 expression in pancreatic islets (n = 3/group). (C) HOMA-IR (n = 4–6/group) (D) Body weight progression, (E) fat pad weight, (F) fasting plasma cholesterol and (G) triglycerides at 25 weeks of age (n = 7–12/group).

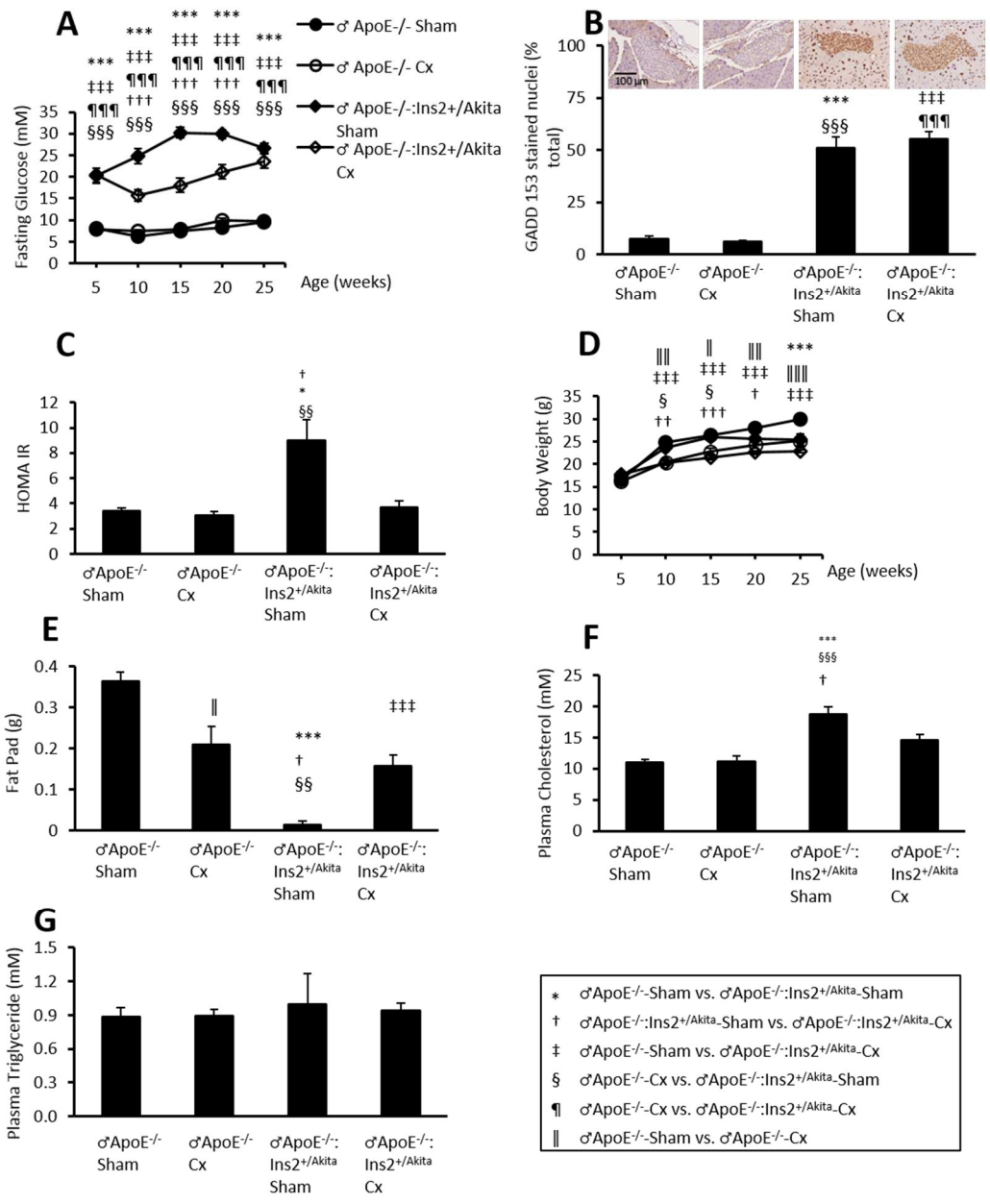
A
Fasting Glucose (mM)
Age (weeks)
♂ ApoE-/- Sham
♂ ApoE-/- Cx
♂ ApoE-/-:Ins2+/Akita Sham
♂ ApoE-/-:Ins2+/Akita Cx
B
GADD 153 stained nuclei (% total)
100 µm
♂ApoE-/- Sham
♂ApoE-/- Cx
♂ApoE-/-: Ins2+/Akita Sham
♂ApoE-/-: Ins2+/Akita Cx
C
HOMA IR
D
Body Weight (g)
Age (weeks)
E
Fat Pad (g)
F
Plasma Cholesterol (mM)
G
Plasma Triglyceride (mM)
* ♂ApoE-/--Sham vs. ♂ApoE-/-:Ins2+/Akita-Sham
† ♂ApoE-/-:Ins2+/Akita-Sham vs. ♂ApoE-/-:Ins2+/Akita-Cx
‡ ♂ApoE-/--Sham vs. ♂ApoE-/-:Ins2+/Akita-Cx
§ ♂ApoE-/--Cx vs. ♂ApoE-/-:Ins2+/Akita-Sham
¶ ♂ApoE-/--Cx vs. ♂ApoE-/-:Ins2+/Akita-Cx
‖ ♂ApoE-/--Sham vs. ♂ApoE-/--Cx

Figure 4.5

Atherosclerosis is reduced in castrated ApoE$^{-/-}$:Ins2$^{+/Akita}$ mice

At 25 weeks of age, the atherosclerotic lesions in the castrated ApoE$^{-/-}$:Ins2$^{+/Akita}$ mice were significantly smaller at the aortic sinus (Figure 4.6A). In addition, these lesions were less advanced, having smaller necrotic cores (Figure 4.6B), less calcification (Figure 4.6C) and a reduction in the number of SMCs but not macrophages (Supplemental Figure 9B and Supplemental Figure 10B, Appendix 2), relative to the sham-operated ApoE$^{-/-}$:Ins2$^{+/Akita}$ mice. Descending aortas of ApoE$^{-/-}$:Ins2$^{+/Akita}$-Cx mice had significantly less atherosclerosis relative to sham-operated controls (Figure 4.6D). Conversely, the castration in the ApoE$^{-/-}$ mice significantly accelerated the development of atherosclerosis (Figure 4.6A–B and Supplemental Figure 9B, Appendix 2).

Figure 4.6. Castration reduces atherosclerotic development in $ApoE^{-/-}$:$Ins2^{+/Akita}$ mice. (A) Atherosclerotic lesion area and volume (n = 8–12/group), (B) necrotic core (n = 7–12/group), (C) calcification in the aortic sinus (n = 8–12/group) and (D) lipid accumulation in *en face* aortas (n = 8–12/group) were quantified in 25-week-old male mice.

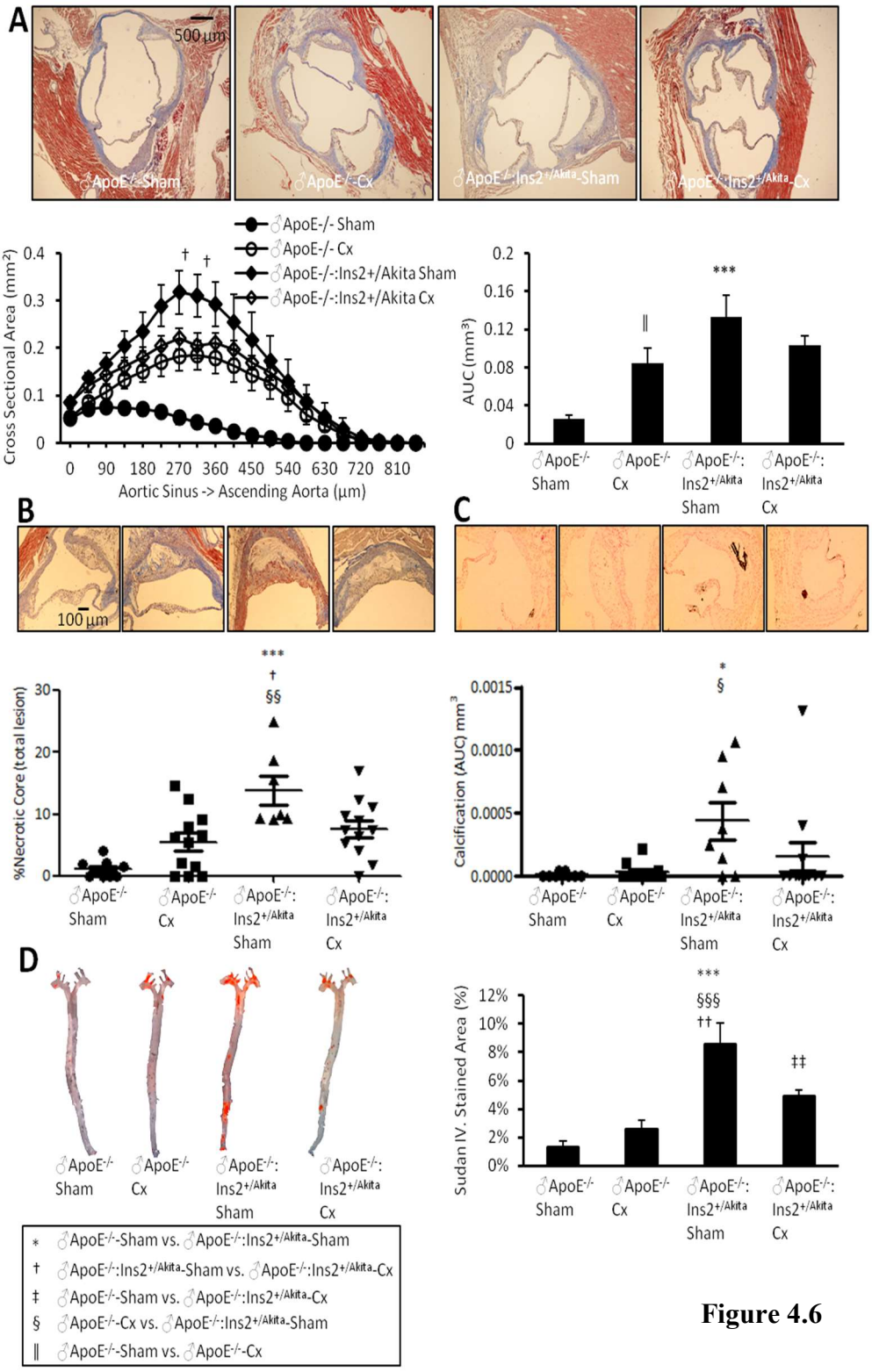
A
500 µm
♂ApoE-/- Sham
♂ApoE-/- Cx
♂ApoE-/-:Ins2+/Akita Sham
♂ApoE-/-:Ins2+/Akita Cx
Cross Sectional Area (mm²)
Aortic Sinus -> Ascending Aorta (µm)
AUC (mm³)
B
100 µm
C
%Necrotic Core (total lesion)
Calcification (AUC) mm³
D
Sudan IV. Stained Area (%)
♂ApoE-/- Sham
♂ApoE-/- Cx
♂ApoE-/-: Ins2+/Akita Sham
♂ApoE-/-: Ins2+/Akita Cx
* ♂ApoE-/-Sham vs. ♂ApoE-/-:Ins2+/Akita-Sham
† ♂ApoE-/-:Ins2+/Akita-Sham vs. ♂ApoE-/-:Ins2+/Akita-Cx
‡ ♂ApoE-/-Sham vs. ♂ApoE-/-:Ins2+/Akita-Cx
§ ♂ApoE-/-Cx vs. ♂ApoE-/-:Ins2+/Akita-Sham
‖ ♂ApoE-/-Sham vs. ♂ApoE-/-Cx

Figure 4.6

4.6 DISCUSSION

In this report we have characterized the sex-specific differences of the ApoE$^{-/-}$:Ins2$^{+/Akita}$ mouse model of hyperglycemia-accelerated atherosclerosis. Specifically, male ApoE$^{-/-}$:Ins2$^{+/Akita}$ mice develop chronic hyperglycemia and significantly accelerated atherosclerosis by 25 weeks of age. Castration slows the development of atherosclerosis in ApoE$^{-/-}$:Ins2$^{+/Akita}$ mice but enhances disease progression in the normoglycemic controls. Female ApoE$^{-/-}$:Ins2$^{+/Akita}$ mice are only transiently hyperglycemic with glucose levels normalizing by 15 weeks of age. Still, transiently hyperglycemic female mice develop accelerated atherosclerosis. Ovariectomized ApoE$^{-/-}$:Ins2$^{+/Akita}$ mice are chronically hyperglycemic and show indications of advanced atherosclerosis.

Differences in the incidence and the prevalence of DM between sexes do exist [26, 27]. In fact, sex differences in prevalence extend to dyslipidemia [28, 29], obesity [30, 31], hypertension [32], atherosclerotic development [33] and the risk of myocardial infarction [34]. Pre-menopausal women have a lower incidence of DM and evidence suggests that estrogen protects against pancreatic beta cell failure in rodent models [35, 36]. Other studies have focused upon the multiple benefits of androgens in men [37]. Testosterone levels tend to decrease with age [38] and this drop could explain the increased prevalence of age-related disease. In the STZ-hyperglycemic male rats [39] the lack of circulating insulin leads to the decrease of the circulating pituitary hormones, FSH and LH, which has a direct impact in the availability of testosterone. Similarly, in human males, an inverse correlation

between testosterone levels and type 2 DM has been described [40, 41] where an increase of the insulin resistance is associated with a deficiency of testosterone.

We observe that castration significantly accelerates the development of atherosclerosis in normoglycemic ApoE$^{-/-}$ mice, which is consistent with a protective vascular effect of androgens [42–44]. When the Ins2^{Akita} mutation is incorporated into the male ApoE$^{-/-}$ mice, we and others [45], have observed the early onset of chronic hyperglycemia, enhanced hypercholesterolemia and the accelerated progression of atherosclerosis. We also observed a significant reduction in insulin sensitivity. In these hyperglycemic mice, the testosterone levels are significantly lower than in normoglycemic controls. This is consistent with previous observation in hyperglycemic rodents [39] and humans [40, 41]. Decreased testosterone combined with chronic hyperglycemia and enhanced hypercholesterolemia would exacerbate the development of atherosclerosis. Interestingly, when the castration is carried out in the hyperglycemic ApoE$^{-/-}$:Ins2$^{+/Akita}$ mice atherosclerosis is attenuated. This effect may be explained by the corresponding reduction in blood glucose and non-HDL-cholesterol levels and the improved insulin sensitivity associated with castration. Together, these results support a model in which testosterone confers vascular protection in the male normoglycemic ApoE$^{-/-}$ mice, but in diabetic mice, testosterone appears to exacerbate hyperglycemia, hypercholesterolemia, and ultimately atherosclerosis. Further investigations are required to fully delineate the underlying mechanisms of these effects.

Female $Ins2^{+/Akita}$ mice have been reported to be hyperglycemic, but with lower blood glucose levels than male $Ins2^{+/Akita}$ mice [19]. In this study we show that, by 15 weeks of age, blood glucose levels in female $ApoE^{-/-}$:$Ins2^{+/Akita}$ mice are similar to $ApoE^{-/-}$ controls. This phenomenon is partially dependent upon ApoE-deficiency because significant hyperglycemia is sustained at 15 weeks of age in heterozygous $ApoE^{+/-}$:$Ins2^{+/Akita}$ females. The underlying mechanisms by which female (but not male) mice can produce functional insulin in the presence of the $Ins2^{Akita}$ mutation have not been explained. We show that female $ApoE^{-/-}$:$Ins2^{+/Akita}$ mice have significantly less beta cell stress (indicated by GADD153 staining) compared to males. We also demonstrate that the transient hyperglycemia in female $ApoE^{-/-}$:$Ins2^{+/Akita}$ mice does not exacerbate the already dyslipidemic profile of $ApoE^{-/-}$ mice, but does promote accelerated atherosclerosis. Ovariectomization of $ApoE^{-/-}$:$Ins2^{+/Akita}$ mice induces sustained hyperglycemia, effectively abolishing the observed protection from beta cell stress (chronically induced by the $Ins2^{Akita}$ mutation) in the pancreatic beta-cells and reducing the ability to produce functional insulin. The atherosclerotic lesion volumes of the ovariectomized $ApoE^{-/-}$:$Ins2^{+/Akita}$ mice are similar to those observed in the sham-operated $ApoE^{-/-}$:$Ins2^{+/Akita}$ and the $ApoE^{-/-}$ mice, but specific characteristics of the lesions appear to be advanced in addition to the lipid accumulation in the whole aortas.

The effects of estrogen on pancreas [35, 36] and the vasculature [46] have been elegantly demonstrated in animal models and in *in vitro* studies. However, the protective effects of estrogen replacement therapy in menopausal women are

questioned due to disparate results [47] and the potential cancerogenic effects of estrogens [48]. Finan B. et al. (2012) have recently overcome these obstacles and re-positioned estrogens as a real alternative to the treatment of the metabolic syndrome [49].

It is important to note that, in addition to the tissue specific or cell specific effects described for sex hormones, alterations in their circulating levels may also affect vascular health through indirect mechanisms. Specifically, evidence suggests that sex hormones modulate levels of lipoprotein particles including HDL, LDL and VLDL as well as levels of ApoA1, ApoB100, ApoB48 and ApoC-III [50–53]. In addition, modulations in hormone levels have been linked to alterations in the concentration of vasodilators, vasoconstrictors, inflammatory cytokine profiles and the response of immune cells to modified LDL particles [54, 55]. These multiple targets and interactions contribute to the complex array of effects observed when sex hormone levels are manipulated.

In conclusion, we have characterized the sex-specific differences of the $ApoE^{-/-}$:$Ins2^{+/Akita}$ mouse model of hyperglycemia-accelerated atherosclerosis. Using this model we have shown that the hormonal component from each sex is playing an important role in diabetes and the development of atherosclerosis by affecting the function of the pancreas as well as pathogenesis in the artery wall. Importantly, in this model, testosterone can have athero-protective or pro-atherogenic effects, depending upon the glycemic status of the mouse. These

findings may have important clinical implications with regard to androgen replacement therapies in the context of chronic disease.

4.7 REFERENCES FOR CHAPTER 4

[1] Goraya TY, Liebson CL, Palumbo PJ: Coronary atherosclerosis in DM: a population based study. J Am Coll Cardiol. 2002, 40:946–953

[2] D'Souza A, Hussain M, Howarth F, Woods NM, Bidasee K and Singh J: Pathogenesis and pathophysiology of accelerated atherosclerosis in the diabetic heart. Mol Cell Biochem. 2009, 331:89–116

[3] Haffner SM, Lehto S, Ronnemaa T, Tyorala K and Laakso M: Mortality from coronary heart disease in subjects with type 2 diabetes and in nondiabetic subjects with and without prior myocardial infarction. N Eng J Med. 1998, 339:229–234

[4] Steinberger J, Daniels SR; American Heart Association Atherosclerosis, Hypertension, and Obesity in the Young Committee (Council on Cardiovascular Disease in the Young); American Heart Association Diabetes Committee (Council on Nutrition, Physical Activity, and Metabolism): Obesity, insulin resistance, diabetes, and cardiovascular risk in children: an American Heart Association scientific statement from the Atherosclerosis, Hypertension, and Obesity in the Young Committee (Council on Cardiovascular Disease in the Young) and the Diabetes Committee (Council on Nutrition, Physical Activity, and Metabolism). Circulation. 2003, 107:1448–1453

[5] Wu KK, Huan Y: Diabetic atherosclerosis mouse models. Atherosclerosis. 2007, 191:241–249

[6] Lenzen S: The mechanisms of alloxan- and streptozotocin-induced diabetes. Diabetologia. 2008, 51:216–226

[7] Park L, Raman KG, Lee KJ, Lu Y, Ferran LJ Jr, Chow WS, Stern D, Schmidt AM: Suppression of accelerated diabetic atherosclerosis by the soluble receptor for advanced glycation endproducts. Nat Med. 1998, 4:1025–1031

[8] Werstuck GH, Khan MI, Femia G, Kim AJ, Tedesco V, Trigatti B and Shi YY: Glucosamine-induced endoplasmic reticulum stress is associated with accelerated atherosclerosis in a hyperglycemic mouse model. Diabetes. 2006, 55:93–101

[9] Veerman KJ, Venegas-Pino D, Khan MI, Shi Y, Gerstein HC, Werstuck GH: Hyperglycaemia is associated with impaired vasa vasorum neovascularisation and accelerated atherosclerosis in apolipoprotein-E deficient mice. Atherosclerosis. 2013, 227:250–258

[10] Bowes AJ, Khan MI, Shi Y, Robertson L, Werstuck GH: Valproate Attenuates Accelerated Atherosclerosis in Hyperglycemic ApoE-Deficient Mice: Evidence in Support of a Role for Endoplasmic Reticulum Stress and Glycogen Synthase Kinase-3 in Lesion Development and Hepatic Steatosis. Am J Pathol. 2009, 174:330–342

[11] Lee JH, Yang SH, Oh JM, and Lee MG: Pharmacokinetics of drugs in rats with diabetes mellitus induced by alloxan or streptozocin: comparison with those in patients with type I diabetes mellitus. J Pharm Pharmacol. 2010, 62:1–23

[12] Muller YD, Golshayan D, Ehirchiou D, Wyss JC, Giovannoni L, Meier R, Serre-Beinier V, Puga Yung G, Morel P, Bühler LH, Seebach JD: Immunosuppressive effects of streptozotocin-induced diabetes result in absolute lymphopenia and a relative increase of T regulatory cells. Diabetes. 2011, 60:2331–2340

[13] Grossman EJ, Lee DD, Tao J, Wilson RA, Park SY, Bell GI, Chong AS: Glycemic control promotes pancreatic beta-cell regeneration in streptozotocin-induced diabetic mice. PLoS One. 2010, 5:e8749

[14] Wang J, Takeuchi T, Tanaka S, Kubo SK, Kayo T, Lu D, Takata K, Koizumi A, Izumi T: A mutation in the insulin 2 gene induces diabetes with severe pancreatic beta-cell dysfunction in the Mody mouse. J Clin Invest. 1999, 103:27–37

[15] Oyadomari S, Koizumi A, Takeda K, Gotoh T, Akira S, Araki E, Mori M: Targeted disruption of the Chop gene delays endoplasmic reticulum stress-mediated diabetes. J Clin Invest. 2002, 109:525–532

[16] Ron D: Proteotoxicity in the endoplasmic reticulum: lessons from the Akita diabetic mouse. J Clin Invest. 2002, 109:443–445

[17] Gupta S, McGrath B, Cavener DR: PERK (EIF2AK3) regulates proinsulin trafficking and quality control in the secretory pathway. Diabetes. 2010, 59:1937–1947

[18] Liu M, Hodish I, Rhodes CJ, Arvan P: Proinsulin maturation, misfolding, and proteotoxicity. Proc Natl Acad Sci U S A. 2007, 104:15841–15846

[19] Yoshioka M, Kayo T Ikeda T, Koizumi A: A novel locus, Mody4, distal to D7Mit189 on chromosome 7 determines early-onset NIDDM nonobese C57BL/6 (Akita) mutant mice. Diabetes. 1997, 46:887–894

[20] Venegas-Pino DE, Banko N, Khan MI, Shi Y, Werstuck GH: Quantitative analysis and characterization of atherosclerotic lesions in the murine aortic sinus. J Vis Exp. 2013, 82:e50933

[21] Thim T, Hagensen MK, Wallace-Bradley D, Granada JF, Kaluza GL, Drouet L, Paaske WP, Bøtker HE, Falk E: Unreliable assessment of necrotic core by virtual histology intravascular ultrasound in porcine coronary artery disease. Circ Cardiovasc Imaging. 2010, 3:384–391

[22] Jeziorska M, McCollum C, Woolley DE: Calcification in atherosclerotic plaque of human carotid arteries: associations with mast cells and macrophages. J Pathol. 1998, 185:10–17

[23] Oyadomari S, Mori M: Roles of CHOP/GADD153 in endoplasmic reticulum stress. Cell Death Differ. 2004, 4:381–389

[24] Matthews DR, Hosker JP, Rudenski AS, Naylor BA, Treacher DF, Turner RC: Homeostasis model assessment: insulin resistance and beta-cell function from fasting plasma glucose and insulin concentrations in man. Diabetologia. 1985, 28:412–419

[25] Katz A, Nambi SS, Mather K, Baron AD, Follmann DA, Sullivan G, Quon MJ: Quantitative insulin sensitivity check index: a simple, accurate method for assessing insulin sensitivity in humans. J Clin Endocrinol Metab. 2000, 85:2402–2410

[26] Gale EA, Gillespie KM: Diabetes and gender. Diabetologia. 2001, 44:3–15

[27] Meisinger C, Thorand B, Schneider A, Stieber J, Döring A, Löwel H: Sex differences in risk factors for incident type 2 diabetes mellitus: the MONICA Augsburg cohort study. Arch Intern Med. 2002, 162:82–89

[28] Freedman DS, Jacobsen SJ, Barboriak JJ, Sobocinski KA, Anderson AJ, Kissebah AH, Sasse EA, Gruchow HW: Body fat distribution and male/female differences in lipids and lipoproteins. Circulation. 1990, 81:1498–1506

[29] Goff DC Jr, Bertoni AG, Kramer H, Bonds D, Blumenthal RS, Tsai MY, Psaty BM: Dyslipidemia prevalence, treatment, and control in the Multi-Ethnic Study of Atherosclerosis (MESA): gender, ethnicity, and coronary artery calcium. Circulation. 2006, 113:647–656

[30] Ogden CL, Carroll MD, Kit BK, Flegal KM: Prevalence of obesity in the United States, 2009–2010. NCHS Data Brief. 2012, 82:1–8

[31] Lovejoy JC, Sainsbury A; Stock Conference 2008 Working Group: Sex differences in obesity and the regulation of energy homeostasis. Obes Rev. 2009, 10:154-167

[32] Reckelhoff JF: Gender differences in the regulation of blood pressure. Hypertension. 2001, 37:1199–1208

[33] Joakimsen O, Bonaa KH, Stensland-Bugge E, Jacobsen BK: Age and sex differences in the distribution and ultrasound morphology of carotid atherosclerosis: the Tromsø Study. Arterioscler Thromb Vasc Biol. 1999, 19:3007–3013

[34] Njølstad I, Arnesen E, Lund-Larsen PG: Smoking, serum lipids, blood pressure, and sex differences in myocardial infarction. A 12-year follow-up of the Finnmark Study. Circulation. 1996, 93:450–456

[35] Tiano JP, Delghingaro-Augusto V, Le May C, Liu S, Kaw MK, Khuder SS, Latour MG, Bhatt SA, Korach KS, Najjar SM, Prentki M, Mauvais-Jarvis F: Estrogen receptor activation reduces lipid synthesis in pancreatic islets and prevents β cell failure in rodent models of type 2 diabetes. J Clin Invest. 2011, 121:3331–3342

[36] Le May C, Chu K, Hu M, Ortega CS, Simpson ER, Korach KS, Tsai MJ, Mauvais-Jarvis F: Estrogens protect pancreatic beta-cells from apoptosis and prevent insulin-deficient diabetes mellitus in mice. Proc Natl Acad Sci U S A. 2006, 103:9232–9237

[37] Jones RD, Nettleship JE, Kapoor D, Jones HT, Channer KS: Testosterone and atherosclerosis in aging men: purported association and clinical implications. Am J Cardiovasc Drugs. 2005, 5:141–154

[38] Vermeulen A: Clinical review 24: Androgens in the aging male. J Clin Endocrinol Metab. 1991, 73:221–224

[39] Ballester J, Muñoz MC, Domínguez J, Rigau T, Guinovart JJ, Rodríguez-Gil JE: Insulin-dependent diabetes affects testicular function by FSH- and LH-linked mechanisms. J Androl. 2004, 25:706–719

[40] Corona G, Monami M, Rastrelli G, Aversa A, Sforza A, Lenzi A, Forti G, Mannucci E, Maggi M: Type 2 diabetes mellitus and testosterone: a meta-analysis study. Int J Androl. 2011, 34:528–540

[41] Tomar R, Dhindsa S, Chaudhuri A, Mohanty P, Garg R, Dandona P: Contrasting testosterone concentrations in type 1 and type 2 diabetes. Diabetes Care. 2006, 29:1120–1122

[42] Bosco C, Bosnyak Z, Malmberg A, Adolfsson J, Keating NL, Van Hemelrijck M: Quantifying observational evidence for risk of fatal and nonfatal cardiovascular disease following androgen deprivation therapy for prostate cancer: a meta-analysis. Eur Urol. 2015, 68:386–396

[43] Vlachopoulos C, Ioakeimidis N, Miner M, Aggelis A, Pietri P, Terentes-Printzios D, Tsekoura D, Stefanadis C: Testosterone deficiency: a determinant of aortic stiffness in men. Atherosclerosis. 2014, 233:278–283

[44] Doğan BA, Karakılıç E, Tuna MM, Arduç A, Berker D, Güler S: Effect of androgen replacement therapy on atherosclerotic risk markers in young-to-middle-aged men with idiopathic hypogonadotropic hypogonadism. Clin Endocrinol (Oxf). 2015, 82:422–428

[45] Jun JY, Ma Z, Segar L: Spontaneously diabetic Ins2(+/Akita):apoE-deficient mice exhibit exaggerated hypercholesterolemia and atherosclerosis. Am J Physiol Endocrinol Metab. 2011, 301:145–154

[46] Bourassa PA, Milos PM, Gaynor BJ, Breslow JL, Aiello RJ: Estrogen reduces atherosclerotic lesion development in apolipoprotein E-deficient mice. Proc Natl Acad Sci U S A. 1996, 93:10022–10027

[47] Mikkola TS, Clarkson TB: Estrogen replacement therapy, atherosclerosis, and vascular function. Cardiovasc Res. 2002, 53:605–619

[48] Persson I, Weiderpass E, Bergkvist L, Bergström R, Schairer C: Risks of breast and endometrial cancer after estrogen and estrogen-progestin replacement. Cancer Causes Control. 1999, 10:253–260

[49] Finan B, Yang B, Ottaway N, Stemmer K, Müller TD, Yi CX, Habegger K, Schriever SC, García-Cáceres C, Kabra DG, Hembree J, Holland J, Raver C, Seeley RJ, Hans W, Irmler M, Beckers J, de Angelis MH, Tiano JP, Mauvais-Jarvis F, Perez-Tilve D, Pfluger P, Zhang L, Gelfanov V, DiMarchi RD, Tschöp MH: Targeted estrogen delivery reverses the metabolic syndrome. Nat Med. 2012, 12:1847–1856

[50] Surra JC, Guillén N, Arbonés-Mainar JM, Barranquero C, Navarro MA, Arnal C, Orman I, Segovia JC, Osada J: Sex as a profound modifier of atherosclerotic lesion development in apolipoprotein E-deficient mice with different genetic backgrounds. J Atheroscler Thromb. 2010, 17:712–721

[51] Gardner CD, Tribble DL, Young DR, Ahn D, Fortmann SP: Population frequency distributions of HDL, HDL(2), and HDL(3) cholesterol and apolipoproteins A-I and B in healthy men and women and associations with age, gender, hormonal status, and sex hormone use: the Stanford Five City Project. Prev Med. 2000, 31:335–345

[52] Wolfe BM, Barrett PH, Laurier L, Huff MW: Effects of continuous conjugated estrogen and micronized progesterone therapy upon lipoprotein metabolism in postmenopausal women. J Lipid Res. 2000, 41:368–375

[53] Khoo C, Campos H, Judge H, Sacks FM: Effects of estrogenic oral contraceptives on the lipoprotein B particle system defined by apolipoproteins E and C-III content. J Lipid Res. 1999, 40:202–212

[54] Tam NN, Leav I, Ho SM: Sex hormones induce direct epithelial and inflammation-mediated oxidative/nitrosative stress that favors prostatic carcinogenesis in the noble rat. Am J Pathol. 2007, 171:1334–1341

[55] Caligiuri G, Nicoletti A, Zhou X, Törnberg I, Hansson GK: Effects of sex and age on atherosclerosis and autoimmunity in apoE-deficient mice. Atherosclerosis. 1999, 145:301–308

CHAPTER 5: Evidence of Extensive Atherosclerosis, Coronary Artery Disease and Hypertrophy in the ApoE$^{-/-}$:Ins2$^{+/Akita}$ Mouse Fed a Western Type Diet

Daniel E. Venegas-Pino, Andrew Lagrotteria, Pei-Wen Wang, Cassaundra Clapdorp, Yuanyuan Shi, Geoff H. Werstuck

From the Departments of Biochemistry and Biomedical Sciences (D.E.V.P., A.L., G.H.W.), Medicine (G.H.W.), and the Thrombosis and Atherosclerosis Research Institute (D.E.V.P., A.L., P.W.W., C.C., Y.S., G.H.W.), McMaster University, Hamilton, Ontario, Canada

5.1 FOREWORD

This study investigates the effects of a western-type diet on the hyperglycemic ApoE$^{-/-}$:Ins2$^{+/Akita}$ mice. We demonstrate the pernicious phenotype of the mice leading to accelerated death correlated with massive atherosclerosis that extended to the aortic sinus, ascending and descending aorta, brachiocephalic artery and coronary arteries, and also accompanied by hypertrophy.

This manuscript is in preparation to be submitted. The experiments in this study were conducted by Daniel E. Venegas-Pino with assistance from the co-authors. The manuscript was written by Daniel E. Venegas-Pino in collaboration with Dr. Geoff Werstuck.

5.2 ABSTRACT

Background: Diabetic patients with no history of cardiac infarction have a prevalence of coronary atherosclerosis and a risk of heart attack equivalent to euglycemic patients who have coronary atherosclerosis and have suffered a prior myocardial infarction. In an intent to establish a diabetic mouse model with coronary artery disease we have fed the ApoE$^{-/-}$:Ins2$^{+/Akita}$ mice with a western-type diet in order to predisposed a pernicious phenotype in these mice and explore the cardiovascular disease.

Methods: 5-week-old ApoE$^{-/-}$:Ins2$^{+/Akita}$ mice were fed a western-type diet—rich in fat and cholesterol—until the 25 weeks of age, and metabolic parameters and pathomorphological characteristics were determined.

Results: We found massive atherosclerotic development at multiple vascular sites: aortic sinus, ascending and descending aorta, brachiocephalic artery and coronary arteries which was accompanied by extreme cholesterolemia and triglyceridemia, hypertrophy and a significant reduction of lifespan in the male ApoE$^{-/-}$:Ins2$^{+/Akita}$ mice. Female ApoE$^{-/-}$:Ins2$^{+/Akita}$ and ApoE$^{-/-}$ mice presented a parallel increase in plasma lipids, atherosclerosis, and no effects on mortality during the study time.

Conclusion: We have established a diabetic mouse model—the western-diet-fed male ApoE$^{-/-}$:Ins2$^{+/Akita}$ mouse—with profound cardiovascular disease: massive atherosclerosis, coronary artery disease and hypertrophy. This may represent the main cause or one of the main causes for shortening the lifespan of these mice.

5.3 INTRDOCUTION

Diabetes mellitus (DM) is associated with a cardiovascular disease mortality rate that exceeds 70%, and patients with type 2 diabetes who have no history of cardiac infarction have a prevalence of coronary atherosclerosis and a risk of heart attack equivalent to euglycemic patients who have coronary atherosclerosis and have suffered a prior myocardial infarction [1–3].

To facilitate the investigation and identification of the relevant molecular and physiological mechanisms that link diabetes and atherosclerosis, several different mouse models of diabetes-induced atherosclerosis have been developed. The $Ins2^{+/Akita}$ mouse represents a genetic alternative to chemically induced hyperglycemia. This mouse carries a spontaneous (C96Y) mutation in the *insulin 2* gene that disrupts a disulfide bond between the insulin A and B chains. The resulting insulin protein cannot be properly processed leading to endoplasmic reticulum (ER) stress and beta cell dysfunction [4]. It has been postulated that ER stress-induced beta cell death is the major cause of insulinopenia in the $Ins2^{+/Akita}$ mouse. Subsequent studies have suggested that the formation of mutant proinsulin-derived aggregates sequester the wild type proinsulin leading to the ER retention and degradation of mutant-wild proinsulin as the cause of the decrease in circulating insulin [5–8].

Recently, it has been reported that, when crossed into an $ApoE^{-/-}$ genetic background and fed a regular chow diet [9, 10], $Ins2^{+/Akita}$ male mice develop accelerated atherosclerosis. We have independently created an $ApoE^{-/-}$:$Ins2^{+/Akita}$

mouse strain in a C57BL/J6 genetic background and confirmed the accelerated atherosclerosis. In addition, we have noted striking sex-dependent differences in this mouse model that were not previously reported. To summarize, female ApoE$^{-/-}$:Ins2$^{+/Akita}$ mice are only transiently hyperglycemic and do not develop relative dyslipidemia compared to age matched ApoE$^{-/-}$ controls. Male ApoE$^{-/-}$:Ins2$^{+/Akita}$ mice are chronically hyperglycemic, develop enhanced dyslipidemia and apparent insulin resistance.

Despite the advanced atherosclerosis quantified at the aortic sinus of the ApoE$^{-/-}$:Ins2$^{+/Akita}$ mouse, no effects on mortality and coronary arteries were detected at up to 25 weeks of age. Here, we hypothesize that the combination of chronic hyperglycemia and a diet rich in fat content will produce a more severe model of accelerated atherosclerosis that may affect the cardiac anatomy and/or physiology of the ApoE$^{-/-}$:Ins2$^{+/Akita}$ mouse.

5.4 MATERIALS AND METHODS

Mice

Male ApoE$^{+/+}$:Ins2$^{+/Akita}$ mice (Jackson Laboratory) were crossed with female ApoE$^{-/-}$:Ins2$^{+/+}$ mice. The resulting male ApoE$^{+/-}$:Ins2$^{+/Akita}$ offspring were crossed with female ApoE$^{-/-}$:Ins2$^{+/+}$ mice. The male ApoE$^{-/-}$:Ins2$^{+/Akita}$ offspring produced from this cross and female ApoE$^{-/-}$:Ins2$^{+/+}$ were set up as breeding pairs to produce the ApoE$^{-/-}$:Ins2$^{+/Akita}$ and control ApoE$^{-/-}$:Ins2$^{+/+}$ littermates that were used in the following experiments. Genotypes were confirmed by PCR using

primers specific for *Ins2* and *ApoE* genes. The restriction enzyme Fnu4HI was used to identify the presence of the $Ins2^{Akita}$ mutation. All the mice used in this study were fed a regular chow diet (RD) which corresponds to 18% of calories derived from fat (2018 Teklad Global 18% Protein Rodent Diet; Harlan Teklad). At 5 weeks of age, mice were randomly allocated to continue receiving the regular chow diet or to receive a western-type diet (WD) with a high fat content (Teklad Adjusted Calories TD 97363; Harlan Teklad) containing 0.2% of cholesterol and 21% of anhydrous milk lipids which correspond to 42% of calories derived from fat. Survival curves were based upon the outcomes of RD-fed $ApoE^{-/-}$ mice (n = 8–10/gender), RD-fed $ApoE^{-/-}$:$Ins2^{+/Akita}$ mice (n = 8–9/gender), WD-fed $ApoE^{-/-}$ mice (n = 8–10/gender) and WD-fed $ApoE^{-/-}$:$Ins2^{+/Akita}$ mice (n = 8–14/gender). Mice were euthanized once they reached endpoint or 25 weeks of age. Endpoint was identified as exhibiting one or more of the following symptoms: breathing rate very slow and labored, unsteady gait, hunched posture, and ruffled fur.

Atherosclerosis was assessed at 25 weeks of age in male and female RD-fed $ApoE^{-/-}$ mice (n = 8/males and 4/females), WD-fed $ApoE^{-/-}$ mice (n = 8/males and 4/females), RD-fed $ApoE^{-/-}$:$Ins2^{+/Akita}$ mice (n = 8/males and 4/females) and WD-fed $ApoE^{-/-}$:$Ins2^{+/Akita}$ mice (n = 6/males and 4/females). All the procedures were pre-approved by the McMaster University Animal Research Ethics Board.

Harvesting and storing

Mice were anesthetized with isoflurane and blood was extracted. Mice were sacrificed by cervical dislocation and the vasculature was rinsed with 5mL of 0.9% saline. Liver and fat pad were removed and the vasculature was perfusion fixed with 10% neutral buffered formalin (NBF). The heart, pancreas and aorta were extracted. All the organs were stored in 10% NBF at room temperature.

Atherosclerosis in the aortic sinus

The harvested hearts were transversely cut along the plane of the aortic sinus and the top portions were embedded in paraffin. Paraffin-embedded hearts were sectioned using a microtome and 4.5μm serial sections from the aortic sinus were collected on glass slides until atherosclerotic lesions were no longer observed, as previously described [11]. The area, volume and necrotic core of the atherosclerotic lesions were estimated by Masson's trichrome staining (Sigma) [11, 12]. Calcified lesion areas were detected and quantified by von Kossa staining [13]. All images were captured with an Olympus DP71 digital camera (Olympus) mounted on a Leitz Laborlux S bright field microscope (Leica Microsystems), and assessed using Image J software.

Atherosclerosis in brachiocephalic arteries

Dissected arteries were manually processed as follows: 10% neutral buffered formalin for 1 hour at 42º C, 70% ethanol for 30 minutes at 40º C, 85%

ethanol for 30 minutes at 40º C, 100% ethanol for 45 minutes at 40º C, 100% ethanol for 45 minutes at 40º C, 100% ethanol for 45 minutes at 40º C, Xylene for 1 hour at 40º C, and Xylene for 1 hour at 40º C. They were then embedded in paraffin and sectioned into 8μm serial sections to be stained and analysed as described above.

Atherosclerosis in coronary arteries

The bottom portions of the hearts (i.e., the ventricles) were processed and embedded into paraffin blocks for sectioning. Using a microtome, the entire tissue was cross sectioned (from base to apex) and 8 μm sections were collected. Representative sections were stained with Masson's Trichrome (Sigma) to identify atherosclerotic lesions in the coronary arteries. For each section, the total number of coronary arteries was determined, and each artery was assessed for its degree of occlusion due to atherosclerotic plaque. A grade of 0% occlusion, <50% occlusion, >50% occlusion and 100% occlusion was assigned and an atherosclerotic profile for each heart, indicating the proportion of diseased arteries, was generated [14].

Atherosclerosis in *en face* aortas

The fixed aortas were cleaned of surrounding muscle and adventitial fat. They were longitudinally opened and stained for lipid content with Sudan IV (Sigma). Images of the whole aorta were captured using a L320 digital camera

(Nikon) and the percentage of the atherosclerotic area was assessed using Image J software.

Analysis of plasma

Fasting (6 hours) blood glucose levels were measured using a glucometer (LifeScan). Plasma lipid levels were determined in nonfasting and fasting conditions using the colorimetric diagnostic kit for total cholesterol and triglyceride (Thermo Scientific). Fasting plasma lipoproteins were separated by fast protein liquid chromatography, and total cholesterol and triglycerides were measured in each fraction. Insulin content was determined by ELISA kit (Crystal Chem) and surrogate indexes of beta cell function and insulin resistance were calculated from fasting blood glucose and plasma insulin concentrations as follows: HOMA-%β = $[(20 * I_0) / (G_0 - 3.5)]$ where G_0 is fasting glucose (mmol/l) and I_0 is fasting insulin (μIU/ml); and HOMA-IR = $[(G_0 * I_0) / 22.5]$ where G_0 is fasting glucose (mmol/l) and I_0 is fasting insulin (μIU/ml) [15].

Data analysis

Data were analyzed by one or two-way ANOVA, followed by the Bonferroni multiple comparison test between all groups. Data are expressed as arithmetic means ± SEM. For all experiments a *p value* of 0.05 was considered statistically significant. * $p<0.05$; ** $p<0.01$; *** $p<0.001$.

5.5 RESULTS

Western-type diet significantly reduces the life span of male ApoE$^{-/-}$:Ins2$^{+/Akita}$ mice

Survival of the WD-fed ApoE$^{-/-}$:Ins2$^{+/Akita}$ mice was studied until 25 weeks of age. This corresponds to the time point when differences in atherosclerotic lesion volume were detected and established in the aortic sinus of RD-fed mice [9, 10]. In accordance with previous pilot experiments, we found that only 20% of the WD-fed male ApoE$^{-/-}$:Ins2$^{+/Akita}$ mice reached this age since the majority of the mice reached endpoint between 20–23 weeks of age (Figure 5.1). No shortening of the life span was detected, during the same time frame, in any of the other WD-fed or RD-feed groups including female ApoE$^{-/-}$:Ins2$^{+/Akita}$ mice. For this reason, the major focus of this study is on male WD-fed mice.

Figure 5.1. Survival curve of male and female ApoE$^{-/-}$ and ApoE$^{-/-}$:Ins2$^{+/Akita}$ mice after feeding with a regular chow diet (RD) and a western-type diet (WD). After separation from breeders, all offspring were maintained in a RD until the 5 weeks of age when mice were randomly allocated to continue with the RD or WD until reached endpoint or the 25 weeks of age. (n = 8–14).

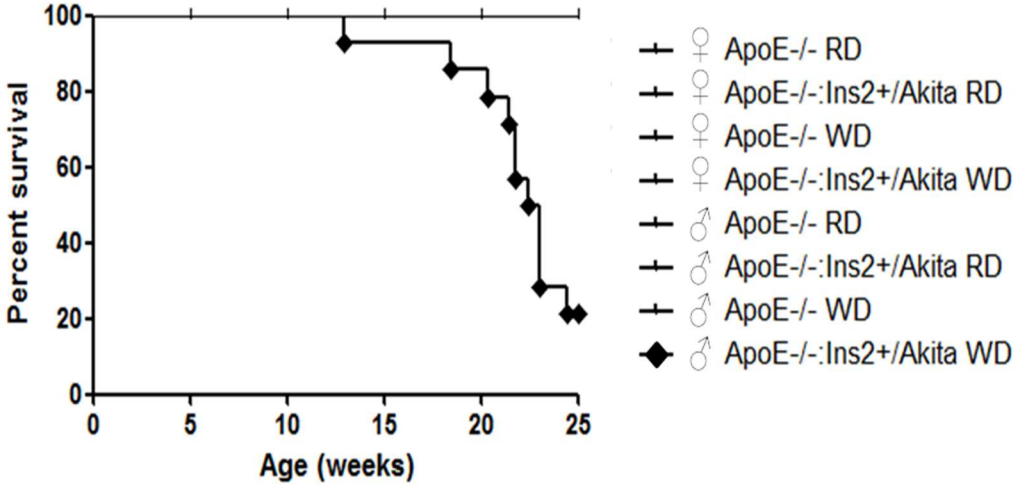
Percent survival
100
80
60
40
20
0
0
5
10
15
20
25
Age (weeks)
♀ ApoE-/- RD
♀ ApoE-/-:Ins2+/Akita RD
♀ ApoE-/- WD
♀ ApoE-/-:Ins2+/Akita WD
♂ ApoE-/- RD
♂ ApoE-/-:Ins2+/Akita RD
♂ ApoE-/- WD
♂ ApoE-/-:Ins2+/Akita WD

Figure 5.1

The effects of western-type diet on the clinical and metabolic parameters

Fasting blood glucose levels were not affected by WD feeding in the male ApoE$^{-/-}$:Ins2$^{+/Akita}$ mice that showed glucose levels of 30.9±1.4mM vs. 30.8±1.2mM under RD and WD feeding (Figure 5.2A), respectively. WD feeding in male apoE$^{-/-}$ mice resulted in a non-significant but noticeable increase of fasting glucose levels of 9.3±0.5mM compared to 7.5±0.6mM under RD feeding (Figure 5.2A). Insulin sensitivity, as evaluated by HOMA-IR and beta-cell function evaluated by HOMA-%β indexes, was significantly impaired in the WD-fed male ApoE$^{-/-}$:Ins2$^{+/Akita}$ mice compared to control diet fed mice (Figure 5.2B–C). No significant changes were observed in male ApoE$^{-/-}$ mice with respect to these indexes (Figure 5.2B–C). Female mice presented with similar glucose levels that also were not affected by the WD (Supplemental Figure 1, Appendix 3). HOMA-IR and HOMA-%β were also similar among all female mice (Supplemental Figure 1, Appendix 3).

Corresponding to previous observations related to RD-fed male ApoE$^{-/-}$:Ins2$^{+/Akita}$ mice, WD-fed male ApoE$^{-/-}$:Ins2$^{+/Akita}$ mice presented with a significant loss of body weight accompanied by the absence of epididymal fat when compared to male ApoE$^{-/-}$ mice (Figure 5.2D–E). Male ApoE$^{-/-}$ mice showed a nonsignificant increase of body mass equivalent to 3g after WD feeding (Figure 5.2D). This increase of body mass was accompanied by an increase of epididymal fat (Figure 5.2E). Liver mass was also affected in the WD-fed male ApoE$^{-/-}$:Ins2$^{+/Akita}$ mice, gaining more than 0.6g (50% net increase) compared to mice fed the regular chow diet (Figure 5.2F). This significant increment of the liver mass was also

accompanied by an aberrant increment of the plasma lipid content where WD-fed male ApoE$^{-/-}$:Ins2$^{+/Akita}$ mice presented with increased amounts of total cholesterol and triglycerides with respect to all other groups (Figure 5.2G–H). Plasma lipoprotein profiles correlated the increase of lipids with the elevation of the cholesterol- and triglyceride-VLDL and cholesterol- and triglyceride-LDL peaks (Figure 5.2I–J). Total cholesterol, but not triglycerides levels, were also significantly augmented in WD-fed male ApoE$^{-/-}$ mice (Figure 5.2G). Female mice showed no significant changes in body weight or epididymal fat content between diets or strains (Supplemental Figure 1, Appendix 3). A slight increase in liver weight and plasma lipid level was observed in WD-fed female mice (Supplemental figure 1, Appendix 3).

Figure 5.2. Analysis of metabolic parameters of male RD-fed and WD-fed mice at 25 weeks of age. (A) Fasting blood glucose levels. (B) Insulin resistance estimated by HOMA-IR index. (C) Beta-cell function evaluated by HOMA-%β index. (D) Body weight. (E) Epididymal fat content. (F) Liver weight. (G) Total cholesterol levels in plasma. (H) Total triglyceride levels in plasma. (I) Lipoprotein-cholesterol profile. (J) Lipoprotein-triglyceride profile. (n = 8–6)

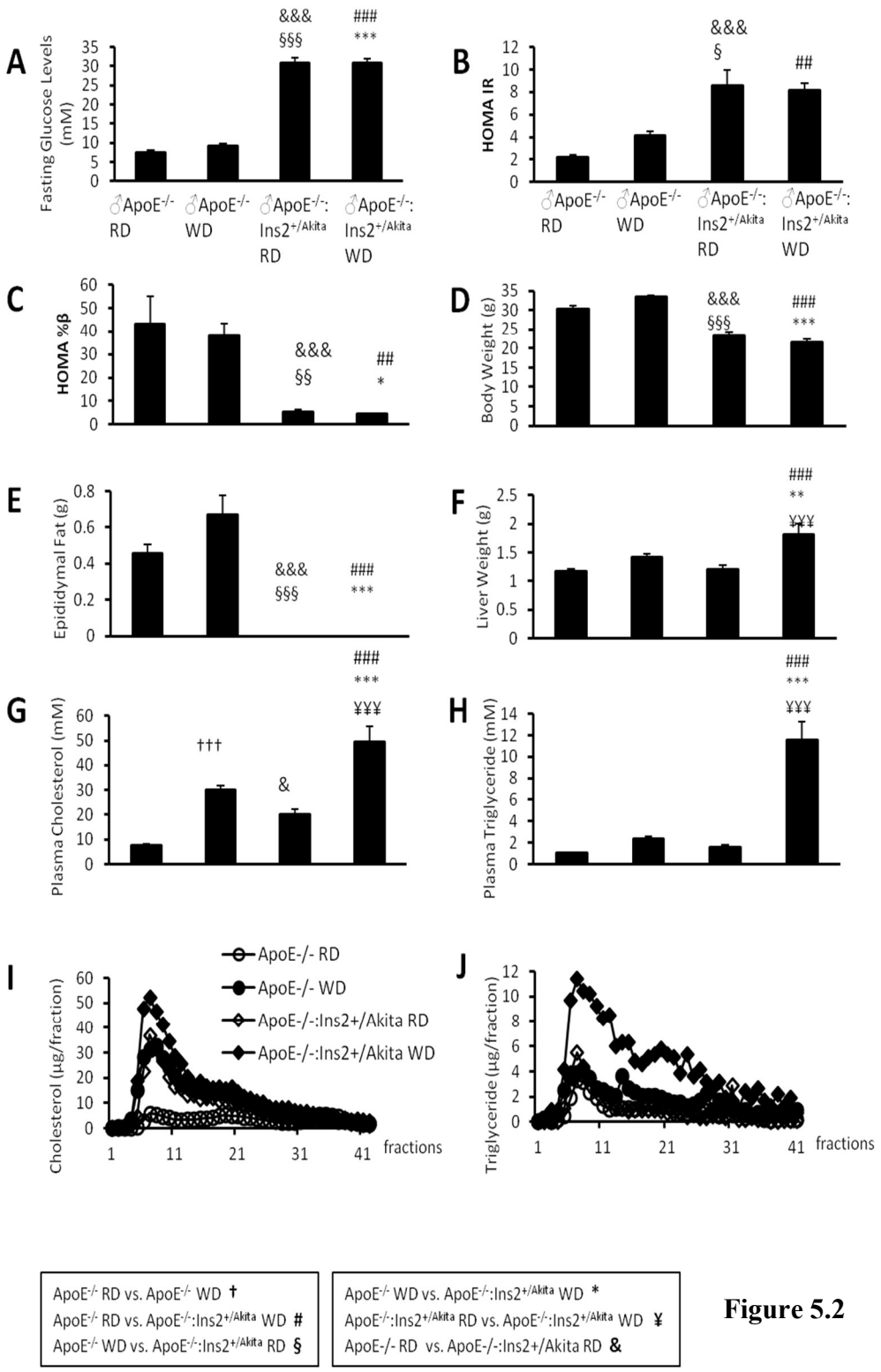
A
Fasting Glucose Levels (mM)
B
HOMA IR
C
HOMA %β
D
Body Weight (g)
E
Epididymal Fat (g)
F
Liver Weight (g)
G
Plasma Cholesterol (mM)
H
Plasma Triglyceride (mM)
I
Cholesterol (µg/fraction)
J
Triglyceride (µg/fraction)
fractions
♂ApoE-/- RD
♂ApoE-/- WD
♂ApoE-/-:Ins2+/Akita RD
♂ApoE-/-:Ins2+/Akita WD
ApoE-/- RD
ApoE-/- WD
ApoE-/-:Ins2+/Akita RD
ApoE-/-:Ins2+/Akita WD
ApoE-/- RD vs. ApoE-/- WD †
ApoE-/- RD vs. ApoE-/-:Ins2+/Akita WD #
ApoE-/- WD vs. ApoE-/-:Ins2+/Akita RD §
ApoE-/- WD vs. ApoE-/-:Ins2+/Akita WD *
ApoE-/-:Ins2+/Akita RD vs. ApoE-/-:Ins2+/Akita WD ¥
ApoE-/- RD vs. ApoE-/-:Ins2+/Akita RD &

Figure 5.2

Atherosclerotic development at the aortic sinus

Previously, we and others have shown that 25-week-old male ApoE$^{-/-}$:Ins2$^{+/Akita}$ mice presented with lesions 4X larger than 25-week-old male ApoE$^{-/-}$ mice fed the same regular chow diet [9, 10]. Under the effect of the WD (see representative images in 5.3A–D), we observed even larger atherosclerotic lesions in both male ApoE$^{-/-}$ and male ApoE$^{-/-}$:Ins2$^{+/Akita}$ mice (Figure 5.3E–F). WD-fed male ApoE$^{-/-}$:Ins2$^{+/Akita}$ mice presented with lesions 20X larger than the RD-fed male ApoE$^{-/-}$, 4X larger than the RD-fed male ApoE$^{-/-}$:Ins2$^{+/Akita}$, and almost 2X larger than the WD-fed male ApoE$^{-/-}$ mice. Despite the massive atherosclerosis, no significant reduction was detected of the cross sectional lumen area in WD-fed male mice (Figure 5.3G–L). In female mice, the effect of WD was similar in the ApoE$^{-/-}$ and ApoE$^{-/-}$:Ins2$^{+/Akita}$ strains (Supplemental Figure 2, Appendix 3).

Atherosclerotic lesions were also characterized with respect to necrotic core size (Figure 5.4A–D) and calcification (Figure 5.4G–J). WD-fed male ApoE$^{-/-}$:Ins2$^{+/Akita}$ mice presented with larger necrotic cores, occupying approximately 17% of the total lesion volume (Figure 5.4E–F). Interestingly, the necrotic core presented by WD-fed male ApoE$^{-/-}$ was larger than the one observed in the RD-fed male ApoE$^{-/-}$:Ins2$^{+/Akita}$ mice, but each occupied less than 10% of the total lesion volume (Figure 5.4E–F). Calcification of the atherosclerotic lesions was also significantly enhanced in the WD-fed male ApoE$^{-/-}$:Ins2$^{+/Akita}$ mice when compared to all other groups of mice (Figure 5.4K–L).

Figure 5.3. Quantification of atherosclerosis in the aortic sinus and ascending aorta of male RD-fed and WD-fed mice. (A–D) Representative images of the atherosclerotic development at the aortic sinus. (E) Atherosclerotic lesion areas through the aortic sinus-ascending aorta. (F) Atherosclerotic lesion volume through aortic sinus-ascending aorta. (G–J) Representative images of the atherosclerotic development in the ascending aorta. (K) Percentage of cross-sectional lesion respect to the cross-sectional-aorta caliber through the ascending aorta. (L) Average cross-sectional-lumen area in the ascending aorta. (n = 8–6)

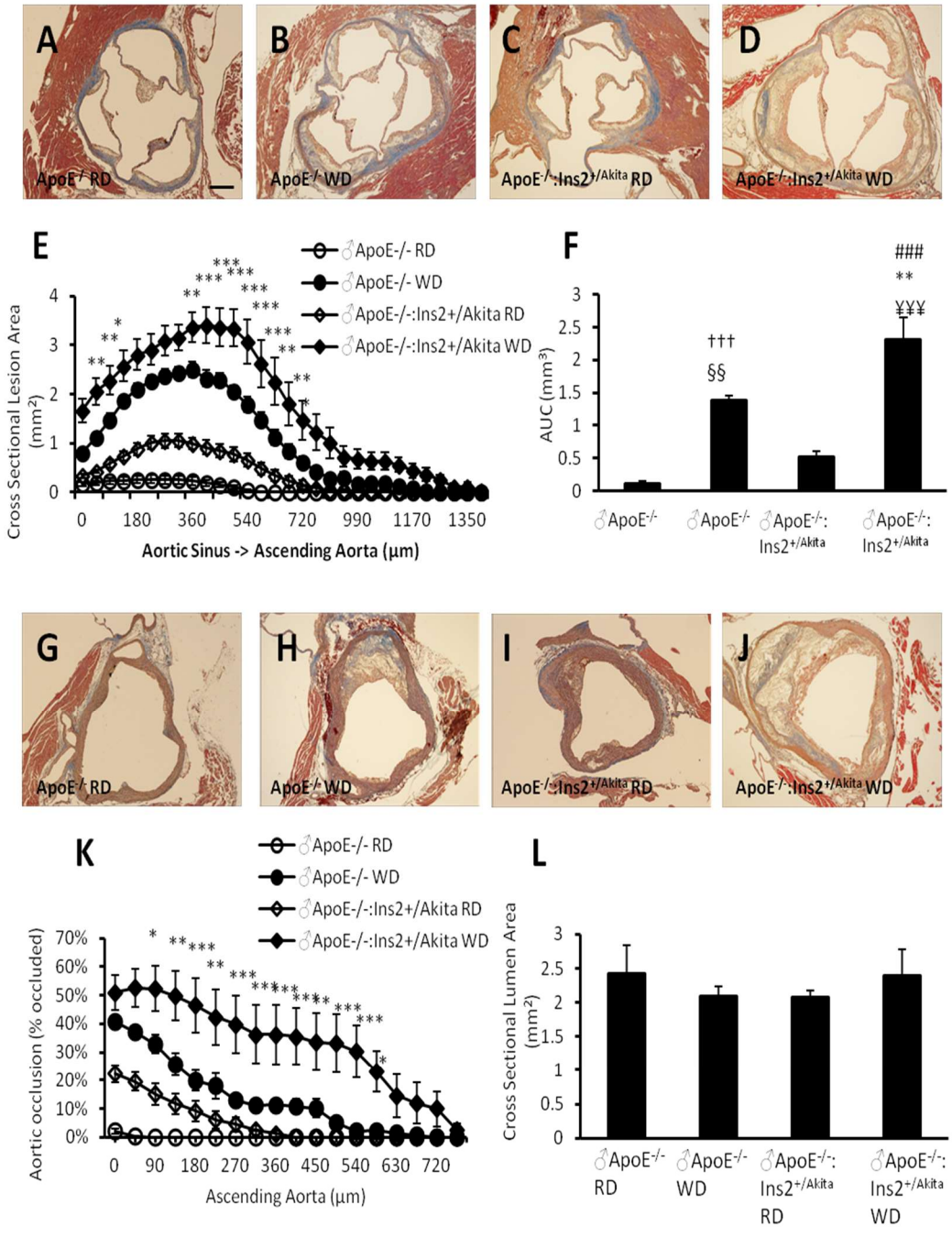

ApoE$^{-/-}$ RD vs. ApoE$^{-/-}$ WD †
ApoE$^{-/-}$ RD vs. ApoE$^{-/-}$:Ins2$^{+/Akita}$ WD #
ApoE$^{-/-}$ WD vs. ApoE$^{-/-}$:Ins2$^{+/Akita}$ RD §

ApoE$^{-/-}$ WD vs. ApoE$^{-/-}$:Ins2$^{+/Akita}$ WD *
ApoE$^{-/-}$:Ins2$^{+/Akita}$ RD vs. ApoE$^{-/-}$:Ins2$^{+/Akita}$ WD ¥
ApoE-/- RD vs. ApoE-/-:Ins2+/Akita RD &

Figure 5.3

Figure 5.4. Quantification of the necrotic core and calcification content in atherosclerotic lesions located in the aortic sinus and ascending aorta of male RD-fed and WD-fed mice. (A–D) Representative images of necrotic core in the atherosclerotic lesions. (E) Total volume of the necrotic core. (F) Percentage of necrotic core volume respect to the total lesion volume. (G–J) Representative images of intimal calcification. (K) Total volume of the intimal calcification. (L) Percentage of calcification volume respect to the total lesion volume. (n = 8–6)

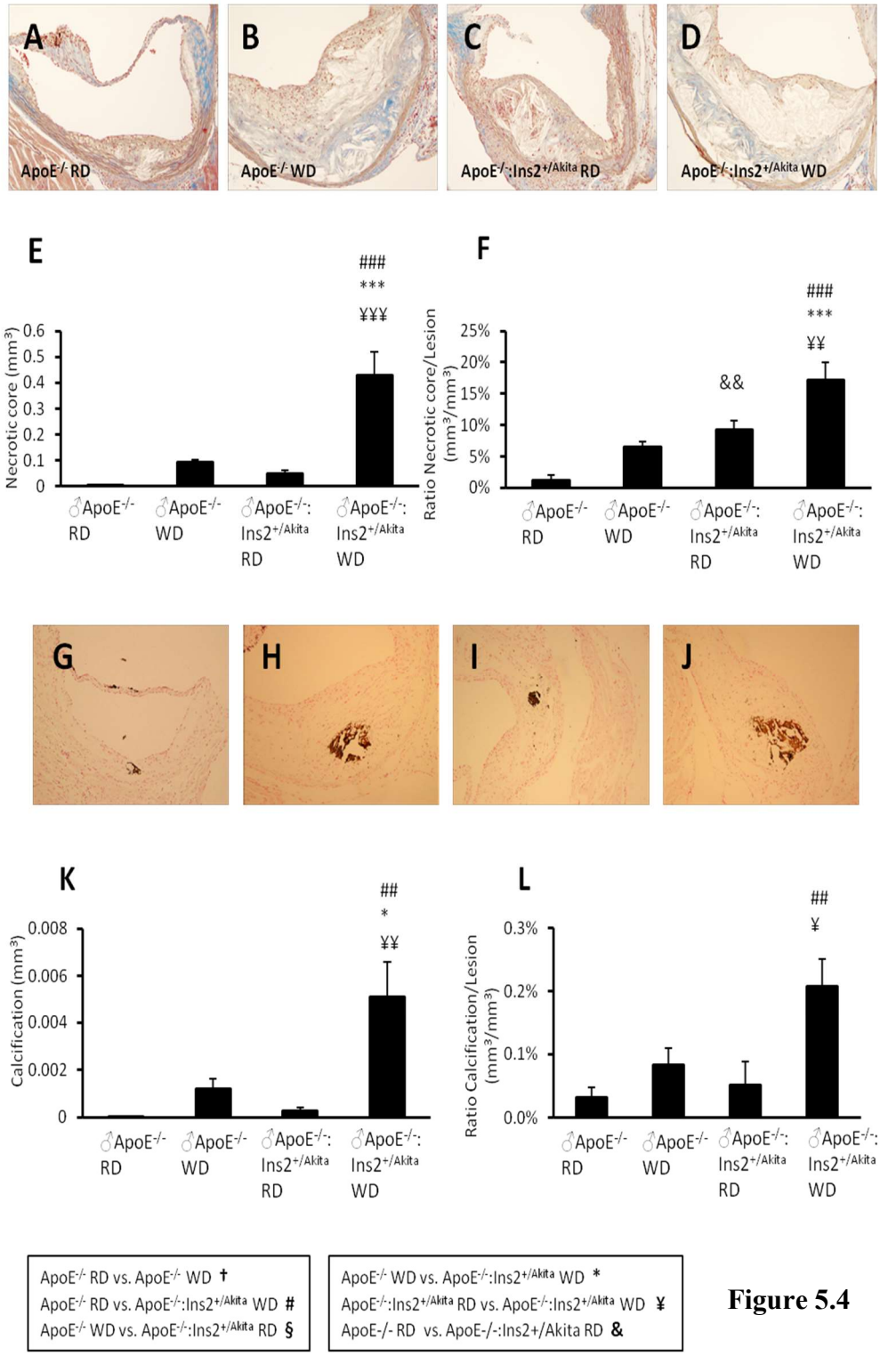
A
ApoE-/- RD
B
ApoE-/- WD
C
ApoE-/-:Ins2+/Akita RD
D
ApoE-/-:Ins2+/Akita WD
E
Necrotic core (mm³)
0.6
0.5
0.4
0.3
0.2
0.1
0
###
***
¥¥¥
♂ApoE-/- RD
♂ApoE-/- WD
♂ApoE-/-: Ins2+/Akita RD
♂ApoE-/-: Ins2+/Akita WD
F
Ratio Necrotic core/Lesion (mm³/mm³)
25%
20%
15%
10%
5%
0%
&&
###
***
¥¥
G
H
I
J
K
Calcification (mm³)
0.008
0.006
0.004
0.002
0
##
*
¥¥
L
Ratio Calcification/Lesion (mm³/mm³)
0.3%
0.2%
0.1%
0.0%
##
¥
ApoE-/- RD vs. ApoE-/- WD †
ApoE-/- RD vs. ApoE-/-:Ins2+/Akita WD #
ApoE-/- WD vs. ApoE-/-:Ins2+/Akita RD §
ApoE-/- WD vs. ApoE-/-:Ins2+/Akita WD *
ApoE-/-:Ins2+/Akita RD vs. ApoE-/-:Ins2+/Akita WD ¥
ApoE-/- RD vs. ApoE-/-:Ins2+/Akita RD &

Figure 5.4

Atherosclerosis in the brachiocephalic arteries and whole aortas

Although RD-fed male ApoE$^{-/-}$:Ins2$^{+/Akita}$ presented with significantly larger lesions than RD-fed male ApoE$^{-/-}$, the development of atherosclerosis at the brachiocephalic artery was profoundly accelerated by the WD in both normoglycemic and hyperglycemic mice (see representative images in Figure 5.5A–D and quantification in Figure 5.5E). As a result, there was no difference between the size of the lesions from WD-fed male ApoE$^{-/-}$ and WD-fed male ApoE$^{-/-}$:Ins2$^{+/Akita}$ mice. However, the lumen of the WD-fed male ApoE$^{-/-}$:Ins2$^{+/Akita}$ mice showed evidence of narrowing (Figure 5.5F). Another important feature present in the lesions of WD-fed mice is the presence of hemorrhagic regions (black arrows in Figure 5.5B–D) characteristic of leaky neovascularization or the rupture of advanced lesions.

Atherosclerosis in the whole aorta followed a similar trend (see representative images in Figure 5.5G–J) as observed in the aortic sinus. There was a significant increase of lipid accumulation in aortas from WD-fed male mice, but with even larger and massive extensions of atherosclerotic areas in the male ApoE$^{-/-}$:Ins2$^{+/Akita}$ mice, covering up 40% of the total internal-artery surface (Figure 5.5K).

Figure 5.5. Quantification of atherosclerosis at the brachiocephalic artery and lipid accumulation in whole aortas. (A–D) Representative images of atherosclerosis development at the brachiocephalic artery from RD-fed apoE$^{-/-}$, WD-fed apoE$^{-/-}$, RD-fed apoE$^{-/-}$:Ins2$^{+/Akita}$ and WD-fed apoE$^{-/-}$:Ins2$^{+/Akita}$ mice. (E) Cross sectional representation of the averaged percentage occupied by lesion respect to the total caliber of the brachiocephalic artery. (F) Average cross sectional lumen area in the brachiocephalic artery. (A–D) Representative images of aortas stained with Sudan IV. (E) Percentage of lipid-stained area respect to the total internal area of the aorta. (n = 8–6)

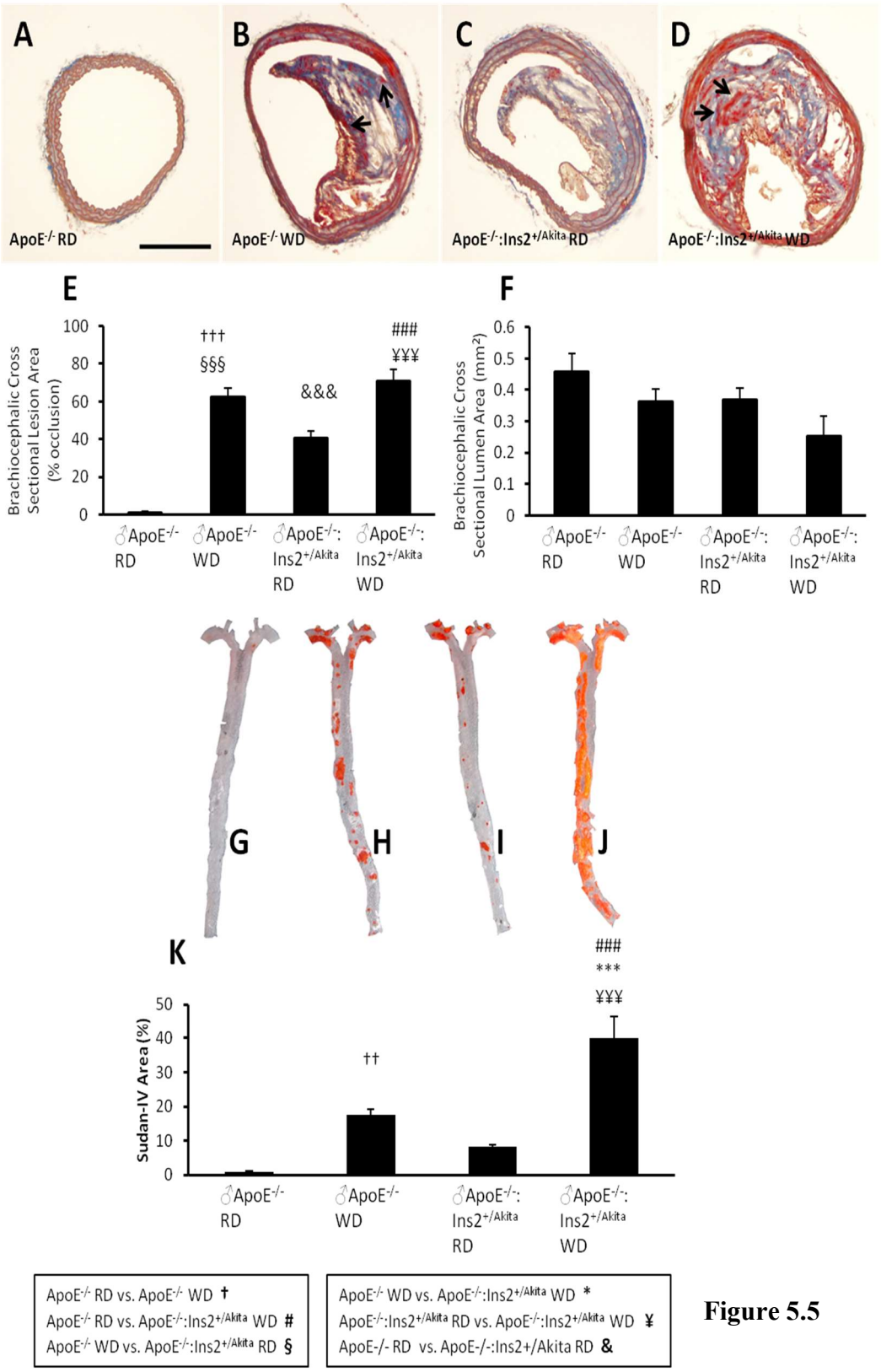
A
B
C
D
ApoE-/- RD
ApoE-/- WD
ApoE-/-:Ins2+/Akita RD
ApoE-/-:Ins2+/Akita WD
E
Brachiocephalic Cross Sectional Lesion Area (% occlusion)
100
80
60
40
20
0
†††
§§§
&&&
###
¥¥¥
♂ApoE-/- RD
♂ApoE-/- WD
♂ApoE-/-: Ins2+/Akita RD
♂ApoE-/-: Ins2+/Akita WD
F
Brachiocephalic Cross Sectional Lumen Area (mm²)
0.6
0.5
0.4
0.3
0.2
0.1
0
♂ApoE-/- RD
♂ApoE-/- WD
♂ApoE-/-: Ins2+/Akita RD
♂ApoE-/-: Ins2+/Akita WD
G
H
I
J
K
Sudan-IV Area (%)
50
40
30
20
10
0
††
###
***
¥¥¥
♂ApoE-/- RD
♂ApoE-/- WD
♂ApoE-/-: Ins2+/Akita RD
♂ApoE-/-: Ins2+/Akita WD
ApoE-/- RD vs. ApoE-/- WD †
ApoE-/- RD vs. ApoE-/-:Ins2+/Akita WD #
ApoE-/- WD vs. ApoE-/-:Ins2+/Akita RD §
ApoE-/- WD vs. ApoE-/-:Ins2+/Akita WD *
ApoE-/-:Ins2+/Akita RD vs. ApoE-/-:Ins2+/Akita WD ¥
ApoE-/- RD vs. ApoE-/-:Ins2+/Akita RD &

Figure 5.5

Coronary artery disease and hypertrophy

The development of coronary artery disease has not been previously described in the ApoE$^{-/-}$:Ins2$^{+/Akita}$ mouse. We found that after the WD feeding, mice presented with a significant percentage of coronary arteries partially and totally occluded (Representative images in Figure 5.6A–D and quantification in Figure 5.6E). The percentage of coronaries totally occluded in the WD-fed male ApoE$^{-/-}$:Ins2$^{+/Akita}$ mice was significantly higher than RD-fed male ApoE$^{-/-}$ and ApoE$^{-/-}$:Ins2$^{+/Akita}$ mice (Figure 5.6E). The percentage of coronaries partially occluded in the WD-fed male ApoE$^{-/-}$:Ins2$^{+/Akita}$ mice was significantly higher than WD-fed male ApoE$^{-/-}$. Also WD-fed male ApoE$^{-/-}$:Ins2$^{+/Akita}$ mice showed a higher percentage of coronaries partially occluded than WD-fed male ApoE$^{-/-}$ mice (Figure 5.6E).

Likely as a result of the massive development of atherosclerosis, WD-fed male ApoE$^{-/-}$:Ins2$^{+/Akita}$ mice presented with an increase of heart mass adjusted to the body mass (representative image in Figure 5.6F and quantification in Figure 5.6G). Also an increase of the heart mass was observed in WD-fed male ApoE$^{-/-}$ mice, but when adjusted to the total body mass, it was no longer observed (Figure 5.6G).

Figure 5.6. Quantification of the coronary artery disease and hypertrophy. (A–D) Representative images of coronary arteries with different grade of atherosclerosis. A grade of 0% occlusion, <50% occlusion, >50% occlusion and 100% occlusion was used to generate the profile (E) for each condition. (F) Representative picture of hearts from RD-fed and WD-fed mice. (G) Proportion heart mass/body mass was obtained in order to account for an effect of body mass. (n = 8–6)

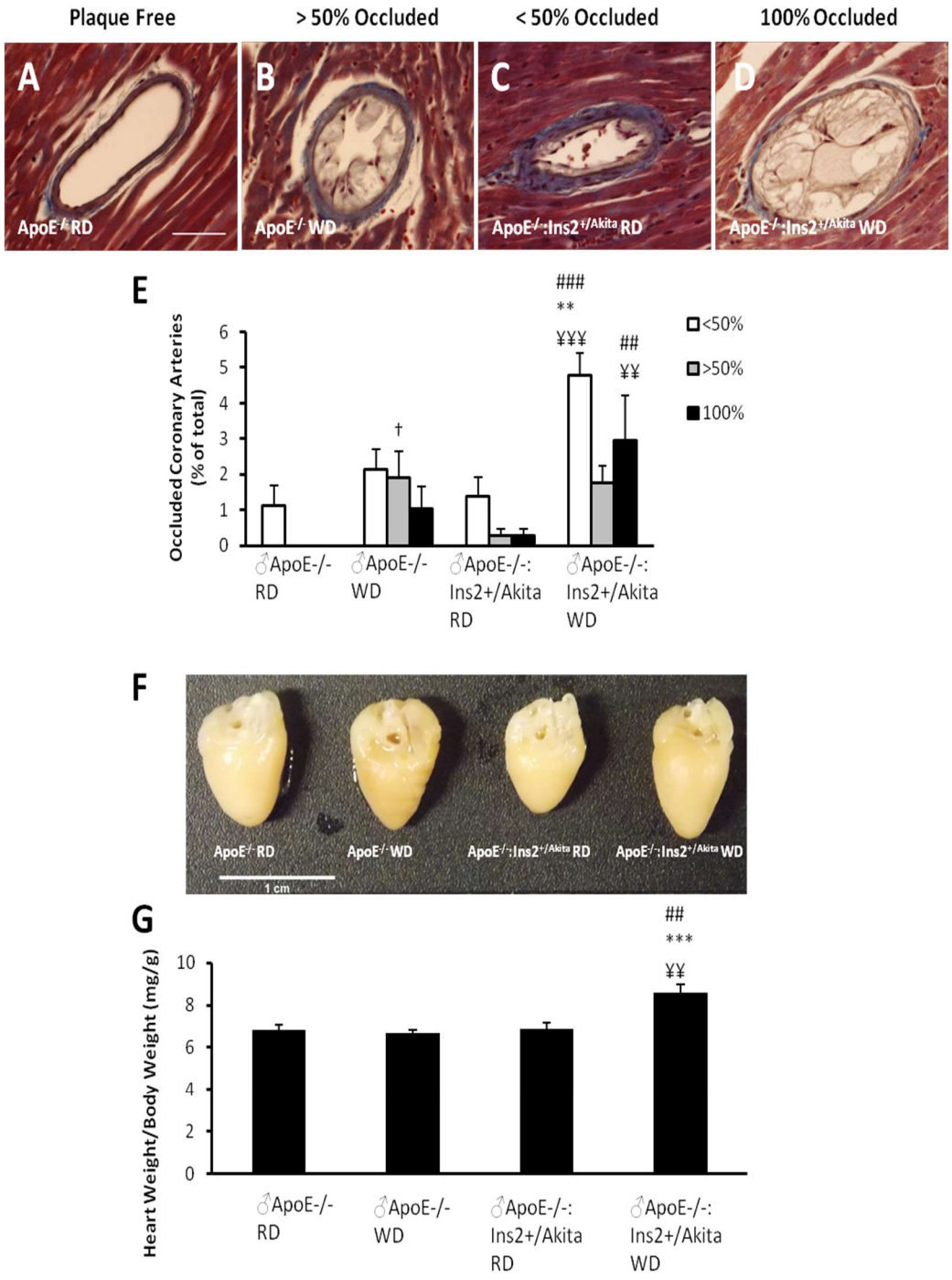

ApoE$^{-/-}$ RD vs. ApoE$^{-/-}$ WD †
ApoE$^{-/-}$ RD vs. ApoE$^{-/-}$:Ins2$^{+/Akita}$ WD #
ApoE$^{-/-}$ WD vs. ApoE$^{-/-}$:Ins2$^{+/Akita}$ RD §

ApoE$^{-/-}$ WD vs. ApoE$^{-/-}$:Ins2$^{+/Akita}$ WD *
ApoE$^{-/-}$:Ins2$^{+/Akita}$ RD vs. ApoE$^{-/-}$:Ins2$^{+/Akita}$ WD ¥
ApoE-/- RD vs. ApoE-/-:Ins2+/Akita RD &

Figure 5.6

5.6. DISCUSSION

Previously, we observed that RD-fed male ApoE$^{-/-}$:Ins2$^{+/Akita}$ mice develop chronic hyperglycemia, enhanced cholesterolemia and significantly accelerated atherosclerosis by 25 weeks of age [9, 10]. In this report we have characterized the effects of a western-type diet, rich in fat and cholesterol, on the ApoE$^{-/-}$:Ins2$^{+/Akita}$ mouse model of hyperglycemia-accelerated atherosclerosis. After feeding the animals with this western-type diet, we have found further enhanced atherosclerosis as well as a significant reduction of lifespan in the male ApoE$^{-/-}$:Ins2$^{+/Akita}$ mice. Female ApoE$^{-/-}$:Ins2$^{+/Akita}$ and ApoE$^{-/-}$ mice presented a parallel increase in atherosclerosis, and no effects on mortality were observed during the study time. Thereby, we have mainly focused our characterization on the study of advanced atherosclerosis and its effects on the heart and vasculature in the WD-fed male ApoE$^{-/-}$:Ins2$^{+/Akita}$ mice.

Rodents are well-known for being resistant to the development of atherosclerosis. Even genetically engineered atherosclerosis-prone mice (ApoE$^{-/-}$, Ldlr$^{-/-}$) are resistant to the development of coronary heart disease [16–18]. Here we have discovered the extreme phenotype shown by the WD-fed male ApoE$^{-/-}$:Ins2$^{+/Akita}$ mouse that includes; i) chronic hyperglycemia (with glucose levels 4X higher than RD-fed male ApoE$^{-/-}$ controls), ii) total plasma cholesterol levels 7X higher than RD-fed male ApoE$^{-/-}$ controls (cholesterol levels that corresponded almost entirely to non-HDL particles), and iii) total plasma triglyceride levels 11X higher than RD-fed male ApoE$^{-/-}$ controls (triglycerides that also corresponded

almost entirely with VLDL and LDL particles). This does not even account for changes in hormonal or inflammatory components that may also be affected, but it certainly established a perfect scenario for atherosclerosis. In addition, we can also compare the WD-fed male ApoE$^{-/-}$:Ins2$^{+/Akita}$ mouse to the double knockout ApoE$^{-/-}$:Ldlr$^{-/-}$ mouse [18, 19], obviously, under a similar western diet that also contains 0.15% cholesterol and 21% (wt/wt) total fat. At around 32 weeks of age, the WD-fed male ApoE$^{-/-}$:Ldlr$^{-/-}$ mouse showed serum cholesterol levels of 26mM, which were not significantly different to the 29mM showed by the WD-fed male ApoE$^{-/-}$ controls [19]. At 25 weeks of age, our WD-fed male ApoE$^{-/-}$:Ins2$^{+/Akita}$ mouse presented with plasma cholesterol levels close to 50mM and significantly different to the 30mM showed by WD-fed male ApoE$^{-/-}$ controls. Clearly establishing a more aggressive lipid profile than the ApoE$^{-/-}$:Ldlr$^{-/-}$ mouse model. Caligiuri et al. also described the development of coronary arteries, myocardial infarction and the increase of mortality in the ApoE$^{-/-}$:Ldlr$^{-/-}$ mouse. Mortality that was increased in mice older than 7 months (28 weeks) of age, later than the time that we predict for our model. One method used by Caligiuri et al. to develop ischemia and infarction in the ApoE$^{-/-}$:Ldlr$^{-/-}$ mouse was hypoxic stress. Ischemia that was prevented by the administration of an endothelin-receptor blocker. Clearly, this hypoxic stressing factor established by Caligiuri et al. is quite attractive for us due to the tight relation between hyperglycemia–hypoxia: i) hyperglycemia decreases HIF-1α stability and activity [21, 22], ii) and directly induces the expression of endothelin-1 [23, 24].

Atherosclerosis is a complex disease that can develop and progress at different rates depending upon the vascular location and internal micro-environmental conditions [25, 26]. Therefore, in this study, we have evaluated lesion development at different vascular regions that are known to be prone to atherosclerosis in order to obtain a complete picture of the general progression of the disease. Generally the term "advanced atherosclerosis" is used when a group of mice develop larger atherosclerotic lesions than a control group at a specific location (preferably at the aortic sinus). However, the clinical significance of having larger lesions at the aortic sinus may not be different, or worse, than a control group with smaller lesions. In other words, the "advanced atherosclerosis" described in the RD-fed $ApoE^{-/-}$:$Ins2^{+/Akita}$ mice when compared to RD-fed male $ApoE^{-/-}$ mice [9, 10] may have limited clinical significance since the expansion that the lesions undergo (lesion volume expanded 4X when fed the WD). In contrast, WD feeding does have a distinct effect on the viability of male $ApoE^{-/-}$:$Ins2^{+/Akita}$ mice that may be the result of massive atherosclerotic development at multiple vascular sites: aortic sinus, ascending and descending aorta, brachiocephalic artery and coronary arteries.

Another important aspect of disease progression is the vascular remodelling of the arteries in the presence of large lesions, which also has an impact on clinical events. For example, the ascending aortas of WD-fed mice were covered with very large atherosclerotic lesions (arterial cross sections covered with 40-50% of lesions), but at the same time the caliber of the arteries expanded leaving the artery

with a lumen size similar to that observed in RD-fed mice. Contrary to this, brachiocephalic arteries in the WD-fed ApoE$^{-/-}$:Ins2$^{+/Akita}$ mice tended to present with reduced lumen size when compared to the other groups. If this observation is repeated in other arteries (that seems to be the case), obstruction of blood flow (mechanical resistance) and exacerbated heart effort may be a link to the observed hypertrophy [27], or an indication of insufficient peripheral tissue oxygenation [28].

Some of the limitations of the present study lie in the effects on multiple organs of the chronic hyperglycemia and the drastic enhancement of circulating lipids. Lipotoxicity at multiple organ levels (severely damaged kidney, advanced steatosis [29, 30], or increased adiposity in the myocardium [31]) could also predict the premature death of the WD-fed male ApoE$^{-/-}$:Ins2$^{+/Akita}$ mice. Also, at this point we still lack a direct measurement of heart failure or infarction.

In conclusion we have established a diabetic mouse model with profound pathomorphological characteristics such as massive atherosclerosis, coronary artery disease and hypertrophy. These may represent the main cause or one of the main causes for shortening the lifespan of the WD-fed male ApoE$^{-/-}$:Ins2$^{+/Akita}$ mouse. In addition to that, these mice have individual metabolic parameters (hyperglycemia, hypercholesterolemia and hypertriglyceridemia) that due to their extremely high levels or combination, they may cause abnormalities in cardiac activity.

5.7. REFERENCES FOR CHAPTER 5

[1] Goraya TY, Liebson CL, Palumbo PJ: Coronary atherosclerosis in DM: a population based study. J Am Coll Cardiol. 2002, 40:946–953

[2] Gregg EW, Cheng YJ, Saydah S, Cowie C, Garfield S, Geiss L, Barker L: Trends in death rates among U.S. adults with and without diabetes between 1997 and 2006: findings from the National Health Interview Survey. Diabetes Care. 2012, 35:1252–1257

[3] Haffner SM, Lehto S, Ronnemaa T, Tyorala K and Laakso M: Mortality from coronary heart disease in subjects with type 2 diabetes and in nondiabetic subjects with and without prior myocardial infarction. N Eng J Med. 1998, 339:229–234

[4] Wang J, Takeuchi T, Tanaka S, Kubo SK, Kayo T, Lu D, Takata K, Koizumi A, Izumi T: A mutation in the insulin 2 gene induces diabetes with severe pancreatic beta-cell dysfunction in the Mody mouse. J Clin Invest. 1999, 103:27–37

[5] Oyadomari S, Koizumi A, Takeda K, Gotoh T, Akira S, Araki E, Mori M: Targeted disruption of the Chop gene delays endoplasmic reticulum stress-mediated diabetes. J Clin Invest. 2002, 109:525–532

[6] Ron D: Proteotoxicity in the endoplasmic reticulum: lessons from the Akita diabetic mouse. J Clin Invest. 2002, 109:443–445

[7] Gupta S, McGrath B, Cavener DR: PERK (EIF2AK3) regulates proinsulin trafficking and quality control in the secretory pathway. Diabetes. 2010, 59:1937–1947

[8] Liu M, Hodish I, Rhodes CJ, Arvan P: Proinsulin maturation, misfolding, and proteotoxicity. Proc Natl Acad Sci U S A. 2007, 104:15841–15846

[9] Jun JY, Ma Z, Segar L: (2011) Spontaneously diabetic Ins2(+/Akita):apoE-deficient mice exhibit exaggerated hypercholesterolemia and atherosclerosis. Am J Physiol Endocrinol Metab. 2011, 301:145–154

[10] Venegas-Pino DE, Wang P, Stoute HK, Singh-Pickersgill NA, Hong BY, Khan MI, Shi Y, Werstuck GH: Sex-Specific Differences in an $ApoE^{-/-}$:$Ins2^{+/Akita}$ Mouse Model of Accelerated Atherosclerosis. Am J Pathol. 2015, 186:67–77

[11] Venegas-Pino DE, Banko N, Khan MI, Shi Y, Werstuck GH: Quantitative analysis and characterization of atherosclerotic lesions in the murine aortic sinus. J Vis Exp. 2013, 82:e50933

[12] Thim T, Hagensen MK, Wallace-Bradley D, Granada JF, Kaluza GL, Drouet L, Paaske WP, Bøtker HE, Falk E: Unreliable assessment of necrotic core

by virtual histology intravascular ultrasound in porcine coronary artery disease. Circ Cardiovasc Imaging. 2010, 3:384–391

[13] Jeziorska M, McCollum C, Woolley DE: Calcification in atherosclerotic plaque of human carotid arteries: associations with mast cells and macrophages. J Pathol. 1998, 185:10–17

[14] Fuller M, Dadoo O, Serkis V, Abutouk D, MacDonald M, Dhingani N, Macri J, Igdoura SA, Trigatti BL: The effects of diet on occlusive coronary artery atherosclerosis and myocardial infarction in scavenger receptor class B, type 1/low-density lipoprotein receptor double knockout mice. Arterioscler Thromb Vasc Biol. 2014, 34:2394–2403

[15] Matthews DR, Hosker JP, Rudenski AS, Naylor BA, Treacher DF, Turner RC: Homeostasis model assessment: insulin resistance and beta-cell function from fasting plasma glucose and insulin concentrations in man. Diabetologia. 1985, 28:412–419

[16] Zhang SH, Reddick RL, Piedrahita JA, Maeda N: Spontaneous hypercholesterolemia and arterial lesions in mice lacking apolipoprotein E. Science. 1992, 258:468–471

[17] Plump AS, Smith JD, Hayek T, Aalto-Setälä K, Walsh A, Verstuyft JG, Rubin EM, Breslow JL: Severe hypercholesterolemia and atherosclerosis in apolipoprotein E-deficient mice created by homologous recombination in ES cells. Cell. 1992, 71:343–353

[18] Ishibashi S, Goldstein JL, Brown MS, Herz J, Burns DK: Massive xanthomatosis and atherosclerosis in cholesterol-fed low density lipoprotein receptor-negative mice. J Clin Invest. 1994, 93:1885–1893

[19] Caligiuri G, Levy B, Pernow J, Thorén P, Hansson GK: Myocardial infarction mediated by endothelin receptor signaling in hypercholesterolemic mice. Proc Natl Acad Sci U S A. 1999, 96:6920–6924

[20] Nakashima Y, Plump AS, Raines EW, Breslow JL, Ross R: ApoE-deficient mice develop lesions of all phases of atherosclerosis throughout the arterial tree. Arterioscler Thromb. 1994, 14:133–140

[21] Thangarajah H, Yao D, Chang EI, Shi Y, Jazayeri L, Vial IN, Galiano RD, Du XL, Grogan R, Galvez MG, Januszyk M, Brownlee M, Gurtner GC: The molecular basis for impaired hypoxia-induced VEGF expression in diabetic tissues. Proc Natl Acad Sci U S A. 2009, 106:13505–13510

[22] Catrina SB, Okamoto K, Pereira T, Brismar K, Poellinger L: Hyperglycemia regulates hypoxia-inducible factor-1alpha protein stability and function. Diabetes. 2004, 53:3226–3232.

[23] Park JY, Takahara N, Gabriele A, Chou E, Naruse K, Suzuma K, Yamauchi T, Ha SW, Meier M, Rhodes CJ, King GL: Induction of endothelin-1 expression by glucose: an effect of protein kinase C activation. Diabetes. 2000, 49:1239–1248

[24] Hargrove GM, Dufresne J, Whiteside C, Muruve DA, Wong NC: Diabetes mellitus increases endothelin-1 gene transcription in rat kidney. Kidney Int. 2000, 58:1534–1545

[25] VanderLaan PA, Reardon CA, Getz GS: Site specificity of atherosclerosis: site-selective responses to atherosclerotic modulators. Arterioscler Thromb Vasc Biol. 2004, 24:12–22

[26] Chatzizisis YS, Coskun AU, Jonas M, Edelman ER, Feldman CL, Stone PH: Role of endothelial shear stress in the natural history of coronary atherosclerosis and vascular remodeling: molecular, cellular, and vascular behavior. J Am Coll Cardiol. 2007, 49:2379–2393

[27] Lavanderos S, Muñoz JP, Salas D, Rodríguez A, Chiong M, Bravo R, Zepeda R, García L: Hipertrofia miocárdica: bases moleculares, modulación e implicancias clínicas / Myocardial hypertrophy: molecular bases, clinical modulation and implications. Cardiol clín. 2007, 23:4–17

[28] Dieter RS, Chu WW, Pacanowski JP Jr, McBride PE, Tanke TE: The significance of lower extremity peripheral arterial disease. Clin Cardiol. 2002, 25:3–10

[29] Kusminski CM, Shetty S, Orci L, Unger RH, Scherer PE: Diabetes and apoptosis: lipotoxicity. Apoptosis. 2009, 14:1484–1495

[30] Schaffer JE: Lipotoxicity: when tissues overeat. Curr Opin Lipidol. 2003, 14:281-287

[31] McGavock JM, Victor RG, Unger RH, Szczepaniak LS; American College of Physicians and the American Physiological Society: Adiposity of the heart, revisited. Ann Intern Med. 2006, 144:517–524

CHAPTER 6: General Discussion

If the predictions for future prevalence of diabetes mellitus and impaired glucose tolerance are accurate, by the year 2025 we will have 333 million people with diabetes and 472 million people with IGT, together representing over 15% of the global adult population [5]. These increases are likely driven by the continued worldwide trends toward increased urbanization, aging populations, disproportionate diets, lack of physical activity, and other unhealthy lifestyles. Furthermore, DM is associated with a cardiovascular mortality rate that exceeds 70%, and diabetic people are 2 to 4 times more likely to die from cardiovascular events than people with no history of diabetes [25]. These facts significantly add to the DM-related health care burden on our society. The main goals of our study were to provide new insights into how diabetes-accelerates development of atherosclerosis, the underlying cause of most CVD. Toward this goal we also established and characterized new mouse models that can be used for further investigation into mechanisms of disease development.

In chapter 3, our results support a direct role for chronic hyperglycemia in the accelerated development of atherosclerotic lesions. In our model, atherogenesis directly correlates with blood glucose levels and accelerated lesion development occurs prior to the onset of overt dyslipidemia. These findings suggest that glucose is primarily responsible for the vascular changes [125, 127]. We investigated the possible effects of hyperglycemia on the vasa vasorum, as well as potential

correlations between vasa vasorum structure and atherosclerosis in our established models.

The vasa vasorum was identified in serial sections of aorta from 5-, 10-, 15- and 20-week-old normoglycemic and hyperglycemic ApoE$^{-/-}$ mice that were immunostained with an antibody against the endothelial marker, von Willebrand Factor (vWF). Microvessel number and cross sectional areas of the atherosclerotic lesions were quantified at the aortic root, an atherosclerosis-prone region where lesions initially develop, as well as in regions of the aorta that are relatively resistant to the development of atherosclerosis. The data indicate that atherosclerotic lesion growth in normoglycemic ApoE$^{-/-}$ mice is associated with expansion in the number of microvessels of the vasa vasorum. This likely corresponds to the increasing blood supply demands of the thickening artery wall and is consistent with observations from other laboratories [156–160]. In contrast, in hyperglycemic ApoE$^{-/-}$ mice, there is no significant expansion of the vasa vasorum in atherosclerotic regions. This is despite the fact that lesions in hyperglycemic mice are at least 2X larger than those in normoglycemic mice at 15 weeks of age. As a control, we have shown that insulin supplementation of STZ-injected ApoE$^{-/-}$ mice normalizes blood glucose levels, attenuates atherosclerosis, and rescues vasa vasorum deficiency.

Taken together these data are the first indication that i) hyperglycemia attenuates neovascularization of the vasa vasorum during normal artery development and especially during atherogenesis and ii) expansion of the vasa

vasorum is not required to support accelerated atherosclerosis in this model. Preliminary investigations into the mechanism(s) underlying these observations suggest that the larger, more advanced, lesions in hyperglycemic mice exhibit significantly increased levels of hypoxia and HIF-1α, but a decrease in VEGF, relative to normoglycemic controls. These findings suggest that there is a disconnection between pro-angiogenic stimuli and response. This observation is consistent with reports from Thangarajah et al. (2009) who suggested that hyperglycemia-induced glycation of the HIF complex cofactor, p300, inhibits HIF-1α activity thereby impairing VEGF expression [161].

One major limitation of this study is the severity of the model. It has been shown that the multiple low doses of STZ, though less impactful that a single high dose, still lead to the elimination of virtually all the pancreatic beta cells after 14 days from the last injection (of a round of 5 daily injections at 40mg/Kg body weight STZ) [147–149]. This is accompanied by the reduction of circulating insulin to the limits of detection (by ELISA) [146, 147, 162] and a dramatic increase in blood glucose concentrations (~30mM). The physiological relevance of these severe changes to the more moderate hyperglycemia observed in humans with T2DM certainly could be challenged. The potential role of insulin was also not addressed in this study. To begin to address some of these limitations, we developed a new atherosclerosis-prone, hyperglycemic mouse model (Chapter 4).

In Chapter 4, we characterize the effects of introducing the $Ins2^{Akita}$ mutation into the $ApoE^{-/-}$ mouse strain as an alternative model to the STZ-injected

$ApoE^{-/-}$ mouse. We observe a very significant, and unexpected, difference between the resulting phenotypes of male and female $ApoE^{-/-}$:$Ins2^{+/Akita}$ mice. To summarize, male $ApoE^{-/-}$:$Ins2^{+/Akita}$ mice present with chronic hyperglycemia that leads to enhanced hypercholesterolemia and advanced atherosclerosis. Female mice with the $Ins2^{Akita}$ mutation develop transient hyperglycemia, which appears to be sufficient to accelerate the development of atherosclerosis, relative to normoglycemia female $ApoE^{-/-}$ mice.

Castration in normoglycemic $ApoE^{-/-}$ mice clearly exposes the protective vascular effect of androgens [163–165]. The castrated mice develop larger atherosclerotic lesions compared to sham-operated age and sex matched controls, but this effect was not observed in the $ApoE^{-/-}$:$Ins2^{+/Akita}$ mice. Measurement of plasma testosterone showed that testosterone levels are significantly lower in these hyperglycemic mice, relative to normoglycemic controls. This is consistent with previous observations in hyperglycemic rodents [166] and humans [167, 168]. Decreased testosterone combined with chronic hyperglycemia and enhanced hypercholesterolemia would be expected to exacerbate the development of atherosclerosis. Interestingly, when the castration is carried out in the hyperglycemic $ApoE^{-/-}$:$Ins2^{+/Akita}$ mice atherosclerosis is attenuated. This effect correlates to the reduction in blood glucose, non-HDL-cholesterol levels and the improved insulin sensitivity. Together, these results support a model in which testosterone confers vascular protection in the male normoglycemic $ApoE^{-/-}$ mice, but in diabetic mice, testosterone appears to exacerbate hyperglycemia,

hypercholesterolemia, and ultimately atherosclerosis. Behind these observations there is a clinical motivation that is worthy of future investigation. Long-term testosterone replacement in diabetic men may bring certain risks which could be associated with the observations in the male ApoE$^{-/-}$:Ins2$^{+/Akita}$ mouse. Future studies should be carried out to directly test the effects of exogenous testosterone in this hyperglycemic mouse model.

Female Ins2$^{+/Akita}$ mice have been reported to be hyperglycemic, but with lower blood glucose levels than male Ins2$^{+/Akita}$ mice [150]. In this study we show that, by 15 weeks of age, blood glucose levels in female ApoE$^{-/-}$:Ins2$^{+/Akita}$ mice are not significantly different from ApoE$^{-/-}$ controls. This phenomenon is partially dependent upon ApoE-deficiency because significant hyperglycemia is sustained at 15 weeks of age in heterozygous ApoE$^{+/-}$:Ins2$^{+/Akita}$ females. The ApoE$^{-/-}$-dependence of this effect is likely why it has not been previously reported.

The underlying mechanisms by which female (but not male) mice can produce functional insulin in the presence of the Ins2^{Akita} mutation have not been explained. We show that female ApoE$^{-/-}$:Ins2$^{+/Akita}$ mice have significantly less beta cell stress (indicated by GADD153 staining) compared to males. It is possible that the presence of estrogen and/or progesterone; i) enhances the ability of the beta cells to properly fold and process nascent wild type insulin and/or ii) enhances the capacity of the beta cell to degrade mutant insulin.

We also demonstrate that the transient hyperglycemia in female ApoE$^{-/-}$:Ins2$^{+/Akita}$ mice does not exacerbate the already dyslipidemic profile of ApoE$^{-/-}$

mice, but does promote accelerated atherosclerosis. Ovariectomization of ApoE$^{-/-}$:Ins2$^{+/Akita}$ mice induces sustained hyperglycemia, effectively abolishing the observed protection from ER stress (chronically induced by the Ins2^{Akita} mutation) in the pancreatic beta-cells and reducing the ability to produce functional insulin. The atherosclerotic lesion volumes of the ovariectomized ApoE$^{-/-}$:Ins2$^{+/Akita}$ mice are similar to those observed in the sham-operated ApoE$^{-/-}$:Ins2$^{+/Akita}$ and the ApoE$^{-/-}$ mice, but specific characteristics of the lesions appear to be advanced in addition to the lipid accumulation in the whole aortas. These findings suggest that a brief exposure to hyperglycemia is sufficient to accelerate the atherogenic process. Once started, atherosclerosis continues at an accelerated pace, even if glucose levels are normalized. This "metabolic memory" (early hyperglycemia is remembered by organs and tissues) is consistent with the findings of the DCCT/EDIC [169, 170] studies that showed that individuals who eventually controlled their blood glucose levels had significant microvascular and cardiovascular complications decades after the end of the study.

Therefore, after the extensive characterization of both sexes of the ApoE$^{-/-}$:Ins2$^{+/Akita}$ mouse we have revealed distinct roles for the hormonal component from each sex in diabetes and the development of atherosclerosis by affecting the function of the pancreas as well as pathogenesis in the artery wall. Differences in the incidence and the prevalence of DM between sexes have been described before [171, 172]. In fact, sex differences in prevalence extend to dyslipidemia [173, 174],

obesity [175, 176], hypertension [177], atherosclerotic development [178] and the risk of myocardial infarction [179].

When we quantify the vasa vasorum in the chronic hyperglycemic male ApoE$^{-/-}$:Ins2$^{+/Akita}$ mice (Supplemental Figure 1, Appendix 4) we observe the vasa vasorum expansion along with the lesion growth. The main reason for this effect may be the enhanced hypercholesterolemia that male ApoE$^{-/-}$:Ins2$^{+/Akita}$ mice develop, which is not observed in the previous model of STZ-injected female ApoE$^{-/-}$ mice. In the current scientific literature, atherosclerotic lesion growth is associated with vasa vasorum neovascularization (expansion) [180, 181]. When the arterial wall becomes thicker during atherosclerosis, hypoxia promotes neovascularization to meet the requirements to maintain the vessel wall and the cells that compose it [182]. Several studies, including ours, have investigated the vasa vasorum in mouse models of high-fat-diet (HFD) accelerated atherosclerosis [156–160]. In these models, lesion size directly correlates to stimulated neovascularization suggesting the direct association between expansive vasa vasorum and atherogenesis, or *vice versa*. According to this the enhanced hypercholesterolemia developed by male ApoE$^{-/-}$:Ins2$^{+/Akita}$ mice may cover the effect of hyperglycemia on the vasa vasorum previously described. The mechanisms by which enhanced dyslipidemia drives angiogenesis are not known.

In Chapter 5, we further developed the ApoE$^{-/-}$:Ins2$^{+/Akita}$ mouse model by examining the effects of a western-type diet on hyperglycemia-accelerated atherosclerosis. After feeding the animals with this diet, we have found further

enhanced atherosclerosis as well as a significant reduction in the lifespan of the male ApoE$^{-/-}$:Ins2$^{+/Akita}$ mice. Here we have discovered the extreme phenotype shown by the WD-fed male ApoE$^{-/-}$:Ins2$^{+/Akita}$ mouse that includes; i) chronic hyperglycemia, ii) chronic hypercholesterolemia, iii) sustained hypertriglyceridemia, iv) cholesterol and triglycerides that corresponded almost entirely with VLDL and LDL particles, v) massive and advanced atherosclerosis in the aortic sinus, ascending and descending aorta and brachiocephalic arteries, vi) coronary artery disease and cardiac hypertrophy, and vii) significantly increased mortality. Also when doing a comparison between the WD-fed ApoE$^{-/-}$:Ins2$^{+/Akita}$ model to another severe phenotype model, the WD-fed male ApoE$^{-/-}$:Ldlr$^{-/-}$ mouse [183, 184], we can basically compare the Ins2^{Akita} mutation to the absence of the LDL receptor. In many respects the phenotype of the hyperglycemic WD-fed ApoE$^{-/-}$:Ins2$^{+/Akita}$ model is more severe. The WD-fed male ApoE$^{-/-}$:Ldlr$^{-/-}$ mouse showed serum cholesterol levels of 26mM at ~32 weeks of age versus the 50mM of plasma cholesterol showed by our WD-fed male ApoE$^{-/-}$:Ins2$^{+/Akita}$ mouse at 25 weeks of age (comparison made under similar western-type diets). Caligiuri et al. also described the development of coronary arteries, myocardial infarction and the increase of mortality in the ApoE$^{-/-}$:Ldlr$^{-/-}$ mouse. Mortality was increased in the ApoE$^{-/-}$:Ldlr$^{-/-}$ mouse, but it seems to be even more accelerated in our model since the endpoint that we observe was around the 23–25 weeks of age. One method used by Caligiuri et al. to develop ischemia and infarction in the ApoE$^{-/-}$:Ldlr$^{-/-}$ mouse was hypoxic stress. They showed that this effect could be prevented by

administration of an endothelin receptor blocker. Clearly, this hypoxic factor established by Caligiuri et al. invite us to continue studying our mouse model because hyperglycemia has been tightly related to hypoxia: decreasing HIF-1α stability and activity [161, 185] and directly inducing the expression of endothelin-1 [186, 187]. In addition to the ApoE$^{-/-}$:Ldlr$^{-/-}$ mouse model, another null mutation—HDL scavenger receptor class B type I—has also been incorporated into the ApoE$^{-/-}$ mouse giving rise to the ApoE$^{-/-}$:SR-BI$^{-/-}$ mouse model. This mouse model is one of the few to exhibit the spontaneous development of myocardial infarctions (MI), as well as hypercholesterolemia, massive atherosclerosis, occlusive coronary arterial lesions, cardiac dysfunction and premature death [188–190]. It is postulated that the addition of the SR-BI null mutation not only induces changes in plasma proatherogenic and antiatherogenic lipoproteins, but also alters cholesterol flux into or out of the artery wall, and alters reverse cholesterol transport [190], making of this model a more complete and aggressive one since there is no need of high-fat supplementation for such phenotype. Evidence has also associated hyperglycemia and the SR-BI expression in hepatocytes [191] and macrophages [192] suggesting for a role in the ApoE$^{-/-}$:Ins2$^{+/Akita}$ model.

The obvious limitations of the WD-fed ApoE$^{-/-}$:Ins2$^{+/Akita}$ model are the severity of the metabolic phenotype. The main advantage, still to be further explored, is the possibility that this model exhibits cardiovascular events—which are extremely rare in rodent models. It in fact appears that extreme models may be required to induce cardiovascular events in mice.

Future Research

Future studies should be focused upon the further study of the ApoE$^{-/-}$:Ins2$^{+/Akita}$ model in three main areas:

i) To investigate the potential protective effects of estrogen/progesterone on beta cells, a procedure for islet isolation has been replicated from Stull ND et al. (2012) [193]. Pancreatic islets from diabetic mice will be treated in culture with estrogen and progesterone in order to study effects on UPR activation and insulin production *ex vivo*.

ii) To further investigate the potential pro-atherogenic effects of testosterone in hyperglycemic mice, testosterone will be administered to ApoE$^{-/-}$ and ApoE$^{-/-}$:Ins2$^{+/Akita}$ using the Alzet pump system. Atherosclerotic lesion development will be examined as previously described.

iii) To further examine the possibility that western-type diet fed ApoE$^{-/-}$:Ins2$^{+/Akita}$ mice develop heart failure and MI, future studies will include heart-related measurements (ECG) and hearts will be more closely examined for fibrosis and indications of infarcts.

With respect to the potential role of the vasa vasorum in atherosclerosis, we can investigate the specific effects of VEGF using mice that are heterozygous for a hypermorphic allele of VEGF-A (VEGF$^{hi/+}$) [194] or heterozygous for a hypomorphic allele for VEGF-A (VEGF$^{lo/+}$) [195]. These heterozygous mice show no overt phenotype, but homozygous VEGF$^{hi/hi}$ and VEGF$^{lo/lo}$ mice are not viable [194, 195]. VEGF expression levels are 2 fold higher in VEGF$^{hi/+}$ mice and 2–4 fold

lower in $VEGF^{lo/+}$ mice relative to wild type littermates [194, 195]. These mice will be crossed with $ApoE^{-/-}$ mice to give $ApoE^{-/-}$:$VEGF^{hi/+}$ and $ApoE^{-/-}$:$VEGF^{lo/+}$. Atherosclerotic development will be measured in normoglycemic and hyperglycemic $ApoE^{-/-}$:$VEGF^{hi/+}$ and $ApoE^{-/-}$:$VEGF^{lo/+}$ mice.

Significance and relevance of the research

The prevalence of diabetes is increasing rapidly around the world. We, the biomedical researchers and healthcare professionals, have made some progress attenuating the consequences of diabetes mellitus that has significantly improved the quality of life and the expected lifespan of people with diabetes. Still, nearly three out of four individuals with diabetes die from CVD. Clearly, there is a lot of work to do. Thus, new evidence as the role of diabetic microvascular disease in the accelerated development of atherosclerosis would represent a paradigm shift in our understanding of how diabetes predisposes individuals to cardiovascular disease. Also, the establishment of the $ApoE^{-/-}$:$Ins2^{+/Akita}$ mouse model offers a new platform to expand the understanding of the mechanisms by which diabetes promotes CVD.

References for General Introduction and General Discussion

[1] American Diabetes Association: Diagnosis and Classification of Diabetes Mellitus. Diabetes Care. 2011, 34: S62–S69

[2] American Diabetes Association: (2) Classification and diagnosis of diabetes. Diabetes Care. 2015, 38:S8–S16

[3] Nathan DM, Davidson MB, DeFronzo RA, Heine RJ, Henry RR, Pratley R, Zinman B; American Diabetes Association: Impaired fasting glucose and impaired glucose tolerance: implications for care. Diabetes Care. 2007, 30:753–759

[4] Zimmet P, Alberti KG, and Shaw J: Global and societal implications of the diabetes epidemic. Nature. 2001, 414:782–788

[5] International Diabetes Federation. IDF Diabetes Atlas, 2nd edition. Brussels, Belgium. 2003

[6] Fong DS, Aiello LP, Ferris FL 3rd, Klein R: Diabetic retinopathy. Diabetes Care. 2004, 27:2540–2553

[7] de Boer IH, Rue TC, Hall YN, Heagerty PJ, Weiss NS, Himmelfarb J. Temporal trends in the prevalence of diabetic kidney disease in the United States. JAMA. 2011, 305:2532–2539

[8] U.S. Renal Data System, USRDS 2013 Annual Data Report: Atlas of Chronic Kidney Disease and End-Stage Renal Disease in the United States, National Institutes of Health, National Institute of Diabetes and Digestive and Kidney Diseases, Bethesda, MD, 2013

[9] Calle-Pascual AL, Redondo MJ, Ballesteros M, Martinez-Salinas MA, Diaz JA, De Matias P, Calle JR, Gil E, Jimenez M, Serrano FJ, Martin-Alvarez PJ, Maranes JP: Nontraumatic lower extremity amputations in diabetic and non-diabetic subjects in Madrid, Spain. Diabetes Metab. 1997, 23:519–523

[10] Bild DE, Selby JV, Sinnock P, Browner WS, Braveman P, Showstack JA: Lower-extremity amputation in people with diabetes. Epidemiology and prevention. Diabetes Care. 1989, 12:24–31

[11] Boulton AJ: Lowering the risk of neuropathy, foot ulcers and amputations. Diabet Med. 1998; 15:S57–S59

[12] Gu K, Cowie CC, Harris MI: Mortality in adults with and without diabetes in a national cohort of the U.S. population, 1971–1993. Diabetes Care. 1998, 21:1138–1145

[13] Geiss LS, Herman WH, Smith PJ: Mortality in non-insulin dependent diabetes. Diabetes in America. Bethesda, MD: National Institutes of Health. 1995, 233–257

[14] D'Adamo E, Caprio S: Type 2 diabetes in youth: epidemiology and pathophysiology. Diabetes Care. 2011, 34:S161–S165

[15] Calcutt NA, Cooper ME, Kern TS, Schmidt AM: Therapies for hyperglycaemia-induced diabetic complications: from animal models to clinical trials. Nat Rev Drug Discov. 2009, 8:417–429

[16] DeFronzo RA: Pharmacologic therapy for type 2 diabetes mellitus. Ann Intern Med. 1999, 131:281–303

[17] UK Prospective Diabetes Study (UKPDS) Group: Intensive blood-glucose control with sulphonylureas or insulin compared with conventional treatment and risk of complications in patients with type 2 diabetes (UKPDS 33). Lancet. 1998, 352:837–853

[18] ADVANCE Collaborative Group, Patel A, MacMahon S, Chalmers J, Neal B, Billot L, Woodward M, Marre M, Cooper M, Glasziou P, Grobbee D, Hamet P, Harrap S, Heller S, Liu L, Mancia G, Mogensen CE, Pan C, Poulter N, Rodgers A, Williams B, Bompoint S, de Galan BE, Joshi R, Travert F: Intensive blood glucose control and vascular outcomes in patients with type 2 diabetes. N Engl J Med. 2008, 358:2560–2572

[19] Action to Control Cardiovascular Risk in Diabetes Study Group, Gerstein HC, Miller ME, Byington RP, Goff DC Jr, Bigger JT, Buse JB, Cushman WC, Genuth S, Ismail-Beigi F, Grimm RH Jr, Probstfield JL, Simons-Morton DG, Friedewald WT: Effects of intensive glucose lowering in type 2 diabetes. N Engl J Med. 2008, 358:2545–2559

[20] Duckworth W, Abraira C, Moritz T, Reda D, Emanuele N, Reaven PD, Zieve FJ, Marks J, Davis SN, Hayward R, Warren SR, Goldman S, McCarren M, Vitek ME, Henderson WG, Huang GD; VADT Investigators. Glucose control and vascular complications in veterans with type 2 diabetes. N Engl J Med. 2009, 360:129–139

[21] Klein R, Klein BE, Moss SE: Relationship of glycemic control to diabetic microvascular complications in diabetes mellitus. Ann Intern Med. 1996, 124:90–96

[22] Beckman JA, Creager MA, Libby P: Diabetes and atherosclerosis: epidemiology, pathophysiology and management. JAMA. 2002, 287:2570–2581

[23] Valmadrid CT, Klein R, Moss SE, Klein BE: The risk of cardiovascular disease mortality associated with microalbuminuria and gross proteinuria in persons with older-onset diabetes mellitus. Arch Intern Med. 2000, 160:1093–1100

[24] Juutilainen A, Lehto S, Rönnemaa T, Pyörälä K, Laakso M: Retinopathy predicts cardiovascular mortality in type 2 diabetic men and women. Diabetes Care. 2007, 30:292–299

[25] Haffner SM, Lehto S, Ronnemaa T, Pyorala K, Laakso M: Mortality from coronary heart disease in subjects with type2 diabetes and in nondiabetic subjects with and without prior myocardial infarction. N Engl J Med. 1998, 339:229–234

[26] Lloyd-Jones D, Adams R, Carnethon M, De Simone G, Ferguson TB, Flegal K, Ford E, Furie K, Go A, Greenlund K, Haase N, Hailpern S, Ho M, Howard V, Kissela B, Kittner S, Lackland D, Lisabeth L, Marelli A, McDermott M, Meigs J, Mozaffarian D, Nichol G, O'Donnell C, Roger V, Rosamond W, Sacco R, Sorlie P, Stafford R, Steinberger J, Thom T, Wasserthiel-Smoller S, Wong N, Wylie-Rosett J, Hong Y; American Heart Association Statistics Committee and Stroke Statistics Subcommittee: Heart disease and stroke statistics—2009 update: a report from the American Heart Association Statistics Committee and Stroke Statistics Subcommittee. Circulation. 2009, 119:e21–181

[27] Norhammar A, Tenerz A, Nilsson G, Hamsten A, Efendíc S, Rydén L, Malmberg K: Glucose metabolism in patients with acute myocardial infarction and no previous diagnosis of diabetes mellitus: a prospective study. Lancet. 2002, 359:2140–2144

[28] Singh DK, Winocour P, Farrington K: Oxidative stress in early diabetic nephropathy: fueling the fire. Nat Rev Endocrinol. 2011, 7:176–184

[29] Aiello LP, Bursell SE, Clermont A, Duh E, Ishii H, Takagi C, Mori F, Ciulla TA, Ways K, Jirousek M, Smith LE, King GL: Vascular endothelial growth factor-induced retinal permeability is mediated by protein kinase C in vivo and suppressed by an orally effective beta-isoform-selective inhibitor. Diabetes. 1997, 46:1473–1480

[30] Cooper ME, Vranes D, Youssef S, Stacker SA, Cox AJ, Rizkalla B, Casley DJ, Bach LA, Kelly DJ, Gilbert RE: Increased renal expression of vascular endothelial growth factor (VEGF) and its receptor VEGFR-2 in experimental diabetes. Diabetes. 1999, 48:2229–2239

[31] Abaci A, Oğuzhan A, Kahraman S, Eryol NK, Unal S, Arinç H, Ergin A: Effect of diabetes mellitus on formation of coronary collateral vessels. Circulation. 1999, 99:2239–2242

[32] Galiano RD, Tepper OM, Pelo CR, Bhatt KA, Callaghan M, Bastidas N, Bunting S, Steinmetz HG, Gurtner GC: Topical vascular endothelial growth factor accelerates diabetic wound healing through increased angiogenesis and by mobilizing and recruiting bone marrow-derived cells. Am J Pathol. 2004, 164:1935–1947

[33] John PR, Thuluvath PJ: Outcome of liver transplantation in patients with diabetes mellitus: a case-control study. Hepatology. 2001, 34:889–895

[34] Costa PZ, Soares R: Neovascularization in diabetes and its complications. Unraveling the angiogenic paradox. Life Sci. 2013, 92:1037–1045

[35] de Vriese AS, Tilton RG, Elger M, Stephan CC, Kriz W, Lameire NH: Antibodies against vascular endothelial growth factor improve early renal dysfunction in experimental diabetes. J Am Soc Nephrol. 2001, 12:993–1000

[36] Galiano RD, Tepper OM, Pelo CR, Bhatt KA, Callaghan M, Bastidas N, Bunting S, Steinmetz HG, Gurtner GC: Topical vascular endothelial growth factor accelerates diabetic wound healing through increased angiogenesis and by mobilizing and recruiting bone marrow-derived cells. Am J Pathol. 2004, 164:1935–1947

[37] Lusis AJ: Atherosclerosis. Nature. 2000, 407:233–241

[38] Kwon HM, Sangiorgi G, Ritman EL, Lerman A, McKenna C, Virmani R, Edwards WD, Holmes DR, Schwartz RS: Adventitial vasa vasorum in balloon-injured coronary arteries: visualization and quantitation by a microscopic three-dimensional computed tomography technique. J Am Coll Cardiol. 1998, 32:2072–2079

[39] Ware JA: Too many vessels? Not enough? The wrong kind? The VEGF debate continues. Nat Med. 2001, 7:403–404

[40] Fleiner M, Kummer M, Mirlacher M, Sauter G, Cathomas G, Krapf R, Biedermann BC: Arterial neovascularization and inflammation in vulnerable patients: early and late signs of symptomatic atherosclerosis. Circulation. 2004, 110:2843–2850

[41] Langheinrich AC, Michniewicz A, Sedding DG, Walker G, Beighley PE, Rau WS, Bohle RM, Ritman EL: Correlation of vasa vasorum neovascularization and plaque progression in aortas of apolipoprotein E(-/-)/low-density lipoprotein(-/-) double knockout mice. Arterioscler Thromb Vasc Biol. 2006, 26:347–352

[42] Parathath S, Mick SL, Feig JE, Joaquin V, Grauer L, Habiel DM, Gassmann M, Gardner LB, Fisher EA: Hypoxia is present in murine atherosclerotic plaques and has multiple adverse effects on macrophage lipid metabolism. Circ Res. 2011, 109:1141–1152

[43] Lucerna M, Zernecke A, de Nooijer R, de Jager SC, Bot I, van der Lans C, Kholova I, Liehn EA, van Berkel TJ, Yla-Herttuala S, Weber C, Biessen EA: Vascular endothelial growth factor-A induces plaque expansion in ApoE knock-out mice by promoting de novo leukocyte recruitment. Blood. 2007, 109:122–129

[44] Petrovan RJ, Kaplan CD, Reisfeld RA, Curtiss LK. DNA vaccination against VEGF receptor 2 reduces atherosclerosis in LDL receptor-deficient mice. Arterioscler Thromb Vasc Biol. 2007, 27:1095–1100

[45] Gössl M, Versari D, Lerman LO, Chade AR, Beighley PE, Erbel R, Ritman EL: Low vasa vasorum densities correlate with inflammation and subintimal thickening: potential role in location – determination of atherogenesis. Atherosclerosis. 2009, 206:362–368

[46] Gössl M, Beighley PE, Malyar NM, Ritman EL: 2004. Role of vasa vasorum in transendothelial solute transport in the coronary vessel wall: a study with cryostatic micro-CT. Am J Physiol Heart Circ Physiol. 2004, 287:H2346–H2351

[47] Ross R: Atherosclerosis—an inflammatory disease. N Engl J Med. 1999, 340:115–126

[48] Hadi HA, Carr CS, Al Suwaidi J: Endothelial dysfunction: cardiovascular risk factors, therapy, and outcome. Vasc Health Risk Manag. 2005, 1:183–198

[49] Hahn C, Schwartz MA: Mechanotransduction in vascular physiology and atherogenesis. Nat Rev Mol Cell Biol. 2009, 10:53–62

[50] Pober JS, Sessa WC: Evolving functions of endothelial cells in inflammation. Nat Rev Immunol. 2007, 7:803–815

[51] Orr AW, Sanders JM, Bevard M, Coleman E, Sarembock IJ, Schwartz MA: The subendothelial extracellular matrix modulates NF-kappaB activation by flow: a potential role in atherosclerosis. J Cell Biol. 2005, 169:191–202

[52] Kuhlencordt PJ, Gyurko R, Han F, Scherrer-Crosbie M, Aretz TH, Hajjar R, Picard MH, Huang PL: Accelerated atherosclerosis, aortic aneurysm formation, and ischemic heart disease in apolipoprotein E/endothelial nitric oxide synthase double-knockout mice. Circulation. 2001, 104:448–454

[53] Landmesser U, Hornig B, Drexler H: Endothelial function: a critical determinant in atherosclerosis? Circulation. 2004, 109:II27–II33

[54] Ley K, Miller YI, Hedrick CC: Monocyte and macrophage dynamics during atherogenesis. Arterioscler Thromb Vasc Biol. 2011, 31:1506–1516

[55] Oram JF, Lawn RM: ABCA1. The gatekeeper for eliminating excess tissue cholesterol. J Lipid Res. 2001, 42:1173–1179

[56] Oram JF: Novel approaches to treating cardiovascular disease: lessons from Tangier disease. Expert Opin Investig Drugs. 2001, 10:427–438

[57] Wang N, Silver DL, Thiele C, Tall AR: ATP-binding cassette transporter A1 (ABCA1) functions as a cholesterol efflux regulatory protein. J Biol Chem. 2001, 276:23742–23747

[58] Wang N, Lan D, Chen W, Matsuura F, Tall AR: ATP-binding cassette transporters G1 and G4 mediate cellular cholesterol efflux to high-density lipoproteins. Proc Natl Acad Sci U S A. 2004, 101:9774–9779

[59] Kennedy MA, Barrera GC, Nakamura K, Baldan A, Tarr P, Fishbein MC, Frank J, Francone OL, Edwards PA: ABCG1 has a critical role in mediating cholesterol efflux to HDL and preventing cellular lipid accumulation. Cell Metab. 2005; 1:121–131

[60] Feng B, Yao PM, Li Y, Devlin CM, Zhang D, Harding HP, Sweeney M, Rong JX, Kuriakose G, Fisher EA, Marks AR, Ron D, Tabas I: The endoplasmic reticulum is the site of cholesterol-induced cytotoxicity in macrophages. Nat Cell Biol. 2003, 5:781–792

[61] Seimon TA, Nadolski MJ, Liao X, Magallon J, Nguyen M, Feric NT, Koschinsky ML, Harkewicz R, Witztum JL, Tsimikas S, Golenbock D, Moore KJ, Tabas I: Atherogenic lipids and lipoproteins trigger CD36-TLR2-dependent apoptosis in macrophages undergoing endoplasmic reticulum stress. Cell Metab. 2010, 12:467–482

[62] Moore KJ, Sheedy FJ, Fisher EA: Macrophages in atherosclerosis: a dynamic balance. Nat Rev Immunol. 2013, 13:709–721

[63] Little WC, Downes TR, Applegate RJ: The underlying coronary lesion in myocardial infarction: implications for coronary angiography. Clin Cardiol. 1991, 14:868–874

[64] Virmani R, Burke AP, Kolodgie F: Morphological characteristics of coronary atherosclerosis in diabetes mellitus. Can J Cardiol. 2006, 22:81B–84B

[65] Burke AP, Kolodgie FD, Zieske A, Fowler DR, Weber DK, Varghese PJ, Farb A, Virmani R: Morphologic findings of coronary atherosclerotic plaques in diabetics: a postmortem study. Arterioscler Thromb Vasc Biol. 2004, 24:1266–1271

[66] Schurgin S, Rich S, Mazzone T: Increased prevalence of significant coronary artery calcification in patients with diabetes. Diabetes Care. 2001, 24:335–338

[67] Mandarino LJ, Finlayson J, Hassell JR: High glucose downregulates glucose transport activity in retinal capillary pericytes but not endothelial cells. Invest Ophthalmol Vis Sci. 1994, 35:964–972

[68] Kaiser N, Sasson S, Feener EP, Boukobza-Vardi N, Higashi S, Moller DE, Davidheiser S, Przybylski RJ, King GL: Differential regulation of glucose transport and transporters by glucose in vascular endothelial and smooth muscle cells. Diabetes. 1993, 42:80–89

[69] Wolff SP, Jiang ZY, Hunt JV: Protein glycation and oxidative stress in diabetes mellitus and ageing. Free Radic Biol Med. 1991, 10:339–352

[70] Eriksson UJ, Borg LA: Diabetes and embryonic malformations. Role of substrate-induced free-oxygen radical production for dysmorphogenesis in cultured rat embryos. Diabetes. 1993, 42:411–419

[71] Du X, Matsumura T, Edelstein D, Rossetti L, Zsengellér Z, Szabó C, Brownlee M: Inhibition of GAPDH activity by poly(ADP-ribose) polymerase activates three major pathways of hyperglycemic damage in endothelial cells. J Clin Invest. 2003, 112:1049–1057

[72] Sawa A, Khan AA, Hester LD, Snyder SH: Glyceraldehyde-3-phosphate dehydrogenase: nuclear translocation participates in neuronal and nonneuronal cell death. Proc Natl Acad Sci U S A. 1997, 94:11669–11674

[73] Schmidtz HD: Reversible nuclear translocation of glyceraldehyde-3-phosphate dehydrogenase upon serum depletion. Eur J Cell Biol. 2001, 80:419–427

[74] Du XL, Edelstein D, Rossetti L, Fantus IG, Goldberg H, Ziyadeh F, Wu J, Brownlee M: Hyperglycemia-induced mitochondrial superoxide overproduction activates the hexosamine pathway and induces plasminogen activator inhibitor-1 expression by increasing Sp1 glycosylation. Proc Natl Acad Sci U S A. 2000, 97:12222–12226

[75] González RG, Barnett P, Aguayo J, Cheng HM, Chylack LT Jr: Direct measurement of polyol pathway activity in the ocular lens. Diabetes. 1984, 33:196–199

[76] Morrison AD, Clements RS Jr, Travis SB, Oski F, Winegrad AI: Glucose utilization by the polyol pathway in human erythrocytes. Biochem Biophys Res Commun. 1970, 40:199–205

[77] Lee AY, Chung SS: Contributions of polyol pathway to oxidative stress in diabetic cataract. FASEB J. 1999, 13:23–30

[78] Markus HB, Raducha M, Harris H: Tissue distribution of mammalian aldose reductase and related enzymes. Biochem Med. 1983, 29:31–45

[79] Vikramadithyan RK, Hu Y, Noh HL, Liang CP, Hallam K, Tall AR, Ramasamy R, Goldberg IJ: Human aldose reductase expression accelerates diabetic atherosclerosis in transgenic mice. J Clin Invest. 2005, 115:2434–2443

[80] Goldin A, Beckman JA, Schmidt AM, Creager MA: Advanced glycation end products: sparking the development of diabetic vascular injury. Circulation. 2006, 114:597–605

[81] Soro-Paavonen A, Watson AM, Li J, Paavonen K, Koitka A, Calkin AC, Barit D, Coughlan MT, Drew BG, Lancaster GI, Thomas M, Forbes JM, Nawroth PP, Bierhaus A, Cooper ME, Jandeleit-Dahm KA: Receptor for advanced glycation end products (RAGE) deficiency attenuates the development of atherosclerosis in diabetes. Diabetes. 2008, 57:2461–2469

[82] Park L, Raman KG, Lee KJ, Lu Y, Ferran LJ Jr, Chow WS, Stern D, Schmidt AM: Suppression of accelerated diabetic atherosclerosis by the soluble receptor for advanced glycation endproducts. Nat Med. 1998, 4:1025–1031

[83] Koya D, King GL: Protein kinase C activation and the development of diabetic complications. Diabetes. 1998, 47:859–866

[84] Xia P, Inoguchi T, Kern TS, Engerman RL, Oates PJ, King GL: Characterization of the mechanism for the chronic activation of diacylglycerolprotein kinase C pathway in diabetes and hypergalactosemia. Diabetes. 1994, 43:1122–1129

[85] Kuboki K, Jiang ZY, Takahara N, Ha SW, Igarashi M, Yamauchi T, Feener EP, Herbert TP, Rhodes CJ, King GL: Regulation of endothelial constitutive nitric oxide synthase gene expression in endothelial cells and in vivo: a specific vascular action of insulin. Circulation. 2000, 101:676–681

[86] Pieper GM, Riaz-ul-Haq: Activation of nuclear factor-kappaB in cultured endothelial cells by increased glucose concentration: prevention by calphostin C. J Cardiovasc Pharmacol. 1997, 30:528–532

[87] Feener EP, Xia P, Inoguchi T, Shiba T, Kunisaki M, King GL: Role of protein kinase C in glucose- and angiotensin II-induced plasminogen activator inhibitor expression. Contrib Nephrol. 1996, 118:180–187

[88] Giacco F, Brownlee M: Oxidative stress and diabetic complications. Circ Res. 2010, 107:1058–1070

[89] Buse MG: Hexosamines, insulin resistance, and the complications of diabetes: current status. Am J Physiol Endocrinol Metab. 2006, 290:E1–E8

[90] Du XL, Edelstein D, Dimmeler S, Ju Q, Sui C, Brownlee M: Hyperglycemia inhibits endothelial nitric oxide synthase activity by posttranslational modification at the Akt site. J Clin Invest. 2001, 108:1341–1348

[91] Federici M, Menghini R, Mauriello A, Hribal ML, Ferrelli F, Lauro D, Sbraccia P, Spagnoli LG, Sesti G, Lauro R: Insulin-dependent activation of endothelial nitric oxide synthase is impaired by O-linked glycosylation modification of signaling proteins in human coronary endothelial cells. Circulation. 2002, 106:466–472

[92] Wen Y, Gu J, Li SL, Reddy MA, Natarajan R, Nadler JL: Elevated glucose and diabetes promote interleukin-12 cytokine gene expression in mouse macrophages. Endocrinology. 2006, 147:2518–2525

[93] Kanter JE, Kramer F, Barnhart S, Averill MM, Vivekanandan-Giri A, Vickery T, Li LO, Becker L, Yuan W, Chait A, Braun KR, Potter-Perigo S, Sanda S, Wight TN, Pennathur S, Serhan CN, Heinecke JW, Coleman RA, Bornfeldt KE: Diabetes promotes an inflammatory macrophage phenotype and atherosclerosis through acyl-CoA synthetase 1. Proc Natl Acad Sci U S A. 2012, 109:E715–E724

[94] Parathath S, Grauer L, Huang LS, Sanson M, Distel E, Goldberg IJ, Fisher EA: Diabetes adversely affects macrophages during atherosclerotic plaque regression in mice. Diabetes. 2011, 60:1759–1769

[95] Nagareddy PR, Murphy AJ, Stirzaker RA, Hu Y, Yu S, Miller RG, Ramkhelawon B, Distel E, Westerterp M, Huang LS, Schmidt AM, Orchard TJ, Fisher EA, Tall AR, Goldberg IJ: Hyperglycemia promotes myelopoiesis and impairs the resolution of atherosclerosis. Cell Metab. 2013, 17:695–708

[96] Padmos RC, Schloot NC, Beyan H, Ruwhof C, Staal FJ, de Ridder D, Aanstoot HJ, Lam-Tse WK, de Wit H, de Herder C, Drexhage RC, Menart B, Leslie RD, Drexhage HA; LADA Consortium: Distinct monocyte gene-expression profiles in autoimmune diabetes. Diabetes. 2008, 57:2768–2773

[97] Bala M, Kopp A, Wurm S, Büchler C, Schölmerich J, Schäffler A: Type 2 diabetes and lipoprotein metabolism affect LPS-induced cytokine and chemokine release in primary human monocytes. Exp Clin Endocrinol Diabetes. 2011, 119:370–376

[98] Cipolletta C, Ryan KE, Hanna EV, Trimble ER: Activation of peripheral blood CD14+ monocytes occurs in diabetes. Diabetes. 2005, 54:2779–2786

[99] Devaraj S, Dasu MR, Rockwood J, Winter W, Griffen SC, Jialal I: Increased toll-like receptor (TLR) 2 and TLR4 expression in monocytes from patients with

type 1 diabetes: further evidence of a proinflammatory state. J Clin Endocrinol Metab. 2008, 93:578–583

[100] Mollah ZU, Pai S, Moore C, O'Sullivan BJ, Harrison MJ, Peng J, Phillips K, Prins JB, Cardinal J, Thomas R: Abnormal NF-kappa B function characterizes human type 1 diabetes dendritic cells and monocytes. J Immunol. 2008, 180:3166–3175

[101] Devaraj S, Tobias P, Jialal I: Knockout of toll-like receptor-4 attenuates the pro-inflammatory state of diabetes. Cytokine. 2011, 55:441–445

[102] Fukuhara-Takaki K, Sakai M, Sakamoto Y, Takeya M, Horiuchi S. Expression of class A scavenger receptor is enhanced by high glucose in vitro and under diabetic conditions in vivo: one mechanism for an increased rate of atherosclerosis in diabetes. J Biol Chem. 2005, 280:3355–3364

[103] Sampson MJ, Davies IR, Braschi S, Ivory K, Hughes DA. Increased expression of a scavenger receptor (CD36) in monocytes from subjects with Type 2 diabetes. Atherosclerosis. 2003, 167:129 –134

[104] Li L, Sawamura T, Renier G. Glucose enhances human macrophage LOX-1 expression: role for LOX-1 in glucose-induced macrophage foam cell formation. Circ Res. 2004, 94:892–901

[105] Mauldin JP, Nagelin MH, Wojcik AJ, Srinivasan S, Skaflen MD, Ayers CR, McNamara CA, Hedrick CC: Reduced expression of ATP-binding cassette transporter G1 increases cholesterol accumulation in macrophages of patients with type 2 diabetes mellitus. Circulation. 2008, 117:2785–2792

[106] Mauldin JP, Srinivasan S, Mulya A, Gebre A, Parks JS, Daugherty A, Hedrick CC: Reduction in ABCG1 in Type 2 diabetic mice increases macrophage foam cell formation. J Biol Chem. 2006, 281:21216–21224

[107] Robbins CS, Chudnovskiy A, Rauch PJ, Figueiredo JL, Iwamoto Y, Gorbatov R, Etzrodt M, Weber GF, Ueno T, van Rooijen N, Mulligan-Kehoe MJ, Libby P, Nahrendorf M, Pittet MJ, Weissleder R, Swirski FK: Extramedullary hematopoiesis generates Ly-6C(high) monocytes that infiltrate atherosclerotic lesions. Circulation. 2012, 125:364–374

[108] Bobryshev YV: Transdifferentiation of smooth muscle cells into chondrocytes in atherosclerotic arteries in situ: implications for diffuse intimal calcification. J Pathol. 2005, 205:641–650

[109] Allahverdian S, Chehroudi AC, McManus BM, Abraham T, Francis GA: Contribution of intimal smooth muscle cells to cholesterol accumulation and macrophage-like cells in human atherosclerosis. Circulation. 2014, 129:1551–1559

[110] Lewis GF, Carpentier A, Adeli K, Giacca A: Disordered fat storage and mobilization in the pathogenesis of insulin resistance and type 2 diabetes. Endocr Rev. 2002, 23:201–229

[111] Du X, Edelstein D, Obici S, Higham N, Zou MH, Brownlee M: Insulin resistance reduces arterial prostacyclin synthase and eNOS activities by increasing endothelial fatty acid oxidation. J Clin Invest. 2006, 116:1071–1080

[112] Rask-Madsen C, Li Q, Freund B, Feather D, Abramov R, Wu IH, Chen K, Yamamoto-Hiraoka J, Goldenbogen J, Sotiropoulos KB, Clermont A, Geraldes P, Dall'Osso C, Wagers AJ, Huang PL, Rekhter M, Scalia R, Kahn CR, King GL: Loss of insulin signaling in vascular endothelial cells accelerates atherosclerosis in apolipoprotein E null mice. Cell Metab. 2010, 11:379–389

[113] Baumgartl J, Baudler S, Scherner M, Babaev V, Makowski L, Suttles J, McDuffie M, Tobe K, Kadowaki T, Fazio S, Kahn CR, Hotamisligil GS, Krone W, Linton M, Brüning JC: Myeloid lineage cell-restricted insulin resistance protects apolipoproteinE-deficient mice against atherosclerosis. Cell Metab. 2006, 3:247–256

[114] Han S, Liang CP, DeVries-Seimon T, Ranalletta M, Welch CL, Collins-Fletcher K, Accili D, Tabas I, Tall AR: Macrophage insulin receptor deficiency increases ER stress-induced apoptosis and necrotic core formation in advanced atherosclerotic lesions. Cell Metab. 2006, 3:257–266

[115] González-Navarro H, Vinué A, Vila-Caballer M, Fortuño A, Beloqui O, Zalba G, Burks D, Díez J, Andrés V: Molecular mechanisms of atherosclerosis in metabolic syndrome: role of reduced IRS2-dependent signaling. Arterioscler Thromb Vasc Biol. 2008, 28:2187–2194

[116] Galkina EV, Butcher M, Keller SR, Goff M, Bruce A, Pei H, Sarembock IJ, Sanders JM, Nagelin MH, Srinivasan S, Kulkarni RN, Hedrick CC, Lattanzio FA, Dobrian AD, Nadler JL, Ley K: Accelerated atherosclerosis in Apoe-/- mice heterozygous for the insulin receptor and the insulin receptor substrate-1. Arterioscler Thromb Vasc Biol. 2012, 32:247–256

[117] Shiomi M, Koike T, Ishida T: Genetically modified animal models for lipoprotein research. In: Frank S, Kostner G, editors. Lipoproteins e role in health and diseases. Intechopen Com. 2012, chapter 22:533–560

[118] Heinonen SE, Genové G, Bengtsson E, Hübschle T, Åkesson L, Hiss K, Benardeau A, Ylä-Herttuala S, Jönsson-Rylander AC, Gomez MF: Animal models of diabetic macrovascular complications: key players in the development of new therapeutic approaches. J Diabetes Res. 2015, 2015:404085

[119] Mahley RW, Huang Y, Weisgraber KH: Putting cholesterol in its place: apoE and reverse cholesterol transport. J Clin Invest. 2006, 116:1226–1229

[120] Zhang SH, Reddick RL, Piedrahita JA, Maeda N: Spontaneous hypercholesterolemia and arterial lesions in mice lacking apolipoprotein E. Science. 1992, 258:468–471

[121] Plump AS, Smith JD, Hayek T, Aalto-Setälä K, Walsh A, Verstuyft JG, Rubin EM, Breslow JL: Severe hypercholesterolemia and atherosclerosis in apolipoprotein E-deficient mice created by homologous recombination in ES cells. Cell. 1992, 71:343–353

[122] Reddick RL, Zhang SH, Maeda N: Atherosclerosis in mice lacking apo E. Evaluation of lesional development and progression. Arterioscler Thromb. 1994, 14:141–147

[123] Zhang SH, Reddick RL, Burkey B, Maeda N: Diet-induced atherosclerosis in mice heterozygous and homozygous for apolipoprotein E gene disruption. J Clin Invest. 1994, 94:937–945

[124] Nakashima Y, Plump AS, Raines EW, Breslow JL, Ross R: ApoE-deficient mice develop lesions of all phases of atherosclerosis throughout the arterial tree. Arterioscler Thromb. 1994, 14:133–140

[125] Khan MI, Pichna BA, Shi Y, Bowes AJ, Werstuck GH: Evidence supporting a role for endoplasmic reticulum stress in the development of atherosclerosis in a hyperglycaemic mouse model. Antioxid Redox Signal. 2009, 11:2289–2298

[126] Zeadin M, Butcher M, Werstuck G, Khan M, Yee CK, Shaughnessy SG: Effect of leptin on vascular calcification in apolipoprotein E-deficient mice. Arterioscler Thromb Vasc Biol. 2009, 29:2069–2075

[127] Werstuck GH, Khan MI, Femia G, Kim AJ, Tedesco V, Trigatti B, Shi Y: Glucosamine-induced endoplasmic reticulum dysfunction is associated with accelerated atherosclerosis in a hyperglycemic mouse model. Diabetes. 2006, 55:93–101

[128] Ishibashi S, Goldstein JL, Brown MS, Herz J, Burns DK: Massive xanthomatosis and atherosclerosis in cholesterol-fed low density lipoprotein receptor-negative mice. J Clin Invest. 1994, 93:1885–1893

[129] Lichtman AH, Clinton SK, Iiyama K, Connelly PW, Libby P, Cybulsky MI: Hyperlipidemia and atherosclerotic lesion development in LDL receptor-deficient mice fed defined semipurified diets with and without cholate. Arterioscler Thromb Vasc Biol. 1999, 19:1938–1944

[130] Moon BC, Friedman JM: The molecular basis of the obese mutation in ob2J mice. Genomics. 1997, 42:152–156

[131] Zhang Y, Proenca R, Maffei M, Barone M, Leopold L, Friedman JM: Positional cloning of the mouse obese gene and its human homologue. Nature. 1994, 372:425–432

[132] Lee GH, Proenca R, Montez JM, Carroll KM, Darvishzadeh JG, Lee JI, Friedman JM: Abnormal splicing of the leptin receptor in diabetic mice. Nature. 1996, 379:632–635

[133] Chen H, Charlat O, Tartaglia LA, Woolf EA, Weng X, Ellis SJ, Lakey ND, Culpepper J, Moore KJ, Breitbart RE, Duyk GM, Tepper RI, Morgenstern JP: Evidence that the diabetes gene encodes the leptin receptor: identification of a mutation in the leptin receptor gene in db/db mice. Cell. 1996, 84:491–495

[134] Wu KK, Wu TJ, Chin J, Mitnaul LJ, Hernandez M, Cai TQ, Ren N, Waters MG, Wright SD, Cheng K: Increased hypercholesterolemia and atherosclerosis in mice lacking both ApoE and leptin receptor. Atherosclerosis. 2005, 181:251–259

[135] Gruen ML, Saraswathi V, Nuotio-Antar AM, Plummer MR, Coenen KR, Hasty AH: Plasma insulin levels predict atherosclerotic lesion burden in obese hyperlipidemic mice. Atherosclerosis. 2006, 186:54–64

[136] Hasty AH, Shimano H, Osuga J, Namatame I, Takahashi A, Yahagi N, Perrey S, Iizuka Y, Tamura Y, Amemiya-Kudo M, Yoshikawa T, Okazaki H, Ohashi K, Harada K, Matsuzaka T, Sone H, Gotoda T, Nagai R, Ishibashi S, Yamada N: Severe hypercholesterolemia, hypertriglyceridemia, and atherosclerosis in mice lacking both leptin and the low density lipoprotein receptor. J Biol Chem. 2001, 276:37402–37408

[137] Oldstone MB, Nerenberg M, Southern P, Price J, Lewicki H: Virus infection triggers insulin-dependent diabetes mellitus in a transgenic model: role of anti-self (virus) immune response. Cell. 1991, 65:319–331

[138] Ohashi PS, Oehen S, Buerki K, Pircher H, Ohashi CT, Odermatt B, Malissen B, Zinkernagel RM, Hengartner H: Ablation of "tolerance" and induction of diabetes by virus infection in viral antigen transgenic mice. Cell. 1991, 65:305–317

[139] Renard CB, Kramer F, Johansson F, Lamharzi N, Tannock LR, von Herrath MG, Chait A, Bornfeldt KE: Diabetes and diabetes-associated lipid abnormalities have distinct effects on initiation and progression of atherosclerotic lesions. J Clin Invest. 2004, 114:659–668

[140] Lenzen S: The mechanisms of alloxan- and streptozotocin-induced diabetes. Diabetologia. 2008, 51:216–226

[141] Wu KK, Huan Y: Diabetic atherosclerosis mouse models. Atherosclerosis. 2007, 191:241–249

[142] Olbricht CJ, Geissinger B: Renal hypertrophy in streptozotocin diabetic rats: role of proteolytic lysosomal enzymes. Kidney Int. 1992, 41:966–972

[143] Laguens RP, Candela S, Hernández RE, Gagliardino JJ: Streptozotocin-induced liver damage in mice. Horm Metab Res. 1980, 12:197–201

[144] Rerup CC: Drugs producing diabetes through damage of the insulin secreting cells. Pharmacol Rev. 1970, 22:485–518

[145] Eleazu CO, Eleazu KC, Chukwuma S, Essien UN: Review of the mechanism of cell death resulting from streptozotocin challenge in experimental animals, its practical use and potential risk to humans. J Diabetes Metab Disord. 2013, 12:60

[146] Matsuzaka T, Shimano H, Yahagi N, Amemiya-Kudo M, Okazaki H, Tamura Y, Iizuka Y, Ohashi K, Tomita S, Sekiya M, Hasty A, Nakagawa Y, Sone H, Toyoshima H, Ishibashi S, Osuga J, Yamada N: Insulin-independent induction of sterol regulatory element-binding protein-1c expression in the livers of streptozotocin-treated mice. Diabetes. 2004, 53:560–569

[147] Bonnevie-Nielsen V, Steffes MW, Lernmark A: A major loss in islet mass and B-cell function precedes hyperglycemia in mice given multiple low doses of streptozotocin. Diabetes. 1981, 30:424–429

[148] Sandler S: Protection by dimethyl urea against hyperglycaemia, but not insulitis, in low-dose streptozotocin-induced diabetes in the mouse. Diabetologia. 1984, 26:386–388

[149] Li Z, Karlsson FA, Sandler S: Islet loss and alpha cell expansion in type 1 diabetes induced by multiple low-dose streptozotocin administration in mice. J Endocrinol. 2000, 165:93–99

[150] Yoshioka M, Kayo T, Ikeda T, Koizumi A: A novel locus, Mody4, distal to D7Mit189 on chromosome 7 determines early-onset NIDDM nonobese C57BL/6 (Akita) mutant mice. Diabetes, 1997, 46:887–894

[151] Wang J, Takeuchi T, Tanaka S, Kubo SK, Kayo T, Lu D, Takata K, Koizumi A, Izumi T. A mutation in the insulin 2 gene induces diabetes with severe pancreatic beta-cell dysfunction in the Mody mouse. J Clin Invest. 1999, 103:27–37

[152] Oyadomari S, Koizumi A, Takeda K, Gotoh T, Akira S, Araki E, Mori M: Targeted disruption of the Chop gene delays endoplasmic reticulum stress-mediated diabetes. J Clin Invest. 2002, 109:525–532

[153] Ron D: Proteotoxicity in the endoplasmic reticulum: lessons from the Akita diabetic mouse. J Clin Invest. 2002, 109:443–445

[154] Cavener DR, Gupta S, McGrath BC: PERK in beta cell biology and insulin biogenesis. Trends Endocrinol Metab. 2010, 21:714–721

[155] Liu M, Hodish I, Rhodes CJ, Arvan P: Proinsulin maturation, misfolding, and proteotoxicity. Proc Natl Acad Sci U S A. 2007, 104:15841–15846

[156] Moulton KS, Heller E, Konerding MA, Flynn E, Palinski W, Folkman J: Angiogenesis inhibitors endostatin or TNP-470 reduce intimal neovascularization and plaque growth in apolipoprotein E-deficient mice. Circulation. 1999, 99:1726–1732

[157] Celletti FL, Waugh JM, Amabile PG, Brendolan A, Hilfiker PR, Dake MD: Vascular endothelial growth factor enhances atherosclerotic plaque progression. Nature. 2001, 7:425–429

[158] Wilson SH, Herrmann J, Lerman LO, Holmes DR, Napoli C, Ritman EL, Lerman A: Simvastatin preserves the structure of coronary adventitial vasa vasorum in experimental hypercholesterolemia independent of lipid lowering. Circulation. 2002, 105:415–418

[159] Moulton KS, Vakili K, Zurakowski D Soliman M, Butterfield C, Sylvin E, Lo KM, Gillies S, Javaherian K, Folkman J: Inhibition of plaque neovascularization reduces macrophage accumulation and progression of advanced atherosclerosis. Proc Natl Acad Sci U S A. 2003, 100:4736–4741

[160] Mollmark J, Ravi S, Sun B, Shipman S, Buitendijk M, Simons M, Mulligan-Kehoe MJ: Antiangiogenic activity of rPAI-1(23) promotes vasa vasorum regression in hypercholesterolemic mice through a plasmin-dependent mechanism. Circ Res. 2011, 108:1419–1428

[161] Thangarajah H, Yao D, Chang EI, Shi Y, Jazayeri L, Vial IN, Galiano RD, Du XL, Grogan R, Galvez MG, Januszyk M, Brownlee M, Gurtner GC: The molecular basis for impaired hypoxia-induced VEGF expression in diabetic tissues. Proc Natl Acad Sci U S A. 2009, 106:13505–13510

[162] Fukushima M, Hattori Y, Tsukada H, Koga K, Kajiwara E, Kawano K, Kobayashi T, Kamata K, Maitani Y: Adiponectin gene therapy of streptozotocin-induced diabetic mice using hydrodynamic injection. J Gene Med. 2007, 9:976–985

[163] Bosco C, Bosnyak Z, Malmberg A, Adolfsson J, Keating NL, Van Hemelrijck M: Quantifying observational evidence for risk of fatal and nonfatal cardiovascular disease following androgen deprivation therapy for prostate cancer: a meta-analysis. Eur Urol. 2015, 68:386–396

[164] Vlachopoulos C, Ioakeimidis N, Miner M, Aggelis A, Pietri P, Terentes-Printzios D, Tsekoura D, Stefanadis C: Testosterone deficiency: a determinant of aortic stiffness in men. Atherosclerosis. 2014, 233:278–283

[165] Doğan BA, Karakılıç E, Tuna MM, Arduç A, Berker D, Güler S: Effect of androgen replacement therapy on atherosclerotic risk markers in young-to-middle-aged men with idiopathic hypogonadotropic hypogonadism. Clin Endocrinol (Oxf). 2015, 82:422–428

[166] Ballester J, Muñoz MC, Domínguez J, Rigau T, Guinovart JJ, Rodríguez-Gil JE: Insulin-dependent diabetes affects testicular function by FSH- and LH-linked mechanisms. J Androl. 2004, 25:706–719

[167] Corona G, Monami M, Rastrelli G, Aversa A, Sforza A, Lenzi A, Forti G, Mannucci E, Maggi M: Type 2 diabetes mellitus and testosterone: a meta-analysis study. Int J Androl. 2011, 34:528–540

[168] Tomar R, Dhindsa S, Chaudhuri A, Mohanty P, Garg R, Dandona P: Contrasting testosterone concentrations in type 1 and type 2 diabetes. Diabetes Care. 2006, 29:1120–1122

[169] Nathan DM, Cleary PA, Backlund JY, et al.; Diabetes Control and Complications Trial/Epidemiology of Diabetes Interventions and Complications (DCCT/EDIC) Study Research Group. Intensive diabetes treatment and cardiovascular disease in patients with type 1 diabetes. N Engl J Med. 2005, 353:2643–2653

[170] Ceriello A, Ihnat MA, Thorpe JE: Clinical review 2: The "metabolic memory": is more than just tight glucose control necessary to prevent diabetic complications? J Clin Endocrinol Metab. 2009, 94:410–415

[171] Gale EA, Gillespie KM: Diabetes and gender. Diabetologia. 2001, 44:3–15

[172] Meisinger C, Thorand B, Schneider A, Stieber J, Döring A, Löwel H: Sex differences in risk factors for incident type 2 diabetes mellitus: the MONICA Augsburg cohort study. Arch Intern Med. 2002, 162:82–89

[173] Freedman DS, Jacobsen SJ, Barboriak JJ, Sobocinski KA, Anderson AJ, Kissebah AH, Sasse EA, Gruchow HW: Body fat distribution and male/female differences in lipids and lipoproteins. Circulation. 1990, 81:1498–1506

[174] Goff DC Jr, Bertoni AG, Kramer H, Bonds D, Blumenthal RS, Tsai MY, Psaty BM: Dyslipidemia prevalence, treatment, and control in the Multi-Ethnic Study of Atherosclerosis (MESA): gender, ethnicity, and coronary artery calcium. Circulation. 2006, 113:647–656

[175] Ogden CL, Carroll MD, Kit BK, Flegal KM: Prevalence of obesity in the United States, 2009-2010. NCHS Data Brief. 2012, 82:1–8

[176] Lovejoy JC, Sainsbury A; Stock Conference 2008 Working Group: Sex differences in obesity and the regulation of energy homeostasis. Obes Rev. 2009, 10:154–167

[177] Reckelhoff JF: Gender differences in the regulation of blood pressure. Hypertension. 2001, 37:1199–1208

[178] Joakimsen O, Bonaa KH, Stensland-Bugge E, Jacobsen BK: Age and sex differences in the distribution and ultrasound morphology of carotid atherosclerosis: the Tromsø Study. Arterioscler Thromb Vasc Biol. 1999, 19:3007–3013

[179] Njølstad I, Arnesen E, Lund-Larsen PG: Smoking, serum lipids, blood pressure, and sex differences in myocardial infarction. A 12-year follow-up of the Finnmark Study. Circulation. 1996, 93:450–456

[180] Moreno PR, Purushothaman KR, Fuster V, Echeverri D, Truszczynska H, Sharma SK, Badimon JJ, O'Connor WN: Plaque neovascularization is increased in ruptured atherosclerotic lesions of human aorta: implications for plaque vulnerability. Circulation. 2004, 110:2032–2038

[181] O'Brien ER, Garvin MR, Dev R, Stewart DK, Hinohara T, Simpson JB, Schwartz SM: Angiogenesis in human coronary atherosclerotic plaques. Am J Pathol. 1994, 145:883–894

[182] Rey S, Semenza GL: Hypoxia-inducible factor-1-dependent mechanisms of vascularization and vascular remodelling. Cardiovasc Res. 2010, 86:236–242

[183] Caligiuri G, Levy B, Pernow J, Thorén P, Hansson GK: Myocardial infarction mediated by endothelin receptor signaling in hypercholesterolemic mice. Proc Natl Acad Sci U S A. 1999, 96:6920–6924

[184] Ishibashi S, Herz J, Maeda N, Goldstein JL, Brown MS: The two-receptor model of lipoprotein clearance: tests of the hypothesis in "knockout" mice lacking the low density lipoprotein receptor, apolipoprotein E, or both proteins. Proc Natl Acad Sci U S A. 1994, 91:4431–4435

[185] Catrina SB, Okamoto K, Pereira T, Brismar K, Poellinger L: Hyperglycemia regulates hypoxia-inducible factor-1alpha protein stability and function. Diabetes. 2004, 53:3226–3232

[186] Hargrove GM, Dufresne J, Whiteside C, Muruve DA, Wong NC: Diabetes mellitus increases endothelin-1 gene transcription in rat kidney. Kidney Int. 2000, 58:1534–1545

[187] Park JY, Takahara N, Gabriele A, Chou E, Naruse K, Suzuma K, Yamauchi T, Ha SW, Meier M, Rhodes CJ, King GL: Induction of endothelin-1 expression by glucose: an effect of protein kinase C activation. Diabetes. 2000, 49:1239–1248

[188] Trigatti B, Rayburn H, Viñals M, Braun A, Miettinen H, Penman M, Hertz M, Schrenzel M, Amigo L, Rigotti A, Krieger M: Influence of the high density lipoprotein receptor SR-BI on reproductive and cardiovascular pathophysiology. Proc Natl Acad Sci U S A. 1999, 96:9322–9327

[189] Braun A, Trigatti BL, Post MJ, Sato K, Simons M, Edelberg JM, Rosenberg RD, Schrenzel M, Krieger M: Loss of SR-BI expression leads to the early onset of occlusive atherosclerotic coronary artery disease, spontaneous myocardial infarctions, severe cardiac dysfunction, and premature death in apolipoprotein E-deficient mice. Circ Res. 2002, 90:270–276

[190] Braun A, Zhang S, Miettinen HE, Ebrahim S, Holm TM, Vasile E, Post MJ, Yoerger DM, Picard MH, Krieger JL, Andrews NC, Simons M, Krieger M: Probucol prevents early coronary heart disease and death in the high-density lipoprotein receptor SR-BI/apolipoprotein E double knockout mouse. Proc Natl Acad Sci U S A. 2003, 100:7283–7288

[191] Murao K, Yu X, Imachi H, Cao WM, Chen K, Matsumoto K, Nishiuchi T, Wong NC, Ishida T: Hyperglycemia suppresses hepatic scavenger receptor class B type I expression. Am J Physiol Endocrinol Metab. 2008, 294:E78–E87

[192] Gantman A, Fuhrman B, Aviram M, Hayek T: High glucose stimulates macrophage SR-BI expression and induces a switch in its activity from cholesterol efflux to cholesterol influx. Biochem Biophys Res Commun. 2010, 391:523–528

[193] Stull ND, Breite A, McCarthy R, Tersey SA, Mirmira RG: Mouse islet of Langerhans isolation using a combination of purified collagenase and neutral protease. J Vis Exp. 2012, 67:4137

[194] Miquerol L, Langille BL, Nagy A: Embryonic development is disrupted by modest increases in vascular endothelial growth factor gene expression. Development. 2000, 127:3941–3946

[195] Damert A, Miquerol L, Gertsenstein M, Risau W, Nagy A: Insufficient VEGFA activity in yolk sac endoderm compromises haematopoietic and endothelial differentiation. Development. 2002, 129:1881–1892

APPENDIX 1: Supplemental Material for CHAPTER 3

Quantification of the Necrotic Core

Serial cross sections (4μm) of the aortic root were collected and stained with hematoxylin and eosin for lesion and necrotic core measurement (Supplemental Figure 1). The necrotic core was defined as the acellular area of the atherosclerotic lesion. The necrotic core typically contains visible cholesterol crystals [1].

Supplemental Figure 1. The necrotic core has been defined as the acellular area of the atherosclerotic lesion. This is a similar criteria to that used by Shai et al (2010) [1]. (scale = 100 μm)

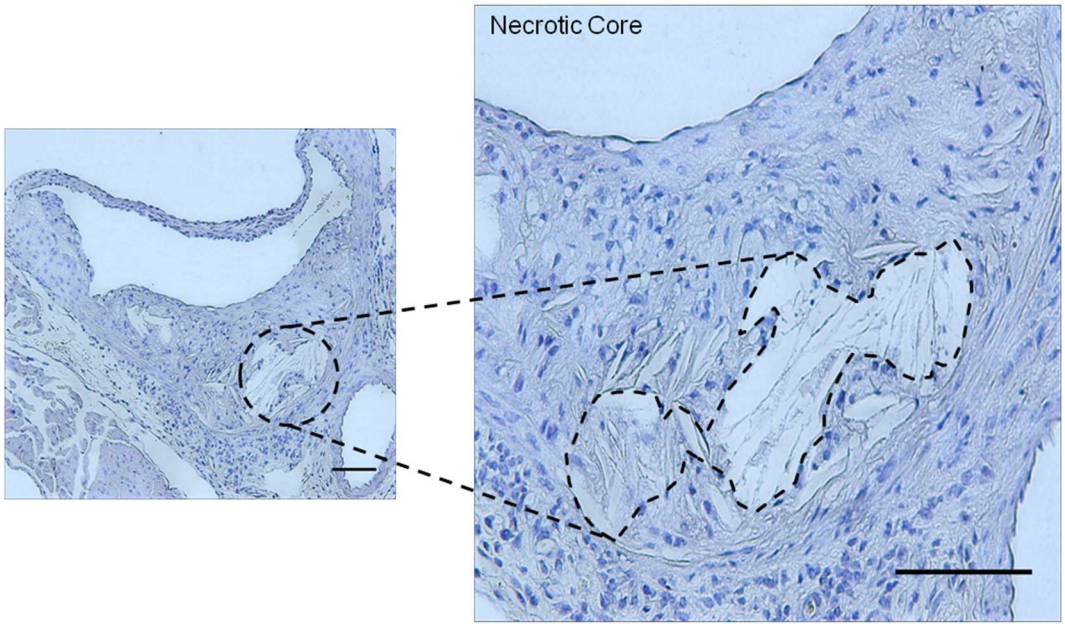

Supplemental Figure 1

Analysis of microvascular changes in the retina

Retinal microvasculature density was calculated using a counting template that was placed over retinal flat mounts (Supplemental Figure 2). The number of vessel intersections with the edges of each sampling box was tallied for central, mid, and peripheral regions of the vasculature [2].

Supplemental Figure 2. Counting template used to quantify retinal microvessel density, defined as the average number of microvessel intersections per quantification box analyzed.

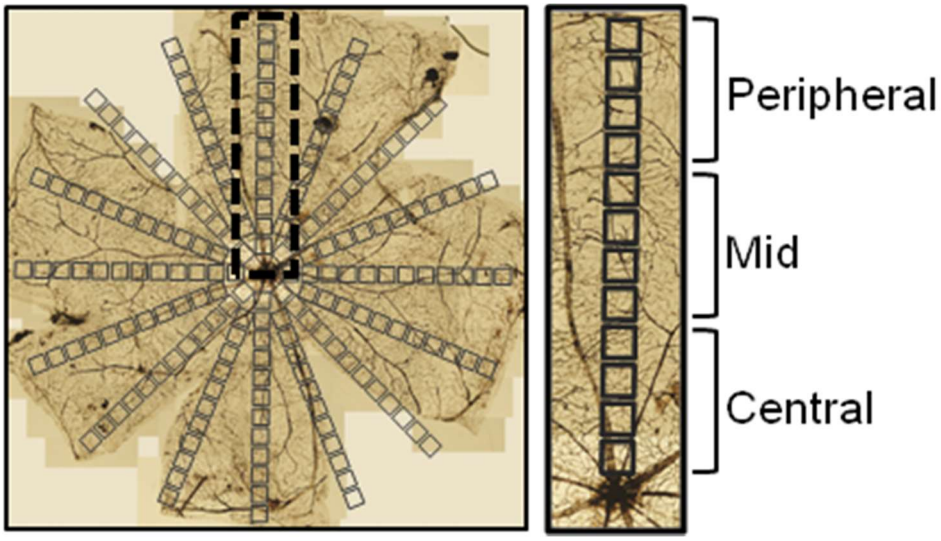

Supplemental Figure 2

Western feeding in ApoE$^{-/-}$ and Ldlr$^{-/-}$ mice is associated with accelerated atherogenesis and vasa vasorum neovascularization at the aortic sinus

In this study, 5-week-old ApoE$^{-/-}$and Ldlr$^{-/-}$ mice were placed on standard chow or high-fat Western diet for 10 weeks. By 15 weeks of age, both ApoE$^{-/-}$ and Ldlr$^{-/-}$ Western-fed mice had significantly elevated serum triglyceride and cholesterol levels compared to controls (Supplemental Table 1); however, blood glucose levels were unaffected.

Consistent with previously reported findings in non-diabetic and normoglycemic models [3–7], we found that high fat diet-fed ApoE$^{-/-}$ and Ldlr$^{-/-}$ mice developed significantly larger atherosclerotic lesions at the aortic sinus than standard diet controls (Supplemental Figure 3B). Accelerated atherogenesis in these models directly corresponds to vasa vasorum neovascularization. By 15 weeks of age, Western-fed ApoE$^{-/-}$ and Ldlr$^{-/-}$ mice had 2.0- and 2.5-times more vasa vasorum microvessels than standard diet controls, respectively (Supplemental Figure 3A and Supplemental Table 1).

Methods: Five-week-old female ApoE$^{-/-}$ (B6.129P2-ApoE^{tm1Unc}) and Ldlr$^{-/-}$ mice were randomized to standard chow diet (TD92078; Harlan Teklad, Madison, WI) or high fat, Western diet (TD97363; Harlan Teklad, Madison, WI). At 15 weeks of age, mice were sacrificed (n = 3–6 per group) and plasma and tissue samples were collected for further examination. All animal procedures were approved by the McMaster University Animal Research Ethics Board.

Control and Western-fed ApoE$^{-/-}$ and Ldlr$^{-/-}$ mice were anaesthetized with isoflurane, flushed with 1x PBS, and perfusion-fixed with 10% neutral buffered formalin. Hearts and aortas were excised and embedded in paraffin blocks. Using the valve leaflets as a point of orientation, serial sections (4um) of the aortic root were collected and used for lesion measurement (hematoxylin and eosin) and immunofluorescence (IF) analysis.

Polyclonal rabbit anti-human von Willebrand Factor (vWF; DakoCytomation) and goat anti-rabbit Alexa 594 (Invitrogen) were used to analyze the vasa vasorum in control and Western-fed ApoE$^{-/-}$ and Ldlr$^{-/-}$ mice. DAPI nuclear counterstaining was performed on all sections, and non-specific staining was controlled for using pre-immune rabbit IgG. For quantification of vWF staining, positively labeled vasa vasorum microvessels residing within the intima, media, and adventitia of the aortic sinus were tallied. Vasa vasorum density was defined as the total number of microvessels residing within the defined regions, per aortic cross-section.

Supplemental Figure 3. Analysis of vasa vasorum density and atherosclerotic lesion area in $ApoE^{-/-}$ or $Ldlr^{-/-}$ mice fed control diets or high fat diets as indicated. (n = 3–6 per group; mean ± SEM) * $p<0.05$

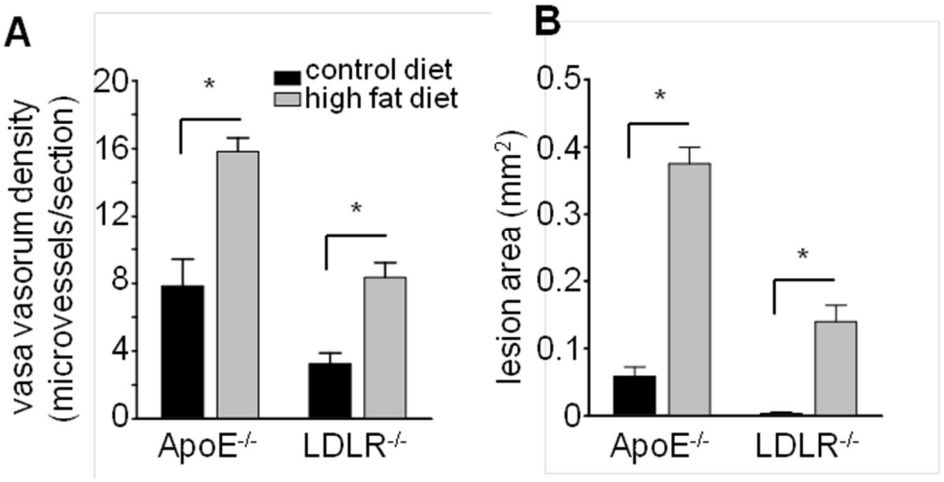

Supplemental Figure 3

Supplemental Table 1. Metabolic parameters. Plasma and tissue parameters of 15 week old ApoE$^{-/-}$ and Ldlr$^{-/-}$ mice on Control or high fat Western diet. *N* values are indicated. Vasa vasorum density defined as the total number of vasa vasorum microvessels per aortic cross section. * $p<0.05$, ** $p<0.01$, $p<0.001$ relative to control.

	ApoE$^{-/-}$			LDLR$^{-/-}$		
Plasma	**Control**	**Western**		**Control**	**Western**	
Blood Glucose (mM)	8.53 ± 0.55	9.05 ± 1.01	**NS**	8.50 ± 0.21	8.80 ± 0.92	**NS**
Triglycerides (mM)	0.40 ± 0.04	0.74 ± 0.03	***	0.28 ± 0.02	1.05 ± 0.15	*
Cholesterol (mM)	4.69 ± 0.46	9.44 ± 1.09	*	2.85 ± 0.04	11.47 ± 0.94	*
Tissues						
Body Weight (g)	21.68 ± 0.64	23.18 ±1.36	**NS**	20.00 ± 0.78	23.43 ± 0.75	*
Lesion Area (mm^2)	0.059 ± 0.014	0.375 ± 0.025	**	0.003 ± 0.002	0.139 ± 0.024	*
Vv Density	7.83 ± 1.58	15.83 ± 0.79	**	3.25 ± 0.73	8.33 ± 0.88	*
N	**3-6**	**4-6**		**3**	**3**	

Supplemental Table 1

Fluorescent microangiography (FMA) imaging of the vasa vasorum.

Fifteen week old normoglycemic and hyperglycemic ApoE$^{-/-}$ mice were injected with fluorescently-labeled microspheres. Fluorescent microangiography analysis of the structure and organization of the vasa vasorum surrounding the aortic sinus support a correlation between hyperglycemia and microvessel deficiency (Supplemental Figure 4).

Methods: Fifteen week old control and hyperglycemic ApoE$^{-/-}$ mice were anaesthetized with isoflurane, flushed with 1x PBS, and perfused with a 0.01% agarose-bead solution containing 0.04μm-diameter fluorescently-labeled microspheres (FluoSpheres® Invitrogen. Upon gel solidification, the heart and aorta were isolated and embedded in a 0.1% agarose gel block. A vibratome was used to section the gel blocks at 100μm-thickness, and serial sections of the aortic arch were collected on pre-coated glass slides for analysis.

Supplemental Figure 4. Sections of the aorta from 15-week-old normoglycemic and hyperglycemic ApoE$^{-/-}$ mice perfused with 0.04μm-diameter fluorescently-labelled microspheres. Panels on the right (scale = 50μm) represent higher-magnification images of boxed regions on the left (scale = 100μm).

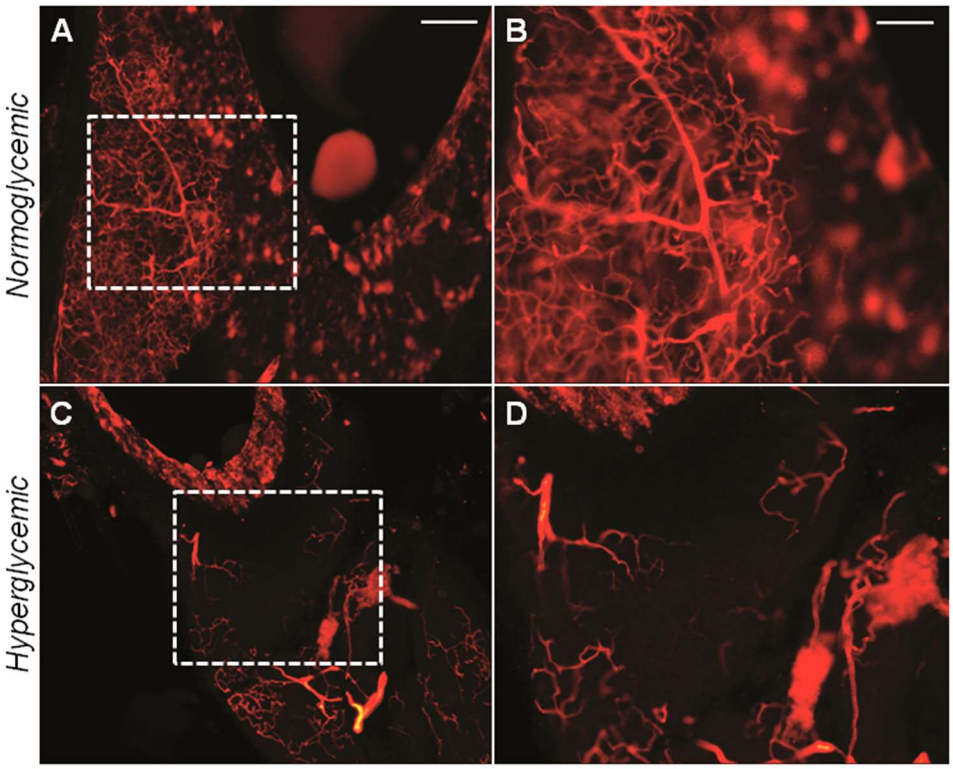

Supplemental Figure 4

REFERENCES FOR APPENDIX 1

[1] Shai SY, Sukhanov S, Higashi Y, Vaughn C, Kelly J, Delafontaine P: Smooth muscle cell-specific insulin-like growth factor-1 overexpression in Apoe$^{-/-}$ mice does not alter atherosclerotic plaque burden but increases features of plaque stability. Arterioscler Thromb Vasc Biol. 2010, 30:1916–1924

[2] Browning J, Wylie CK, Gole G: Quantification of oxygen-induced retinopathy in the mouse. Invest Ophthalmol Vis Sci. 1997, 38:1168–1174

[3] Virmani R, Kolodgie FD, Burke AP, Finn AV, Gold HK, Tulenko TN, Wrenn SP, Narula J: Atherosclerotic plaque progression and vulnerability to rupture: angiogenesis as a source of intraplaque hemorrhage. Arterioscler Thromb Vasc Biol. 2005, 25:2054–2061

[4] Barger AC, Beeuwkes R,3rd, Lainey LL, Silverman KJ: Hypothesis: vasa vasorum and neovascularization of human coronary arteries. A possible role in the pathophysiology of atherosclerosis. N Engl J Med. 1984, 310:175–177

[5] Langheinrich AC, Michniewicz A, Sedding DG, Walker G, Beighley PE, Rau WS, Bohle RM, Ritman EL: Correlation of vasa vasorum neovascularization and plaque progression in aortas of apolipoprotein E(-/-)/low-density lipoprotein(-/-) double knockout mice. Arterioscler Thromb Vasc Biol. 2006, 26:347–352

[6] Moulton KS, Heller E, Konerding MA, Flynn E, Palinski W, Folkman J: Angiogenesis inhibitors endostatin or TNP-470 reduce intimal neovascularization and plaque growth in apolipoprotein E-deficient mice. Circulation. 1999, 99:1726–1732

[7] Moulton KS, Vakili K, Zurakowski D, Soliman M, Butterfield C, Sylvin E, Lo KM, Gillies S, Javaherian K, Folkman J: Inhibition of plaque neovascularization reduces macrophage accumulation and progression of advanced atherosclerosis. Proc Natl Acad Sci U S A. 2003, 100:4736–4741

APPENDIX 2: Supplemental Material for CHAPTER 4

Supplemental Figure 1. Representative results from genotype analysis. (A) The $Ins2^{Akita}$ point mutation is identified by the absence of an Fnu4HI restriction site in a PCR amplified cDNA. (B) ApoE-deficiency is confirmed by PCR analysis using primers specific for the gene knock out.

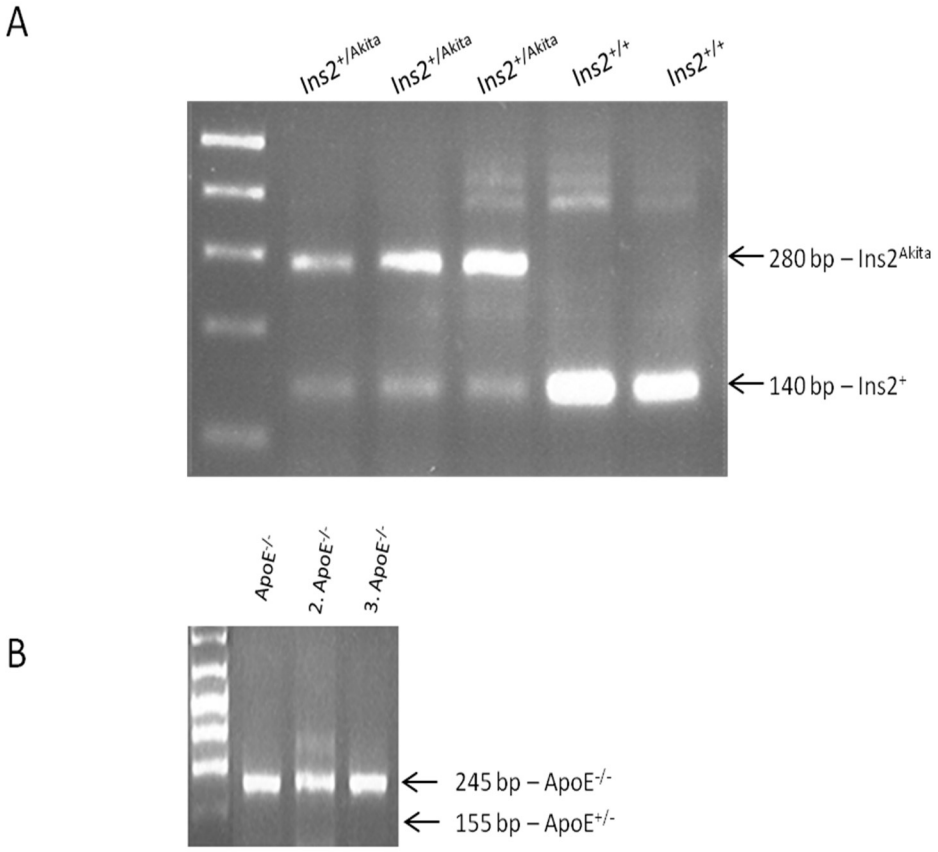

Supplemental Figure 1

Supplemental Figure 2. Fasting blood glucose levels in the heterozygous $ApoE^{+/-}$ mouse with or without the $Ins2^{Akita}$ mutation (n = 12/♂$ApoE^{+/-}$:$Ins2^{+/Akita}$; n = 9/♂$ApoE^{+/-}$; n = 12/♀$ApoE^{+/-}$:$Ins2^{+/Akita}$; n = 12/♀$ApoE^{+/-}$).

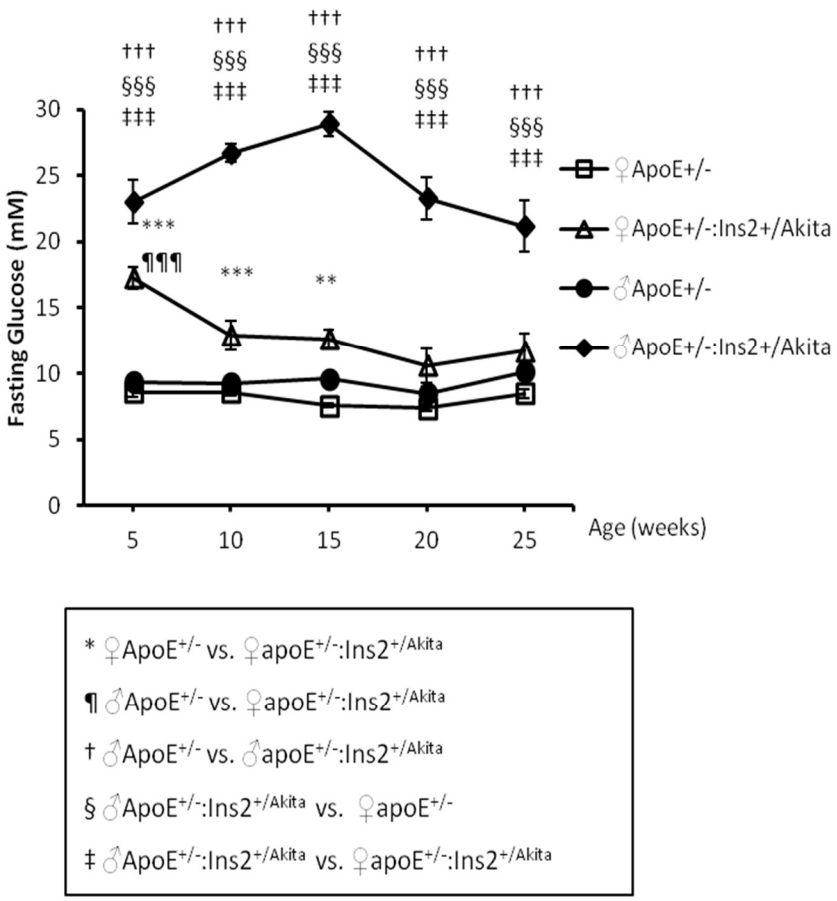

Supplemental Figure 2

Supplemental Figure 3. Atherosclerosis in the 15-week-old male ApoE$^{-/-}$:Ins2$^{+/Akita}$ mice and the 25-week-old female ApoE$^{-/-}$:Ins2$^{+/Akita}$ mice. (A) Atherosclerosis in the aortic sinus of 15-week-old male mice (n = 6/group). (B) Lipid accumulation in the whole aortas of 15-week-old male mice (n = 6/group). (C) Atherosclerosis in the aortic sinus of 25-week-old female mice (n = 5–10/group). (D) Lipid accumulation in the whole aortas of 25-week-old female mice (n = 4/group).

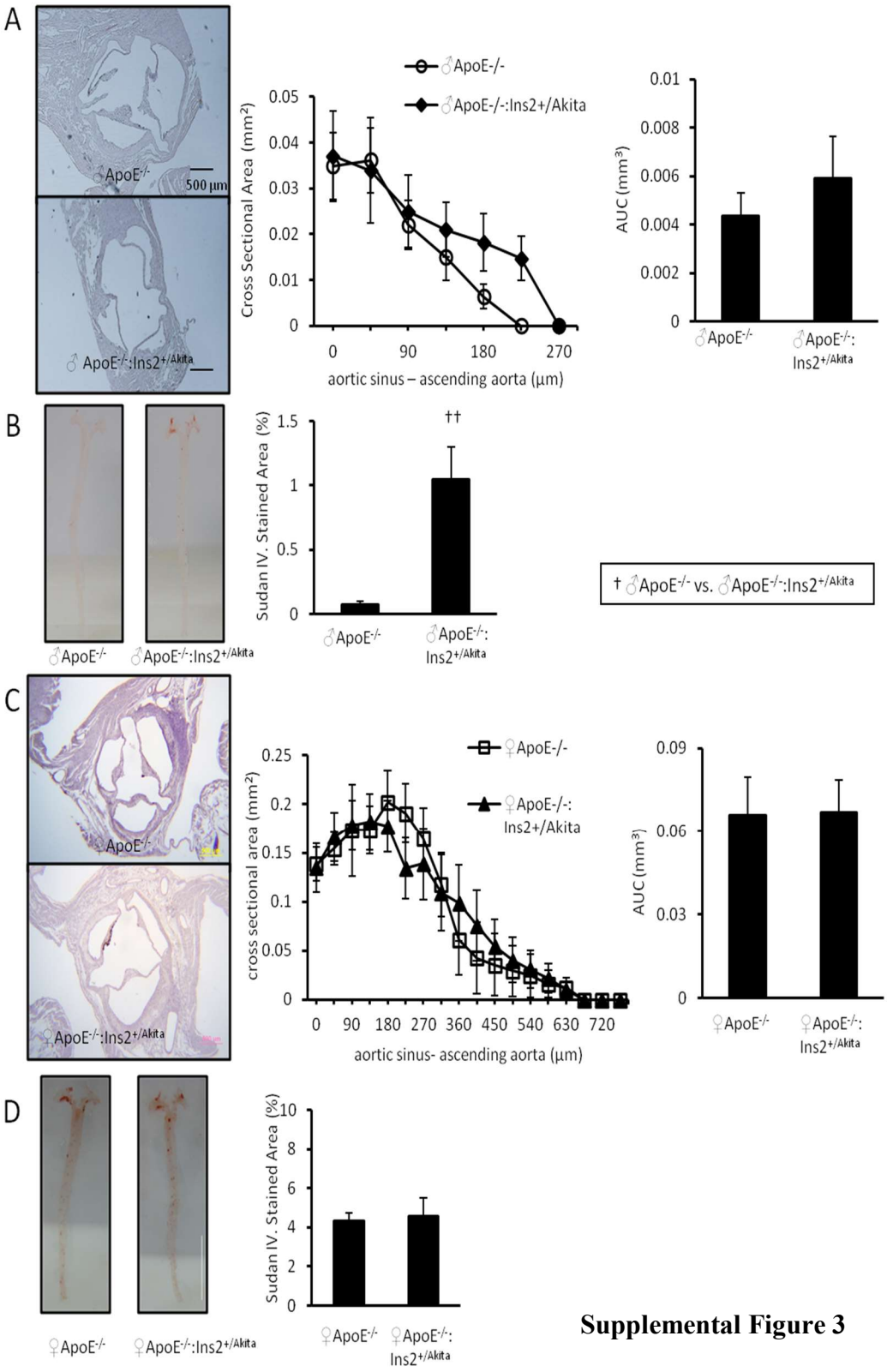

Supplemental Figure 3

Supplemental Figure 4. Surrogate indexes of beta cell function (HOMA-%β) and insulin sensitivity (QUICKI) in female (A–B) and male (C–D) mice (n = 4–6/group).

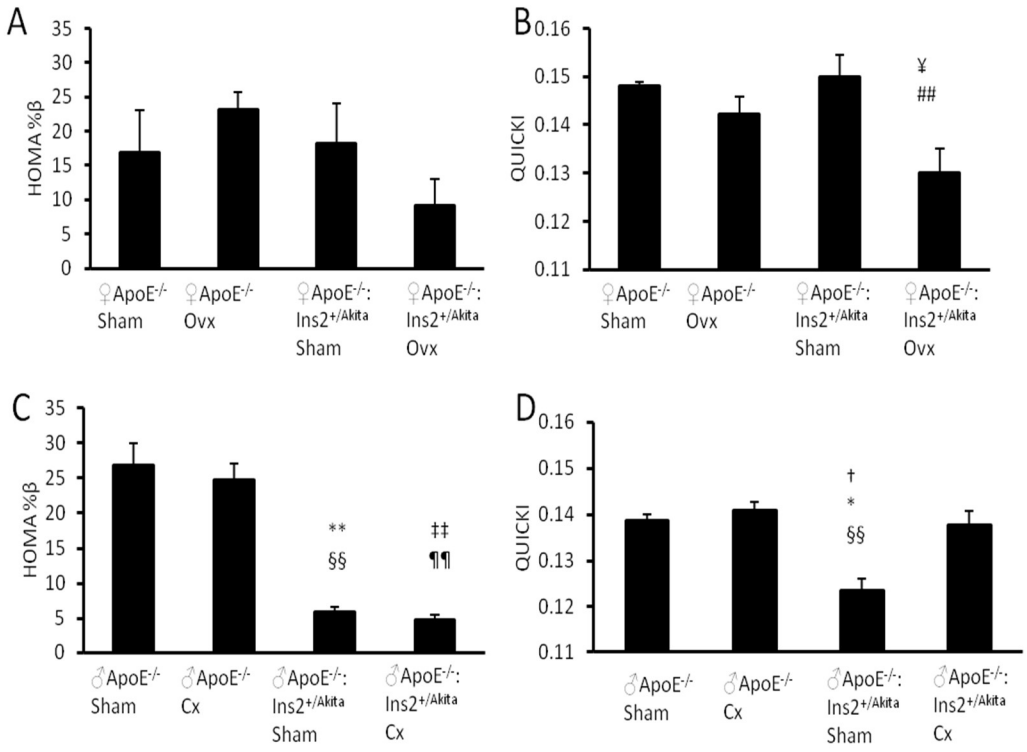

¥♀ ApoE$^{-/-}$:Ins2$^{+/Akita}$-Sham vs. ♀ ApoE$^{-/-}$:Ins2$^{+/Akita}$-Ovx

#♀ApoE$^{-/-}$-Sham vs. ♀ApoE$^{-/-}$:Ins2$^{+/Akita}$-Ovx

*♂ApoE$^{-/-}$-Sham vs. ♂ApoE$^{-/-}$:Ins2$^{+/Akita}$-Sham

†♂ApoE$^{-/-}$:Ins2$^{+/Akita}$-Sham vs. ♂ApoE$^{-/-}$:Ins2$^{+/Akita}$-Cx

‡♂ApoE$^{-/-}$-Sham vs. ♂ApoE$^{-/-}$:Ins2$^{+/Akita}$-Cx

§♂ApoE$^{-/-}$-Cx vs. ♂ApoE$^{-/-}$:Ins2$^{+/Akita}$-Sham

¶ ♂ApoE$^{-/-}$-Cx vs. ♂ApoE$^{-/-}$:Ins2$^{+/Akita}$-Cx

Supplemental Figure 4

Supplemental Figure 5. Measurements of plasma insulin (A) and percent change in plasma insulin (B) after a 2 g oral glucose challenge (n = 3/group).

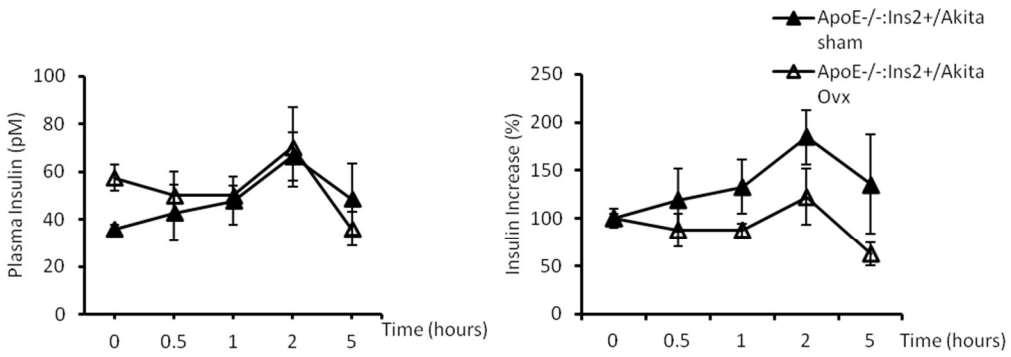

Supplemental Figure 5

Supplemental Figure 6. Liver weights of ovariectomized and castrated $ApoE^{-/-}$:$Ins2^{+/Akita}$ mice. (A) Female mice (n = 7–9/group). (B) Male mice (n = 7–12/group).

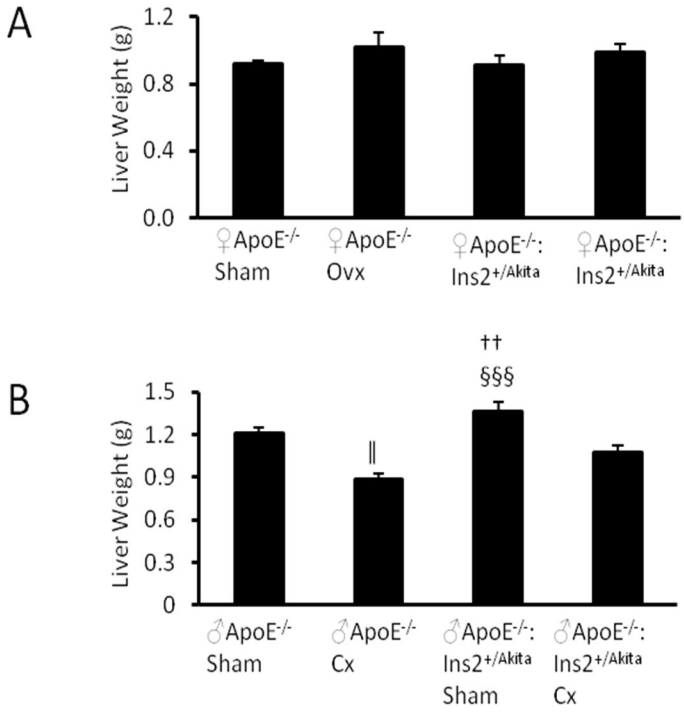

† ♂ApoE$^{-/-}$:Ins2$^{+/Akita}$-Sham vs. ♂ApoE$^{-/-}$:Ins2$^{+/Akita}$-Cx

§ ♂ApoE$^{-/-}$-Cx vs. ♂ApoE$^{-/-}$:Ins2$^{+/Akita}$-Sham

‖ ♂ApoE$^{-/-}$-Sham vs. ♂ApoE$^{-/-}$-Cx

Supplemental Figure 6

Supplemental Figure 7. Plasma lipid profile of ovariectomized and castrated ApoE$^{-/-}$:Ins2$^{+/Akita}$ mice. VLDL-, LDL- and HDL lipoprotein particles were separated by FPLC and cholesterol content was quantified in plasma collected from female (A) and male (B) mice (n = 6/group).

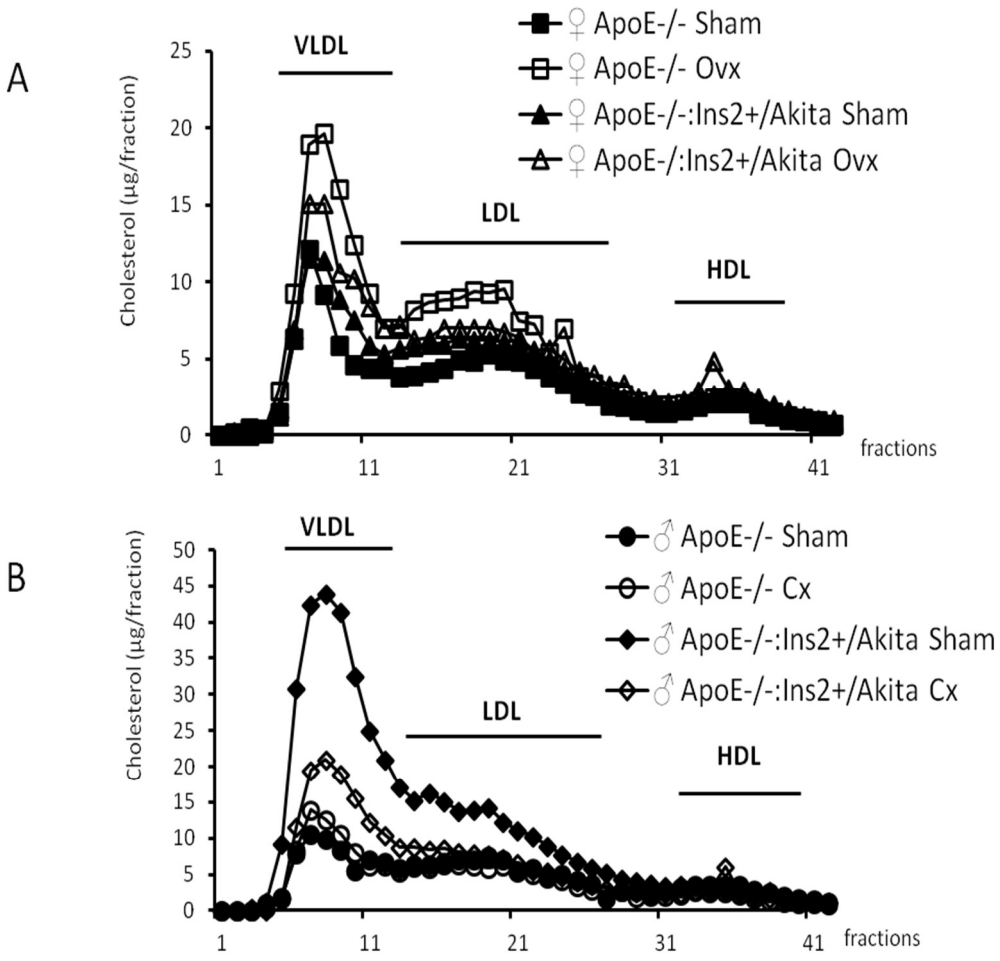

Supplemental Figure 7

Supplemental Figure 8. Estradiol (A) and progesterone (B) levels in the 15-week-old female mice (n = 4–8/group). (C) Testosterone levels in the 25-week-old male mice (n = 7–12/group).

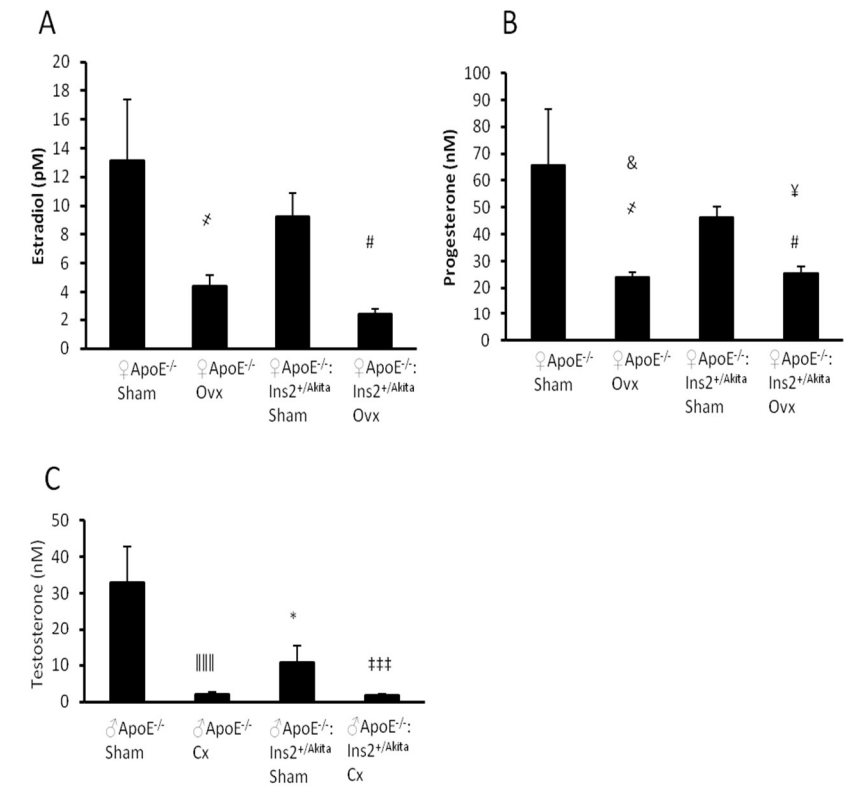

¥♀ ApoE$^{-/-}$:Ins2$^{+/Akita}$-Sham vs. ♀ ApoE$^{-/-}$:Ins2$^{+/Akita}$-Ovx

#♀ApoE$^{-/-}$-Sham vs. ♀ApoE$^{-/-}$:Ins2$^{+/Akita}$-Ovx

&♀ApoE$^{-/-}$-Ovx vs. ♀ApoE$^{-/-}$:Ins2$^{+/Akita}$-Sham

≠♀ApoE$^{-/-}$-Sham vs. ♀ApoE$^{-/-}$-Ovx

* ♂ ApoE$^{-/-}$-Sham vs. ♂ApoE$^{-/-}$:Ins2$^{+/Akita}$-Sham

‡ ♂ApoE$^{-/-}$-Sham vs. ♂ApoE$^{-/-}$:Ins2$^{+/Akita}$-Cx

‖ ♂ApoE$^{-/-}$-Sham vs. ♂ApoE$^{-/-}$-Cx.

Supplemental Figure 8

Supplemental Figure 9. Analysis of the macrophage content of atherosclerotic lesions in the aortic sinus by Mac-3 recognition. Female (A) and male (B) mice at 25 weeks of age (n = 7–12/group).

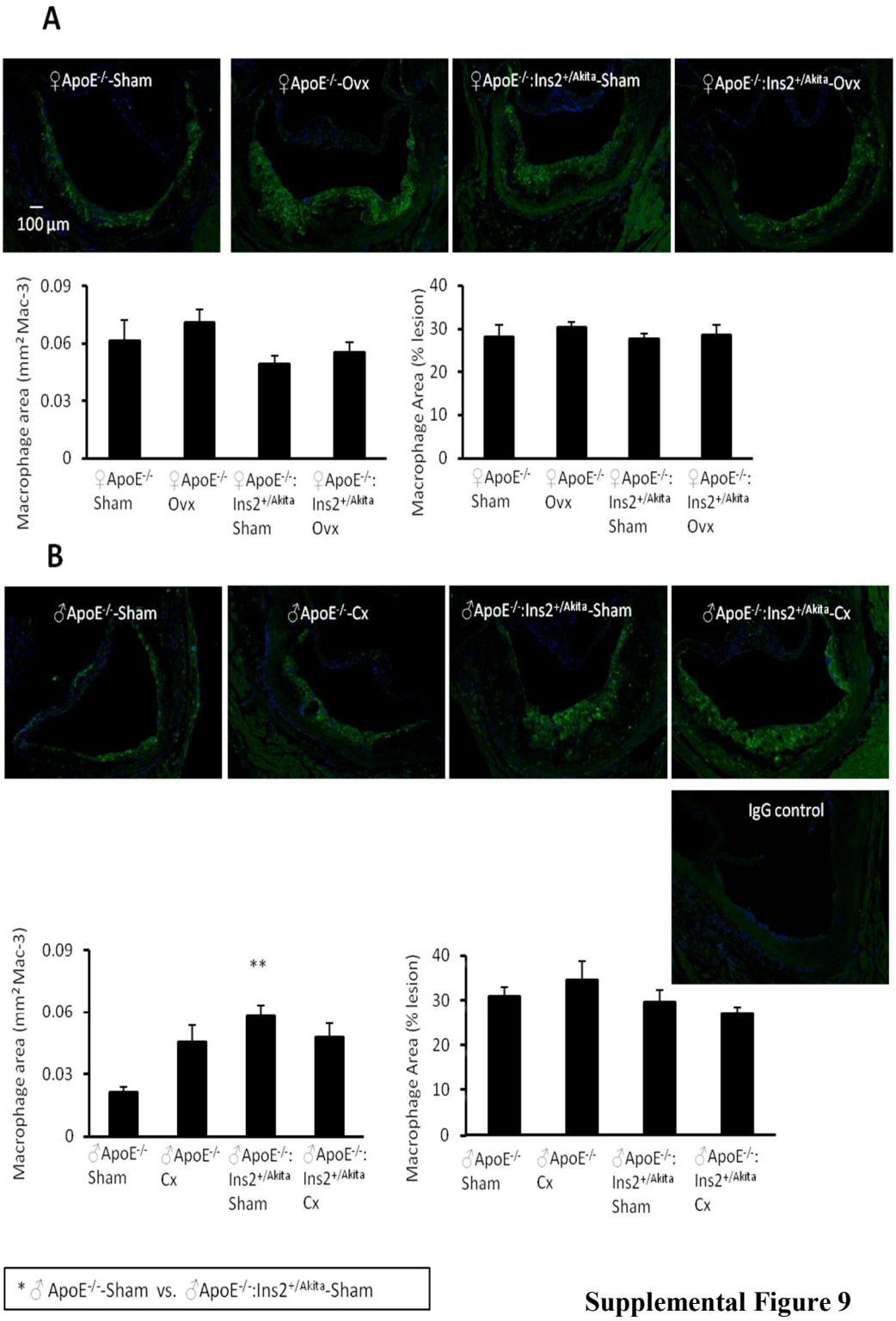

Supplemental Figure 9

Supplemental Figure 10. Analysis of the SMC content of atherosclerotic lesions in the aortic sinus by α-actin recognition. Female (A) and male (B) mice at 25 weeks of age (n = 7–12/group).

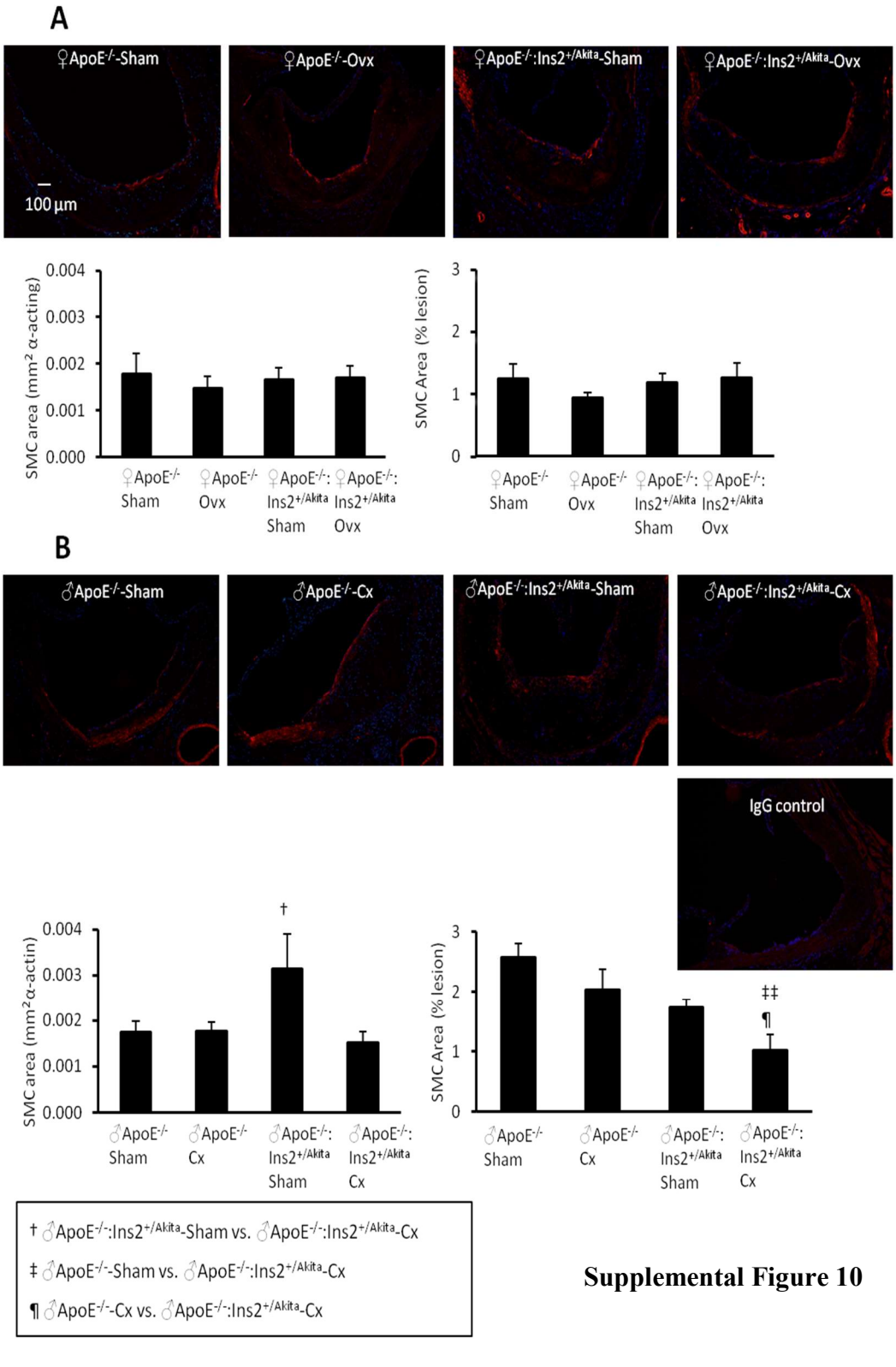

Supplemental Figure 10

APPENDIX 3: Supplemental Material for CHAPTER 5

Supplemental Figure 1. Analysis of metabolic parameters of female RD-fed and WD-fed mice at 25 weeks of age. (A) Fasting blood glucose levels. (B) Insulin resistance estimated by HOMA-IR index. (C) Beta-cell function evaluated by HOMA %β index. (D) Body weight. (E) Epididymal fat content. (F) Liver weight. (G) Total cholesterol levels in plasma. (H) Total triglyceride levels in plasma. (I) Lipoprotein-cholesterol profile. (J) Lipoprotein-triglyceride profile. (n = 4–8)

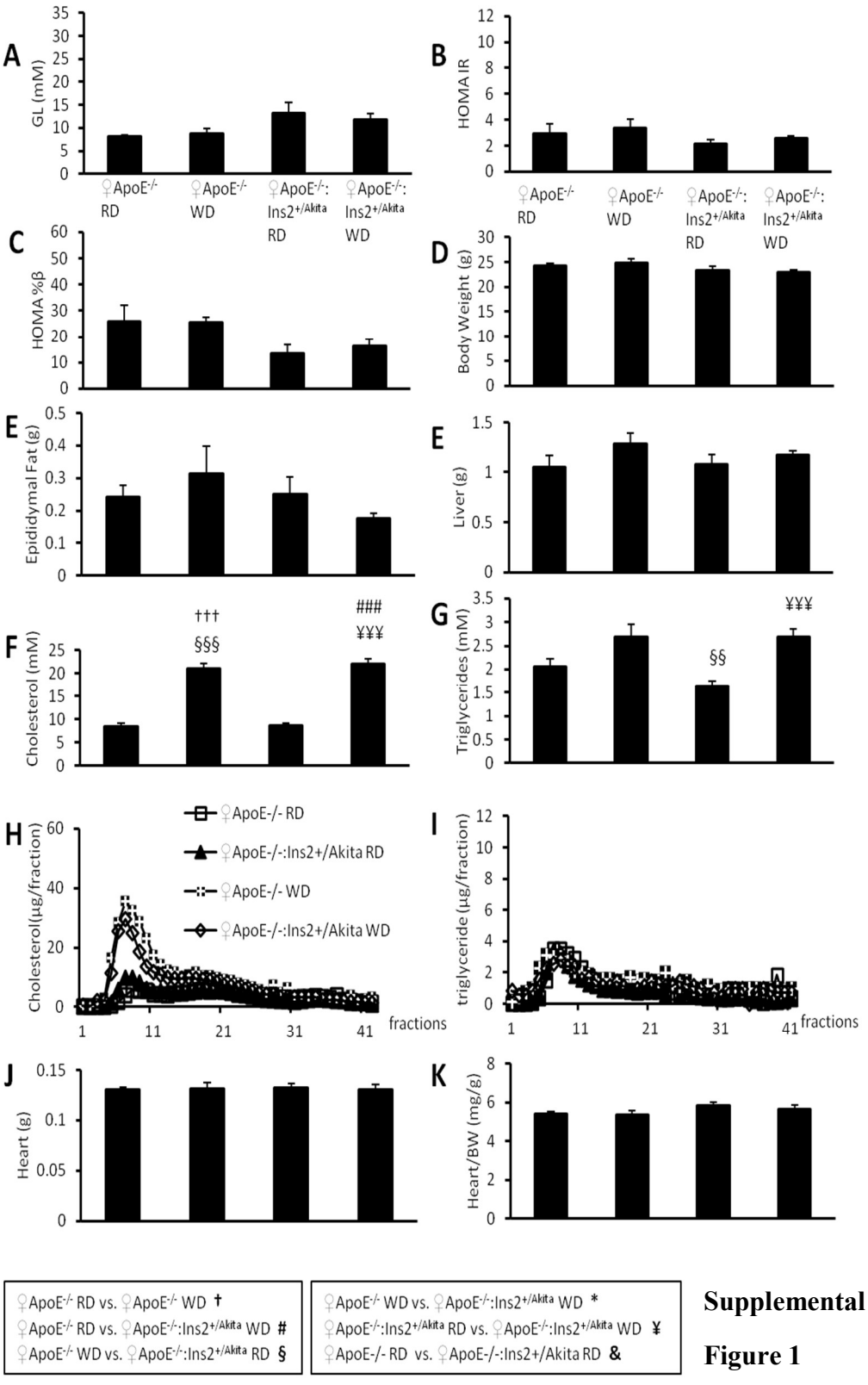

Supplemental Figure 1

Supplemental Figure 2. Quantification of atherosclerosis in the aortic sinus and ascending aorta of female RD-fed and WD-fed mice. (A–D) Representative images of the atherosclerotic development at the aortic sinus. (E) Atherosclerotic lesion areas through the aortic sinus-ascending aorta. (F) Atherosclerotic lesion volume through aortic sinus-ascending aorta. (n = 4–6)

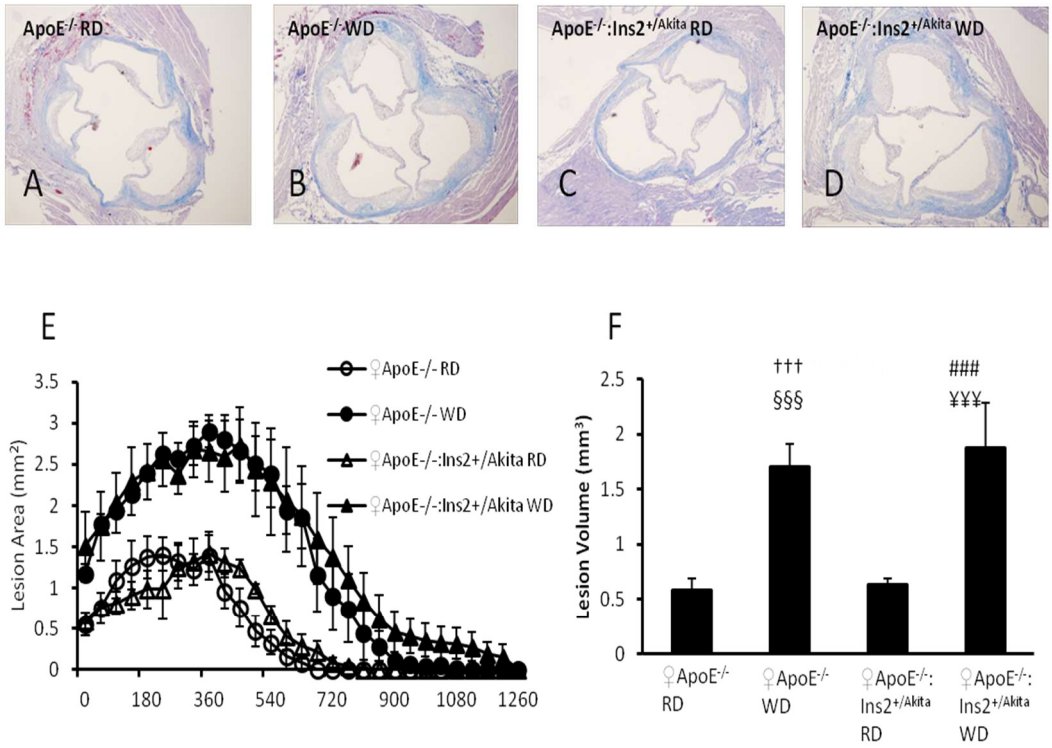

Supplemental Figure 2

APPENDIX 4: Supplemental Material for Chapter 6

Supplemental Figure 1. Vasa Vasorum density. (A) Representative pictures of microvessels at 25 weeks of age in ♂ApoE$^{-/-}$ and ♂ApoE$^{-/-}$:Ins2$^{+/Akita}$ mice. (B) Vasa Vasorum was quantified at 5 (n = 4), 15 (n = 6) and 25 (n = 12–18) weeks of age in male ApoE$^{-/-}$ and ApoE$^{-/-}$:Ins$^{+/Akita}$ mice. *p<0.05, bar = 50 μm.

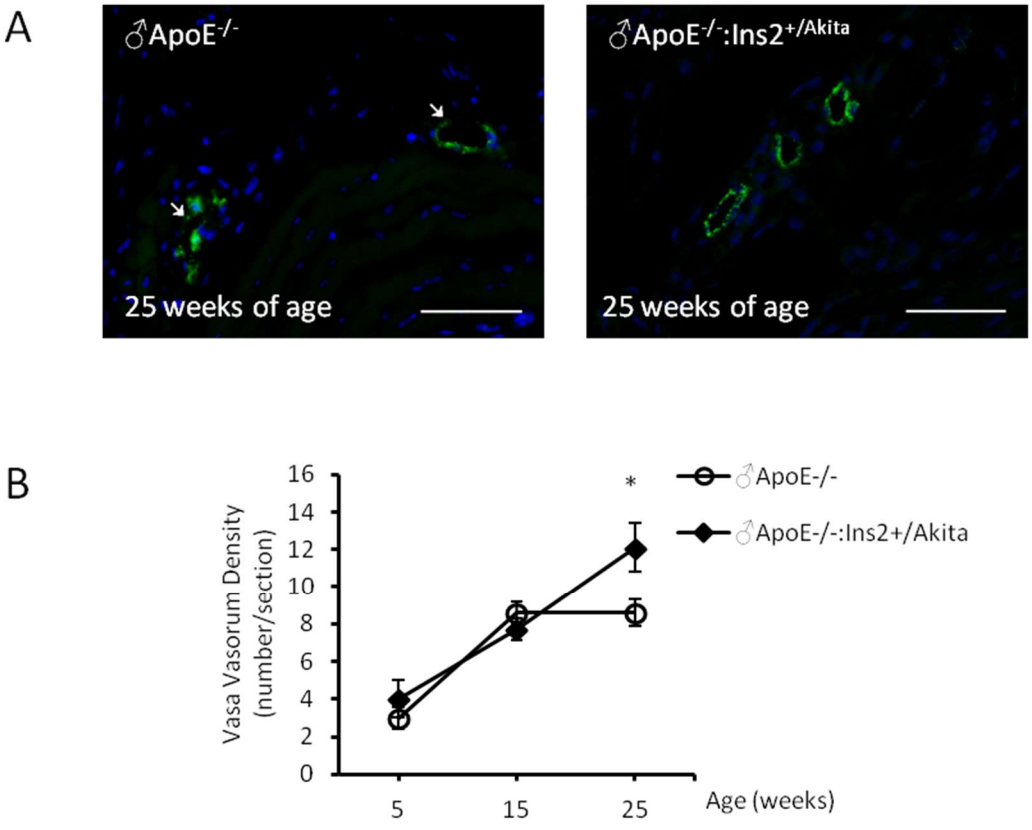

Supplemental Figure 1